Università degli Studi di Milano

Department of Chemistry

Doctoral Course in Chemistry

XXXIII Cycle

Synthesis of carbohydrate antigens and their structural analogues for vaccines development

PhD student: Cristina Manuela Santi

Tutor: Prof. Luigi Lay
Coordinator: Prof. Emanuela Licandro

2017-2020

Abstract

Carbohydrates are multifunctional, stereochemical rich natural molecules. Together with their well-known role of energy sources (glucose, glycogen, amylose) and structural components (cellulose, chitin), they serve important functions in biological processes relevant for health and disease[1] such as molecular recognition, cell communication and adhesion.

A dense layer of oligosaccharides (proteoglycans, glycoproteins, glycolipids and other glycoconjugates) named glycocalyx, covers the membrane of most of cells. Glycocalyx of bacteria often exhibits oligosaccharides different from those found in mammalians, which have an important role in pathogen recognition and immune system activation. For this reason, pathogenic bacteria polysaccharides are widely used for vaccines production. Moreover, the role of symbiont bacteria glycocalyx in immune system activation, development and modulation is object of increasing interest.

In this thesis, the important connection between carbohydrates and immune system is discussed by two different examples.

The first section of the thesis deals with the synthesis of a structural analogue of *Neisseria meningitidis* A (MenA) capsular polysaccharide (CPS), with the final goal of producing a stable glycoconjugate vaccine against meningococcal infections.

Neisseria meningitidis is the major cause of bacterial meningitis. In particular, the serogroup A had been for a long time the leading cause of periodic meningitis epidemics in the area of Africa nicknamed "African meningitis belt"[2]. Despite the introduction a new vaccine named "MenAfriVac" led to a drastic decrease of MenA-related infections[3], the WHO highlighted the importance to persist with a strict vaccination programme.

MenAfriVac, as well as all the other vaccines targeting MenA, is obtained from the extraction and size fragmentation of the capsular polysaccharide of the bacterium.

The natural CPS of MenA is made of *N*-acetylmannosamine repeating units linked through α-(1→6) phosphodiester bonds, prevalently acetylated in position 3 and partially acetylated in position 4. This structure, once isolated from the bacterium, is not stable in water due to

the hydrolysis of the phosphodiester bond. Due to the instability issues, most of the licensed vaccines targeting MenA are distributed in a lyophilized form and the cold chain must be maintained during all the process of distribution and storage. In order to achieve a more stable vaccine, which could be distributed in the more convenient liquid formulation without the need of a strict temperature control, some more stable structural analogues have been developed[4–8]. In particular, the group of Professor Lay synthesized MenA CPS non-acetylated phosphonoester-linked oligomers up to the trimer[4,5]. These analogues showed good stability, however, they resulted to be poorly immunogenic.

Since the acetylation in position 3 was proven to have an important role in the immunogenicity of natural MenA CPS[6,9], this thesis project focused on the synthesis of the 3-O acetylated phosphonate analogues up to the trimer.

The synthetic work developed for the preparation of the 3-O acetylated phosphono analogues is reported in detail and critically discussed in chapter 2.3 of the thesis.

The second section of this thesis deals with the synthesis of glycolipids with the aim of elucidating the structure of new lipid A molecules extracted from *Bacteroides fragilis* and studying their biological potential.

Bacterial lipid A modulate human's innate immune system through their interaction with Toll like receptors (TLR), proteins expressed on dendritic cells and macrophages which play a key role in the development of the innate immunity. TLR activation by bacterial lipid A (di-glucosamines differently O- and N-acylated and phosphorylated) can cause a strong, uncontrolled infection which can even lead to septic shock[10]. However, the use of Monophopshoryl lipid A (MPL) as vaccine adjuvant is the proof that low-toxicity lipid A molecules can also be exploited to boost the efficiency of vaccines via a controlled immune system activation[11,12].

Since symbiont bacteria are well tolerated by the human immune system, the study of their influence on human's immune system is particularly interesting. Potentially, symbiont bacteria's lipid A could be used as a tool to modulate the human immune response.

In 2019, the group of Professor Kasper, isolated novel lipid A molecules from the commensal bacterium *Bacteroides fragilis*[13]. The mixture isolated was composed of tetra- and pentaacylated di-glucosamines (acylated with 15 to 17 carbon atoms linear fatty acid

chains), containing one or no phosphate groups[13]. However, the precise structure of the isolated compounds is still unknown.

As a part of a collaboration with Professor Kasper's group (Harvard Medical School, Boston), a small library of lipid A molecules was designed as a tool to help with *B. fragilis* lipid A structural elucidation. Moreover, structure-activity relationship studies will be performed on the different compounds of the library to achieve a better understanding of the biological potential of symbiont bacteria lipid A.

Preliminary stages of the synthesis of a small library of lipid A molecules from *B. fragilis* are described in chapter 3.4 of this thesis.

Abbreviations and acronyms

[Ir]	(1,5-cyclooctadiene) bis(methyldiphenylphosphine)Iriudim(I) hexafluorophospate
Ac	Acetyl
ACN	Acetonitrile
AIBN	Azobisisobutyronitrile
APC	Antigen-presenting cell
BCR	B-cell receptor
Bn	Benzyl
Cbz	Benzyloxycarbonyl
CD4+ T cells	Helper T cells
CD8+ T cells	Cytotoxic T cells
CM	Cytoplasmic membrane
COSY	Homonuclear correlation spectroscopy
CPS	Capsular polysaccharide
CRM_{197}	Corynebacterium diphtheriae
CSA	Camphorsulfonic acid
DBU	1,5-Diazabiciclo(5.4.0)undec-7-ene
DC	Dentritic cell
DCM	Dichloromethane
DDQ	2,3-Dichloro-5,6-dicyano-1,4-benzoquinone
DFT	Discrete fourier transform
DIAD	Diisopropyl azodicarboxylate
DIBAL-H	Diisobutylaluminium hydride
DIPEA	N,N-Diisopropylethylamine
DMAP	Dimethylamino pyridine
DMF	Dimethyl formamide
DMP	Dess–Martin periodinane
ELISA	Enzyme-linked immunosorbent assay
ESI	Electrospray ionization
Fmoc	Fluorenylmethyloxycarbonyl
GlcN	Glucosamine
Hex	Hexane
HMb	Human microbiota
HMBC	Heteronuclear multiple bond correlation
HMDS	Bis(trimethylsilyl)amine
HMPT	Hexamethylphosphoramide

HPTLC	High-performance thin-layer chromatography
HSA	Human serum albumin
HSQC	Heteronuclear single quantum correlation
IBX	2-Iodoxybenzoic acid\
Ig	Immunoglobulin
IL	Interleukin
IM	Inner membrane
IPV	Inactivated poliovirus vaccine
Kdo	3-deoxy-D-manno-oct-2-ulosonic acid
LC-MS	Liquid chromatography - Mass spectrometry
LPS	Lipopolysaccharide
MALDI	Matrix-assisted laser desorption ionization
Men	*Neisseria meningitidis*
MHC	Major-histocompability-complex
MPL	Monophosphoryl lipid A
Ms	Mesyl
MS	Molecular sieve
MTPA	(+)-α-Methoxy-α-trifluoromethylphenylacetic acid (Mosher's acid)
NLR	NOD-like receptors
NOD	Nucleotide-binding oligomerization domain
NP	Nanoparticle
OM	Outer membrane
PAMP	Pathogen-associated molecular patterns
PDT	1,3-Propanedithiol
PG	Protective group
Ph	Phenyl
PMB	p-Methoxybenzyl
PRR	Pattern-recognition receptor
PS	Polysaccharide
PTSA	p-Toluenesulfonic acid
Py	Pyridine
RIG-I	Retinoic acid-inducible gene-I
RLR	Retinoic acid-inducible gene-I-like receptors
RPTLC	Reverse-phase thin-layer chromatography
RT	Room temperature
SM	Starting material
TBAF	Tetra-n-butylammonium fluoride
TBAI	Tetra-n-butylammonium iodide
TBDPS	tert-Butyldiphenylsilyl

TCR	T-cell receptor
TD	T-dependent
TDS	Dimethylthexylsilyl
TEA	Triethylamine
Tf	Trifluoromethanesulfonyl
Th	Helper T cells
TI	T-independent
TLC	Thin-layer chromatography
TLR	Toll-like receptor
TMAO	Trimethylamine N-oxide
TMS	Trimethylsilyl
Tol	Toluene
WHO	World Health Organization

Index

Introduction

1.1 Introduction on bacteria anatomy

Bacteria are prokaryotic organisms. They present a nucleoid made of a single chromosome, closed in a ring, floating into the cytoplasm. The latter is a granular mass mainly constituted of water, lipids and polysaccharides, which contains discrete structures named inclusions, which function as metabolic reserves or metabolic organelles (which could be provided or not of a specific membrane) and ribosomes. Ribosomes, macromolecular machines that perform biological protein synthesis, have the tendency to lean on the cytoplasmatic membrane, a layer which separates the cytoplasm from the external environment, regulates the input and output of substances from the cell and is the place of all the respiratory enzymes. Moreover, another layer named cell wall covers bacteria, protecting them from mechanical and chemical stress and being involved in their virulence (*Figure 1*).

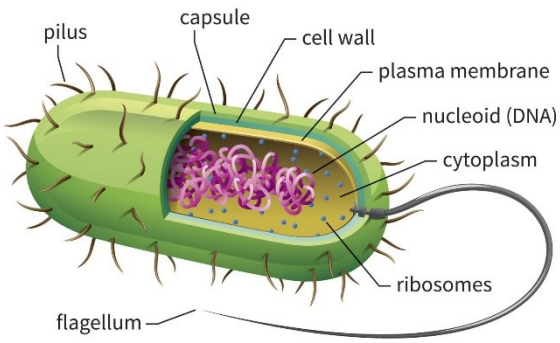

Figure 1. Scheme of bacterial cell structure

Despite all bacteria share some common features, they present structural and functional variability. They can be classified depending on different parameters such as their morphology, their shape, their mode of nutrition, their growth characteristics, etc.

One of the most important classification methods is based on bacteria's staining properties, correlated to their cell wall morphology; indeed, the introduction of the Gram stain by Hans Christian Gram in 1884, allowed to classify bacteria into two categories: bacteria that retain the purple Gram stain are defined as "Gram-positive", while the ones that decolorized are named "Gram-negative"[14].

Bacteria response to Gram stain depends on the different composition and structure of their cell walls. While Gram-positive bacteria have a thick, relatively impermeable wall, mainly composed of peptidoglycans and secondary polymers, Gram-negative bacteria present a thin layer of peptidoglycans, surrounded by a lipid-protein bilayer (outer membrane), which can be disrupted by decolouring with acetone or alcohol[15].

1.1.1 Gram-negative bacterial cell envelope

Gram-negative bacteria cell envelopes are made of three principal layers (*Figure 2)*:

1) The cytoplasmic or inner membrane (IM), made of a phospholipid bilayer and acts as a permeability barrier, location for transport of molecules into the cell, and energy conservation.

2) A thin peptidoglycan cell wall contained in the periplasm (a gel-like matrix in the space between the IM and the outer membrane). The peptidoglycan cell wall is composed by a highly rigid polymer of N-acetyl glucosamine-N-acetyl muramic acid disaccharides, cross-linked by peptide side chains. This cell wall has the aim to protect the bacteria from lysis and, due to its rigidity, it is the responsible for bacteria shape[16].

3) The outer membrane (OM), the most external part of Gram-negative bacteria, which distinguish them from the Gram-positives. It is composed by a lipid bilayer: while the internal part is made of phospholipids, the outer is made of glycolipids, mainly lipopolysaccharides (LPS)[17].

Together with their role in the cell growth development, LPS are involved in several interactions of the cell with other biological systems such as adhesion, recognition, colonization, symbiosis and virulence.

The LPS presents three main domains (*Figure 2)*:

1) O-antigen. This is the most external part of the LPS and consists in a glycan polymer;

2) Core. An oligosaccharide component attached to both the O-antigen and the Lipid A which commonly contains at least one 3-deoxy-D-manno-oct-2-ulosonic acid (Kdo) residue;

3) Lipid A, a phosphorylated disaccharide, usually a di-glucosamine, decorated with multiple fatty acids which anchor the LPS into the bacterial membrane, through hydrophobic and electrostatic interactions[18], while the rest of the LPS projects from the cell surface.

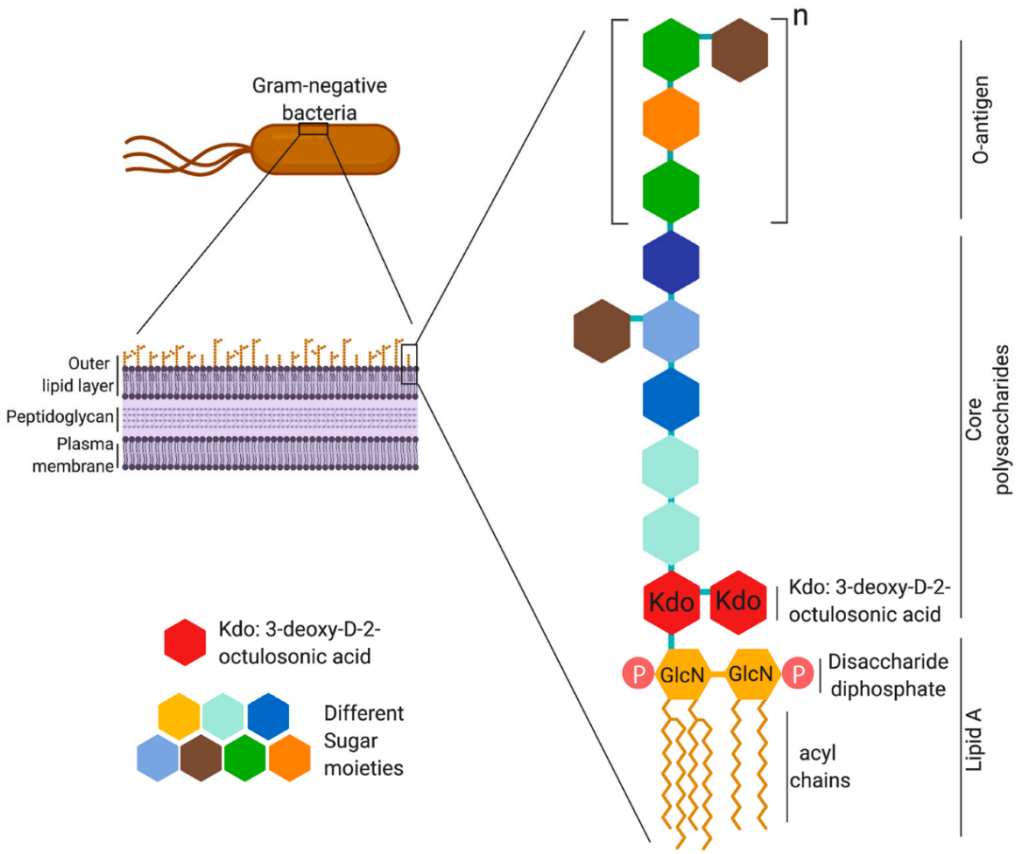

Figure 2. Composition of Gram-negative bacteria envelope.[19]

1.1.2 Encapsulated bacteria

Some bacteria, named "encapsulated bacteria", present a further layer which covers their cell walls, named capsule. The capsule has the role to protect the bacterium from the external environment and to provide defence from host's immune system (in particular from phagocytosis and Complement attacks)[20].

The capsule is constituted of polysaccharides (capsular polysaccharides - CPS), which composition differs among different species.

Many encapsulated bacteria are still leading cause of severe infectious diseases, particularly affecting the most vulnerable population groups (infants, young children and elderly).

Typical examples include both Gram-positive (*Streptococcus pneumoniae*, Group B *Streptococcus*, *Staphylococcus aureus*) and Gram-negative (*Haemophilus influenzae*, *Neisseria meningitidis*, *Salmonella typhi*) bacteria.

The CPS can work as antigen, allowing the host to produce specific antibodies against the bacterium. Since it was demonstrated that immunity against CPS of encapsulated bacteria leads to protection against the disease, these components became an interesting target for vaccine development[21] (*Chapter 1.3.3*).

1.2 The immune system

The immune system is a sophisticated defence system which protects the host from pathogens and allergenic or toxic substances through a series of processes called immune response.

The science dealing with the study of the immune system and response, called immunology, is quite recent: despite its origin is usually dated 1796, when Edward Jenner discovered the first vaccine against smallpox, only in 1882 Elie Metchnikoff discovered macrophages, one of the major players of the innate immunity. Another major advancement in immunology took place quite recently: in 1890s, Emil von Behring and Shibasaburo Kitasato discovered that the serum of animals immune to diphtheria and tetanus contained substances with antitoxic activity, now called antibodies, which are the key elements of the adaptive immune response.

According to these findings, the immune response is now categorized into two main subtypes: the innate and the adaptive immune response.

1.2.1 Innate immune system

The innate immune system is the host's first protection against pathogens and includes physical barriers (skin, epithelial cilia, body hairs), soluble proteins, bioactive small molecules, membrane bound receptors and cytoplasmic proteins.

The name "innate" was given because the defence mechanism is encoded in the host's germline, having been selected over evolution[22].

The innate immune response is rapid (it is activated within minutes or hours) but not specific and it is not able to induce long-lasting immunity against pathogens.

When a microorganism enters the host's body by breaching its physical barriers, the immune system has, at first, the role to recognize it. To do so, it relies on numerous pattern-recognition receptors (PRRs) which can be found as soluble receptors in the blood stream (components of the Complement system), or as membrane-bound receptors on the surface of macrophages and dendritic cells such as Toll-like receptors, TLRs[23].

Receptors belonging to TLR family detects PAMPs (pathogen-associated molecular patterns: specific cell components present on pathogen surface but not on mammalians), expressed on cell surfaces or on the lumen of intracellular vesicles, while intracellular

PAMPs can be detected from retinoic acid-inducible gene-I (RIG-I)-like receptors (RLRs) and nucleotide-binding oligomerization domain (NOD)-like receptors (NLRs)[24].

When the soluble receptors detect the presence of a pathogen, the Complement cascade is activated, causing the stimulation of phagocytic cells (neutrophils and macrophages, which can eliminate the pathogen through phagocytosis), the formation of an inflammation site and the activation of the membrane-attack complex to perforate the cell membranes of pathogens[25].

When PRRs identify PAMPs, they stimulate the production of lipid (such as prostaglandins) and protein (such as cytokines) signalling molecules, which contribute to the inflammatory response. The production of signalling molecules leads to the recruitment at the infection site of neutrophils, macrophages and dendritic cells (DCs).

DCs and macrophages are considered a connection between the innate and adaptive immunity. Indeed, they pick up and process (progressive fragmentation by means of intracellular proteases) antigens driving them to lymph nodes, where they exploit their role of antigen-presenting cells (APCs) by presenting the antigen fragments (peptide fragments, according to the most accepted assumption) to T cell receptor (TCR) of T lymphocytes[23] through the major-histocompatibility-complex (MHC) .

Furthermore, other signalling molecules trigger fever and small blood vessels occlusion to fight the infection and prevent the pathogens to enter the blood stream. However, an uncontrolled inflammatory response is related to septic shock (often fatal) and some chronic conditions such as asthma[23]. For this reason, the regulation of PRRs signalling is crucial to keep the host safe[26].

1.2.2 Adaptive immune response

The adaptive immune response starts from a small number of cells and propagates after encountering the antigen to produce an high number of cells, specific for any individual pathogen, toxin or allergen.

The adaptive response is highly specific but needs more time to be activated, compared to the innate one. Together with the specificity, the ability to develop immunological memory is the key characteristic of the adaptive immune response.

The cellular elements of the adaptive immune system are the T- lymphocytes (effectors of the cellular response) and the B-lymphocytes (which are responsible for antibodies production).
More commonly called T-cells, the T-lymphocytes are generated in the thymus.
All T-cells present on their surfaces several antigen receptors (TCR), different from cell to cell: the huge diversity of TCRs is given by chromosomal recombination and mutations.
When TCRs recognize MHC I-antigen complexes (generated from the degradation of foreign cytosolic proteins), the established immunological synapse (TCR-antigen-MHC I complex) may induce the activation of cytotoxic T-cells (CD8+ T cells), effector cells able to destroy the cells infected by intracellular viruses or bacteria.
Moreover, TCRs can interact with MHC II-antigen complexes. MCH II molecules, normally found on APCs (such as DCs), present peptides deriving from extracellular proteins, after their phagocytosis and digestion. The formation of the TCR-antigen-MHC II complex leads to the proliferation of helper T cells (Th or CD4+ T cells), involved in B cell proliferation and differentiation.

B cells (or B lymphocytes) are the second important class of cells that drive the adaptive immune system. They originate in the bone marrow from a common lymphoid progenitor and, after maturation, they undergo proliferation and may differentiate into plasma cells, i.e. large lymphocytes able to produce antibodies.
Antibodies, also called immunoglobulins, are heterodimeric proteins constituted of two heavy and two light chains. The high variety of immunoglobulins existing is achieved through a complex process of genetic rearrangement and selection.[27]
Once secreted, antibodies circulate throughout the body and, when they find the target antigen, they can neutralize the pathogen by interfering with the receptors used to infect cells or marking the pathogen for destruction by phagocytosis or by the Complement system.
B cells can also evolve into memory B cells: long-living cells (they can be preserved in the bone marrow for decades[28]), responsible for the immunological memory development.
The “Immunological memory” is the ability of the immune system to recognize an antigen that had been already infecting the body and to initiate a fast, strong and specific immune response against it.[29]

1.2.3 T-dependent and T-independent immune response

Depending on the B cell maturation mechanism they activate, antigens can be classified as T independent (TI) or T dependent (TD).

TI antigens activate B cells without involving helper T cells, with consequent maturation to plasma cells and low affinity IgM antibodies production. TI antigens can be further classified into type 1 and type 2.

Type 1 TI antigens, such as lipopolysaccharides and bacterial DNA, are mitogens (polyclonal B cell activators): they can activate B cells independently of their antigenic specificity. In low concentrations, however, they selectively activate B cells specific for the antigen, with monoclonal antibodies production (*Figure 3*).

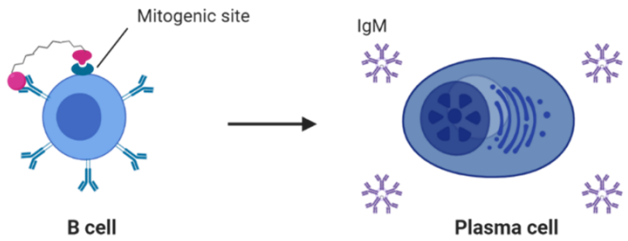

Figure 3. B cell activation by type 1 TI antigens.

Polysaccharides (and other linear polymeric antigens), instead, are mostly type 2 TI antigens. Their polymeric structure allows simultaneous binding to, and cross-linking of, multiple B cell receptors (BCRs), leading to the differentiation of naive B cells into plasma B cells, with the production of low affinity IgG2 and highly unspecific IgM antibodies[21] (*Figure 4*).

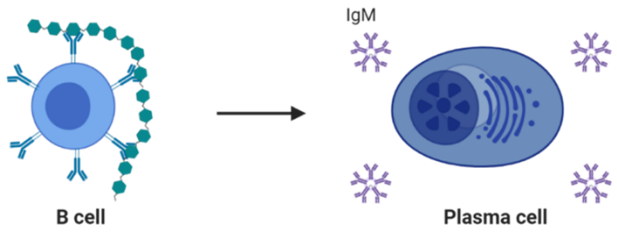

Figure 4. B cell activation by type 2 TI antigens.

TD antigens, typically proteins, activate B cells through a mechanism which requires the intervention of T helper cells. When the antigen enters the host, it is recognized by dendritic cells which internalize and process the antigen by fragmenting it and exposing the fragments to T cell receptors through MHC molecules, with the formation of the MHC-antigen-TCR complex (immunological synapse). If the antigen derives from endogenous pathogens, MHC class I is involved, and T cell will mainly differentiate into cytotoxic T cells. In case of exogenous pathogens, MHC class II is involved and T cells mainly differentiate into T helper cells, which are responsible for B cells activation and their differentiation into plasma cells (with high affinity IgG antibodies production) and memory B cells[21] (*Figure 5*).

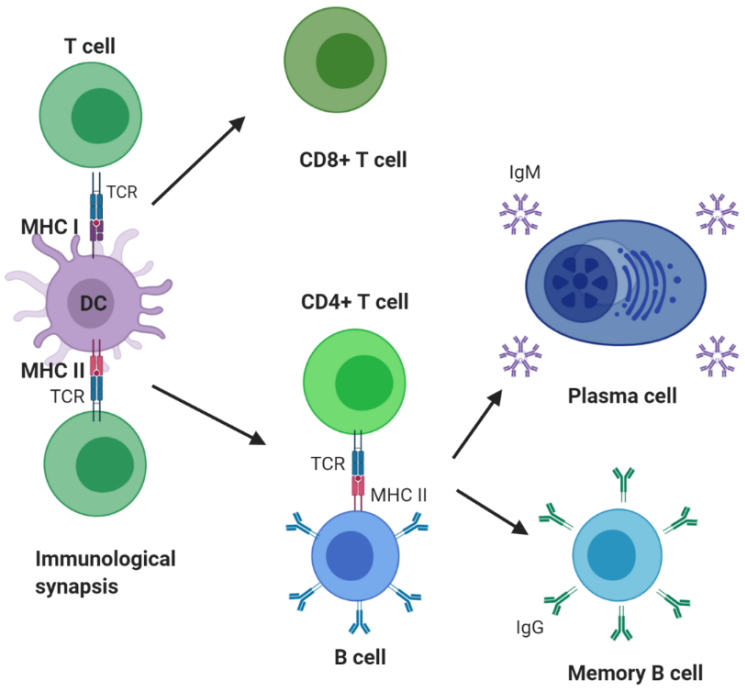

Figure 5. B cell activation by TD antigens.

The ability of an antigen to trigger the production of high affinity antibodies and memory B cells is crucial to achieve a long-term protection of the host from a second attack of the same pathogen and, accordingly, it is crucial in the choice of a suitable antigen for vaccine development.

1.3 Vaccines

Vaccines are biological preparations able to provide acquired immunity against specific infectious diseases. To highlight their importance, World Health Organization (WHO) defined vaccination as "*a key component of primary health care and an indisputable human right*" and as "*one of the most cost-effective ways to prevent diseases*"[30].

Nowadays, vaccines protect against more than 25 debilitating or life-threatening diseases.

1.3.1 Brief history of vaccines

"Vaccine" derives from "*Variolae vaccinae*", the term used by Edward Jenner to describe the protective effect of cowpox against smallpox[31].

Even if the word "vaccine" was coined in 18th century, we must go back centuries to find the beginning of the observations, experiments and trials that led to the birth of vaccinology.

In 430 B.C., it was already been observed that, people who survived smallpox, were immune to a second infection: it was somehow already present the concept of immunity.

The idea of immunizing healthy patients is not that recent too: some records exist showing that, in 10th century, Chinese physicians attempted to transfer the smallpox infection to healthy people with the purpose to make them immune. In fact, they used to open pustules of sick people, dry the matter taken and then put it up the nostrils or inoculate it by scratching it into the skin of the people they wanted to immunize. With this practice, known as "variolation", they could transmit the virus and sometimes immunity[32]. The inoculation procedure was also practiced in Africa and India. In 17th century, this technique was introduced in the Turkish Ottoman Empire and, from there, it arrived in Europe at the beginning of the 18th century[33]. In 1721, variolation eventually came into fashion in Europe, with the support of Lady Montagu. In the same years it was also diffused in America. The variolation procedure demonstrated to be able to lead to patients' immunization but the procedure was not safe, with 2-3% of people death after inoculation and the intrinsic high risk to trigger new epidemics.

In 1796, Edward Jenner had a fundamental role in the development of the one which is considered the first vaccine. Jenner noticed that milkmaids, after being exposed to cowpox, showed immunity to smallpox infection and he experimented the use of cowpox instead of smallpox for inoculation: he achieved the same results in terms of protection but with less side effects. Edward Jenner, however, was not aware of the origin of the infection and of the

mechanism of action of his vaccine. Only later, Louis Pasteur and Robert Koch discovered that germs and microorganisms are the causative agents of diseases. In 1881, Pasteur demonstrated immunization of sheep against anthrax through the injection of a preparation containing an attenuated bacillus form. In 1885, he developed the first live-attenuated vaccine for humans, preparing a protective suspension against rabies[34]. Other live-attenuated or inactivated pathogens and toxins obtained from animal systems were used in the so called "first golden age of vaccines" to create vaccines against diphtheria, tetanus, pertussis and tuberculosis.

The second vaccine's golden age came in 1940s' with the "cell culture revolution"[35]. Enders, Robbins and Weller demonstrated that poliovirus could be grown in cell culture and so, that it is possible to grow human viruses in vitro[36]. These discoveries allowed Salk to grow poliovirus in primary monkey cells for the development of the inactivated poliovirus vaccine (IPV), followed by the development of many other inactivated or attenuated vaccines for hepatitis A, measles, rotavirus, and varicella[37].

In 1970s', the first subunit, polysaccharide-based vaccine against meningococcal strains was introduced by Artenstein, Gottischlich and coworkers[38], followed by pneumococcal vaccines by Heidelberg and Macleod and by *Hemophilus influenzae* type b vaccine by Anderson, Smith, Schneerson, Robbins, and coworkers[39]. These vaccines were developed thanks to the already well-known idea that many pathogens are surrounded by a capsule made of polysaccharides and that the production of antibodies against it could promote phagocytosis. However, polysaccharides revealed to be poorly immunogenic in children. Even if the advantages deriving from polysaccharides' conjugation to proteins were already been shown by Avery and Goebel in 1929, the first glycoconjugate vaccine against *H. influenzae* b was made in 1980[40,41]. Glycoconjugate vaccines proved to induce better antibody response and to be effective in all age groups. Meningococcal and pneumococcal glycoconjugate vaccines were also developed with this strategy. In the same years, Hilleman[42] and co-workers could obtain a vaccine against hepatitis B. The virus does not multiply significantly in cell culture, but it was demonstrated a relationship between the *Australia antigen* (also known as hepatitis B virus surface antigen) present in the blood of some human subjects and the human hepatitis B. The plasma of *Australia antigen* human carriers was treated and then used to immunize healthy patients. The advent of recombinant DNA technique made it possible to produce

large quantities of hepatitis B vaccine in viral-like particles: self-assembling complexes of capsid proteins able to mimic the overall structure of the virus[43].

The huge progress in genomics that took place in the last decades had also an impact on vaccine development. Reverse vaccinology, that led to the development of a meningococcus B vaccine, is indeed based on the rational selection of candidate antigens based on genomic information[44].

Therapeutic use of vaccination is also gaining some importance for the treatment of chronic diseases and cancer.

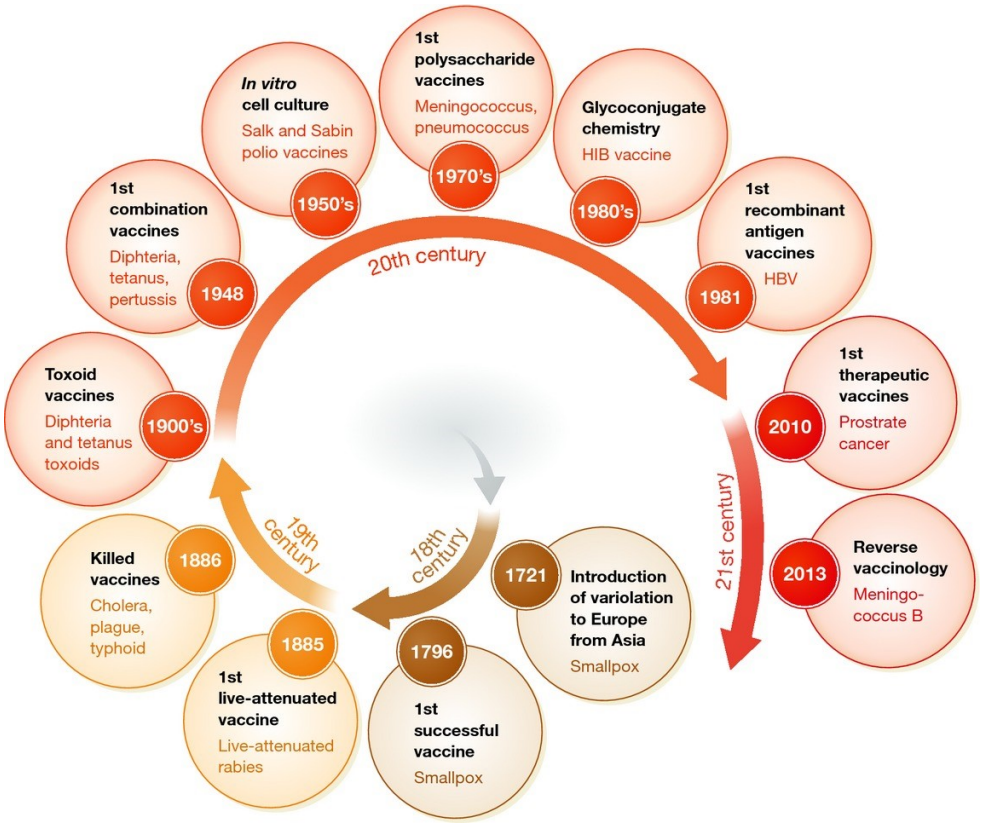

Figure 6. Timeline of vaccines development.[37]

1.3.2 Vaccine components

Vaccines include a variety of ingredients. Each of them serves a specific purpose like providing immunity against a specific disease or keeping the vaccine safe and long lasting. Other compounds deriving from the production of the vaccine can be found in traces.
In this chapter, the main components of vaccines are described.

Active components (antigens)

The active component of a vaccine is represented by the antigen.
The term "antigen" comes from the abbreviation of "antibody-generator" and it is used to indicate molecules recognized by B or T cells[45].
The active component can be obtained from a modified or partial form of the pathogen or it can be produced in the laboratory, mimicking the natural antigen structure.
Vaccines can be classified into categories on the base of the active component they contain[46].

Live-attenuated vaccines: obtained from the weakening of whole pathogens (viruses or bacteria) or from the selection of temperature-sensitive or cold-adapted mutant strains. The attenuated form is not able to replicate sufficiently to cause disease in people with healthy immune systems but is still able to induce an immune response before being eliminated by the immune system.
The protection, obtained with a single dose, is strong and lasting, without the need of adjuvants. This kind of vaccine, however, can cause severe reactions in immunocompromised people, for whom it is not suitable and can lead to side-effects from non-pathogen parts of the vaccine.
Live attenuated vaccines are used, for example, against measles, rubella, yellow fever, rotavirus, varicella, smallpox and influenza[47,48].

Killed or inactivated vaccines: based on the use of a whole pathogen killed, typically through γ-irradiation or chemical agents. These procedures destroy the pathogens' ability to replicate but keep the epitopes intact so that the immune system can still recognize them.
After treatment, the pathogens are no more able to cause the disease even in immunocompromised patients however, they tend to provide a short length of protection, with the need of multiple doses, adjuvants and boosters.
Inactivated vaccines are used to protect against flu, polio, hepatitis A and rabies[47,49].

Toxoid vaccines: in some cases, the disease associated to some pathogen is caused by production of exotoxins. Toxoid vaccines protect against pathogen exotoxins and, doing so, they protect the host from the disease. Toxoids are inactivated versions of exotoxin molecules, obtained by chemical treatment. They can trigger a strong immune response and they are also used to increase the immunogenicity of T-independent antigens.
Toxoid vaccines are mainly used to protect against diphtheria and tetanus.[47]

Subunit vaccines: they contain only some components of the pathogen, which maintain the ability to induce immune response against the full pathogen. They can be obtained either by chemical degradation of a pathogen and isolation of its key antigens, or by production of the antigen through genetic engineering or chemical synthesis.[47]
The first sub-unit vaccines were developed starting from the isolation and purification of the surface antigenic proteins of viruses. This method is labour-intensive and the vaccine production very expensive, especially when it is difficult or impossible to grow the virus in cell cultures or when the purification is hard.
With the introduction of recombinant DNA technology, it became possible to manipulate the DNA of the pathogens: the DNA that encodes for the antigen is introduced into the genome of other organisms which can be easily grow in huge amounts[47,50].
Polysaccharide-based subunit vaccines are suitable to protect against encapsulated bacteria, which are covered by capsular polysaccharides (*Chapter 1.3.3*).

Adjuvants

Adjuvants (from the Latin word "*adiuvare*", meaning "to help") are components which have been used to improve vaccines since when the first vaccines were developed.
Already in the 18th century, at the time of the first smallpox vaccines when nothing was known about vaccinology, nucleic acids and coat components of the pathogens present in the preparations were acting as adjuvants[51].
In the 20s' of 20th century, the French veterinary and biologist Gaston Ramon, better known for the development of the diphtheria vaccine, observed a stronger immune response against diphtheria in the horses in which a stronger inflammation at the injection site was developed. To enhance antibodies production in horses, he injected the antigens with several materials

(tapioca, breadcrumbs,..) and he confirmed his theory: the use of inflaming components could increase the immune response to a vaccine[52].
In the same years, Pope and Glenny showed an increase in the production of antibodies in guinea pig when the tetanus vaccine was administered as adsorbed into insoluble aluminum salts[53].

Nowadays adjuvants are widely clinically used to improve the response to vaccines by increasing antibodies titres and the fraction of people effectively immunised by the vaccine (very important for infants and elderly people). They also facilitate the use of smaller doses of vaccine and the immunization with fewer doses. Adjuvants are also used in pre-clinical and clinical studies to increase the generation of memory cells, to provide functionally appropriate types of immune response and to shorten the time needed to have the initial response to a vaccine (very useful in case of pandemic outbreaks)[54].
Adjuvants can be classified, based on their mechanism of action, into delivery systems and immunostimulatory.

Delivery system adjuvants: they function as carriers for the antigen. They are responsible for the starting of the proinflammatory response in the injection site[55] and for the activation of the innate immune response.
They show high effectiveness in boosting antibodies responses, mainly by stimulating Th2 cells, responsible for the control of immunity against extracellular pathogens[56].
Delivery system adjuvants can be further divided into sub-cathegories[57]. One of the most famous group is the mineral salts, which include aluminium salts (the most widely used), microparticles and lipid particles. Another important group is represented by emulsion adjuvants, which include Freund's adjuvants (water-in-oil emulsion that contains heat-killed mycobacteria) and incomplete Freund's adjuvants (water-in-oil emulsion which does not contain mycobacteria), while microparticles adjuvants include virus-like particles, particles formed by structural viral proteins which mimic intact viruses.
Immune potentiators (immunostimulatory): they activate the innate immune system through PRRs (TLRs, RLRs and NLRs)[58] and induce APC activation and cytokine and chemokine production. Immune potentiators adjuvants can be further classified in categories depending on the type of receptors they can activate.
The main types are TLR3, TLR4, TLR5, TLR7/8, TLR9 and NOD agonists.

TLR4 agonists comprise monophosphoryl lipid A (MPL), an analogue of *Salmonella minnesota* R595 lipid A[59].

Other components

Stabilisers are used to maintain a vaccine effective by stabilising the vaccine's other components during storage[60]. Some examples of stabilisers are glycine, sucrose, lactose, monosodium glutamate and human or bovine serum albumin.

Preservatives are used to prevent contamination of vaccines from fungi and bacteria. The preservatives used include phenol, thiomersal and phenoxyethanol.

Diluents (usually sterile water or saline solution) are liquids provided separately and used to dilute the vaccine.

Other trace components, mostly deriving from the processes of vaccine production, such as antibiotics, inactivating agents (e.g. formaldehyde and glutaraldehyde), egg proteins and yeast can be present[47].

1.3.3 Carbohydrate-based vaccines

Since they are widely expressed on cell surfaces (even on pathogen or damaged cell surfaces) and they are involved in several biological processes, carbohydrates represent attractive targets for sub-unit vaccine design[61].

Carbohydrate-based vaccines can be classified in three "generations".

The first generation consists in the polysaccharide vaccines.

Polysaccharides are extracted from the natural sources, fractionated, purified, and eventually used for vaccine production. However, polysaccharides are mostly TI type 2 antigens (*Chapter 1.2.3*) and they trigger a T-independent immune response, with production of low affinity IgM antibodies and without memory B cells production[62]. Polysaccharides, indeed, showed to provide only short-term protection in adults while they are completely inefficient in children aged below 2 years old and in the elderly, which are the part of population most affected by infectious diseases[63,64].

In 1931, Avery and Goebel[65] reported that polysaccharide immunogenicity can be enhanced through their conjugation to immunogenic proteins. The resulting glycoconjugate vaccines represent the second-generation carbohydrate-based vaccines. They are indeed able to

trigger a T-cell dependent immune response (*Chapter 1.2.3*), which leads to the production of memory B-cells and to the switch from IgM antibodies to polysaccharide-specific IgG[66].
The mechanism of immune system activation by glycoconjugates is still under debate.
In 1970s' Mitchison[67] and co-workers suggested that glycoconjugates could bind the B cell receptors of polysaccharide-specific pre-B cells and could be taken into the endosome, where the protein is "cut" into peptide epitopes by proteases. The peptides could then bind MHC-II and be presented to the CD4+ T cells. Peptide-MHCII-T cell complex could then release cytokines and stimulate B cell maturation and IgM switch to polysaccharide-specific IgG.
A novel mechanism has been proposed by Kasper and coworkers[68,69,70] which suggested that glycopeptide fragments are produced and processed by APCs, leading to the rise of specific T cell clones, called Tcarb, able to induce a TD response against the saccharide.
Although the second-generation vaccine resulted very effective, it also presents some drawbacks. Indeed, the isolation of polysaccharide from microbial cultures makes it impossible to completely avoid microbial contamination and batch-to-batch heterogeneity[71].

The third generation of carbohydrate-based vaccines has the purpose to overcome these problems. Indeed, it consists in the preparation of semi-synthetic glycoconjugate vaccines, in which the saccharide part is synthetic, while the protein carrier is natural. This approach leads to homogeneous, pure and well-defined structures, which can be used for vaccine development or as analytical standards to support the second-generation carbohydrate-based vaccine production. Moreover, the preparation of synthetic saccharides is very useful to support structural analysis to reveal the protective epitope and, furthermore, it makes possible to produce antigens' structural analogues, which can be more stable than the natural ones or can represent a common epitope for the protection against different bacterial stains.
The first example of semi-synthetic glycoconjugate vaccine has been reported in 2004 by Verez-Bencomo, Roy and co-workers[72]. They prepared a fully synthetic oligosaccharide epitope which, after conjugation to tetanus toxoid, provided a commercial vaccine against *Haemophilus influenzae* type b (Quimi Hib®, Heber Biotec, Cuba)[72,73].
Obviously, also this new approach presents some drawbacks, mainly concerning the high production costs and (generally) the lower immunogenicity when compared with larger size carbohydrate vaccines.

Synthesis of an analogue of Neisseria meningitidis A CPS for the development of a glycoconjugate vaccine

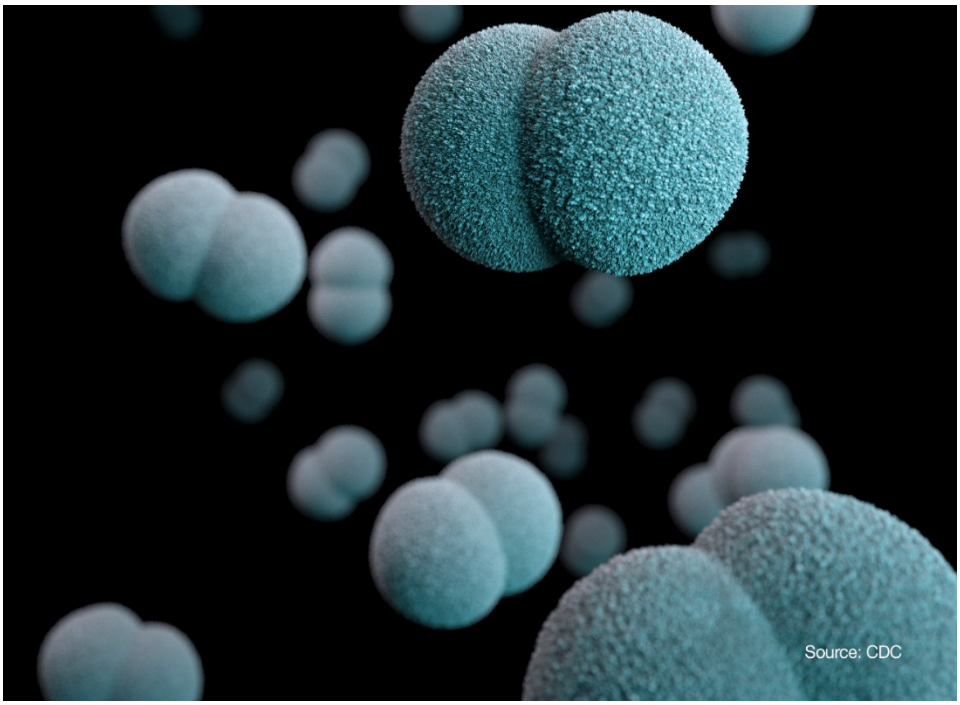

2.1 *Neisseria meningitidis*

Neisseria meningitidis is a Gram-negative, encapsulated, diplococcus bacterium.

Encapsulated bacteria's outer membrane is surrounded by polysaccharide capsules, which protect bacteria from phagocytosis and from the attack of the Complement system and that represent key pathogenicity factors[3] (*Chapter 1.1.2*).

Based on the different composition of their capsular polysaccharides (CPSs), 12 serogroups of *N. meningitidis* have been identified; among them, the serogroups A, B, C, Y, W, X (*Table 1*) are the most relevant in terms of pathogenicity[74]. The relative relevance of the serogroups strictly depends on the geographic area, with serogroups B, C and Y more common in Europe, America and Australia, while infections from serogroup A are mostly found in Africa and Asia[75].

Serogroup	***Repeating unit***	***Linkage***	***O-Acetyl content (mol/mol)***	***Location of O-acetyl groups***
A	2-Acetamindo-2-deoxy-D-mannopyranosyl phosphate	α 1→6	0.7	C-3, C-4
B	N-Acetylneuraminic acid	α 2→8	0	-
C	N-acetylneuraminic acid	α 2→9	1.3	C-7, C-8
W	4-O-α-D-galactopyranosyl-N-acetylneuraminic acid	α 2→6	0	-
Y	4-O-α-D-galactopyranosyl-N-acetylneuraminic acid	α 2→6	1.1	Not specifically located
X	2-Acetamindo-2-deoxy-D-glucopyranosyl phosphate	α1→4	0	-

Table 1. Structure of the main N. meningitidis serogroups[76].

N. meningitidis inhabits the nasopharynx of about 10% of the population[77] without causing any disease: the bacterium is an accidental pathogen and, only rarely, it enters the bloodstream, leading to life-threatening diseases like septicaemia and meningitis. Infants under one year of age, teenagers, people with deficiencies in the complement system and asplenia are the most susceptible to meningococcal disease[78].

Nowadays, *N. meningitidis*-related infections are mostly treated with penicillin G, chloramphenicol or III generation cephalosporins (such as cefotaxime)[79]. However, due to increasing antibiotic bacterial resistance[80,81] and to the high fatality ratio of the disease (higher than 50% when untreated), and considering that the bacterium can sporadically lead to epidemics[82], the WHO defined vaccination as the most effective strategy to fight the spreading of *N. meningitidis*.

Most of the vaccines existing up to date against encapsulated bacteria like *Streptococcus pneumoniae, Haemophilus influenzae* and *Neisseria meningitidis* target their capsular polysaccharides.

Gotschlich and his collaborators[38] have been the first, in 1969, to demonstrate the possibility to extract *N. meningitidis* CPS and, in 1970s[83], the first CPS-based vaccines against *N. meningitidis* were introduced.

Due to the differences in CPS of the different *N. meningitidis* serogroups, it is hard to achieve the formulation of a 12-valent anti-meningococcal vaccine. Indeed, no common epitope was found. Nevertheless, some mono- and oligo-valent vaccines have been licensed.

The first generation of CPS-based vaccines includes bivalent (MenAC), trivalent (MenACW) and tetravalent (MenACWY) formulations. However, the first-generation of polysaccharide-based vaccines showed to be not immunogenic in young children (the most susceptible to the disease) and immunocompromised people. This problem was overcome by conjugation of the CPS to carrier proteins, leading to the introduction of the second-generation polysaccharide-based vaccines: the glycoconjugate vaccines (*Chapter 1.2.3*).

Regarding the second-generation vaccines, Men C conjugate vaccines have been licensed, together with two tetravalent vaccines (MenACWY). In the first one (Menactra®), dated 2005, the CPS is conjugated to diphtheria toxoid, while in the second (Menveo®), dated 2010, CRM_{197} is used as carrier protein.

Although the serogroups A, C, Y and W are suitable for glycoconjugate vaccine production, the serogroup B situation is completely different: the CPS of Men B is constituted of a homopolymer of sialic acid which presents high similarity to human brain glycoproteins[84]. Therefore, Men B CPS is well tolerated from our immune system. Reverse vaccinology was used to develop the first multicomponent Men B vaccine and, in 2017, a new vaccine named Bexsero®, based on two recombinant lipidated factor H binding protein has been licensed for use in EU countries[66].

Unfortunately, no serogroup X vaccine is available nowadays.

2.1.1 Neisseria meningitidis A

The epidemiology of MenA in the African region identified as "African meningitis belt" (mainly comprising Chad, Burkina Faso, Niger and Ethiopia) had been alarming for long time, with the development of periodic epidemic waves during the dry season and large-scale epidemics every 5-12 years (up to 1,000 cases per 100,000 people)[2].

In 2001, Bill and Melinda Gates foundation donated 70 million dollars for the "Meningitis Vaccine Project" to the WHO-PATH partnership (World Health Organization-The Partnership for Advanced Technologies in Healthcare services). The project aim was that to formulate a cheap vaccine against MenA, to be distributed in the African Meningitis Belt. As a result, MenAfriVac was produced as a glycoconjugate vaccine containing MenA CPS conjugated to Tetanus toxoid[85].

The vaccination program with MenAfriVac started in 2010[86] and, by 2017, MenA was responsible for only 0.8% of meningococcal disease cases in the countries where the vaccine had been introduced.[3]

Nevertheless, cases of MenA are still detected in some African countries, Asia and Minor Asia and WHO highlighted the importance of persisting with a strict vaccination program.

2.1.2 N. meningitidis A CPS instability

The natural CPS of MenA, once extracted from the natural source, is not stable in water. Due to stability issues, most of MenA vaccines existing nowadays are distributed in lyophilized formulation. The quadrivalent vaccine Menveo, for example, is made of two parts: one liquid part containing MenCYW and a lyophilized one containing MenA. The stability of the MenA strain, when the conjugate is reconstituted, is only 8 hours at 25°C, after which the vaccine can't be used anymore.

To understand the reasons of the lack of stability on MenA vaccines, we need to look at its chemical structure. The natural capsular polysaccharide of MenA is composed of *N*-acetylmannosamine repeating units linked through α-(1→6) phosphodiester bonds, 3-O acetylated up to 75-90% and 4-O acetylated up to 15-20% (*Figure 7)*.

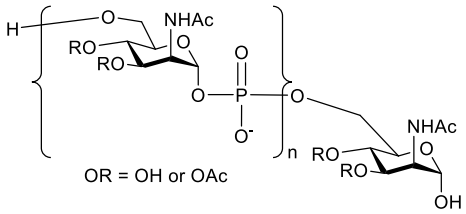

Figure 7. Structure of natural MenA CPS.

In aqueous solution and/or in the presence of specific enzymes, the α-glycosyl phosphodiester bond is unstable, and subject to hydrolysis.

Two different mechanism of hydrolysis are suggested:

- the delocalization of the endocyclic oxygen's lone electron pair to the anomeric carbon (*Figure 8.a*)
- the attack of the carbonyl oxygen of the axially oriented acetamide at C_2 which leads to the formation of a stable oxazoline (*Figure 8.b*)

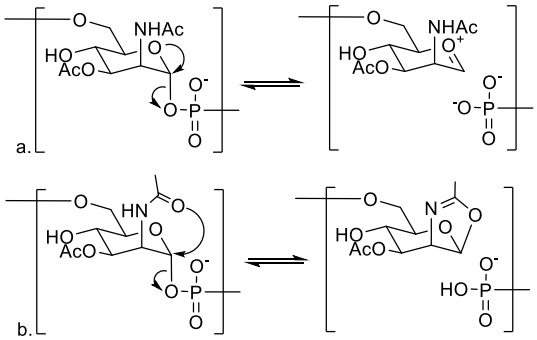

Figure 8. Mechanisms of MenA CPS hydrolysis.

The development of a fully stable MenA vaccine is desirable in order to increase the shelf life and to avoid the use of the cold chain, which represent an additional cost and an organizational problem in particular for the developing countries. Moreover, the possibility to distribute the vaccine in liquid formulation, inside easy to handle classical syringes, would make the administration much easier, reducing the number of specialized personnel required

during the vaccination campaigns and making the vaccine administration faster during the emergency periods.

To obtain a shelf-stable vaccine, a strategy that has been studied in the last years consists in the synthesis of stable analogues of the MenA CPS.

2.1.4 N. meningitidis A CPS structural analogues: state of the art

To increase the stability of the MenA structure, it's necessary to break the acetalic character of the α-glycosyl phosphodiester bond, which represents the key issue for the instability of the structure.

To do so, three different approaches are reported in literature, leading to three different MenA structural analogues, namely carba-analogue, triazolyl-analogue and phosphono-analogue (*Figure9*).

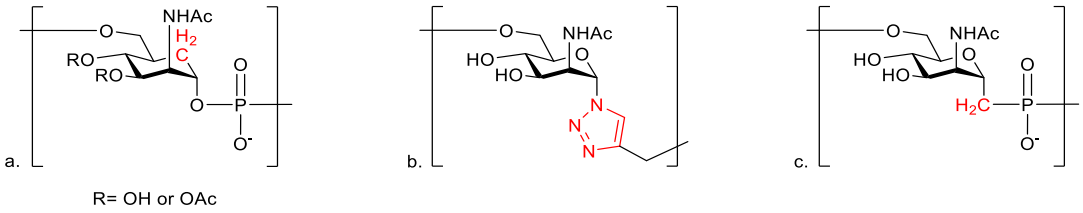

Figure 9. Structure of the repeating units of a) carba-analogue, b) triazolyl-analogue, c) phosphono-analogue

In 2009, Toma et al.[87] published a modelling study with DFT approach on the conformational behaviour of the MenA natural structure, compared to MenA carba and phosphono-analogues. They showed that all the structures' preferred geometry is the pyranose $^4C_1$: for the natural compound, this preference is almost complete, for the phosphono-analogue it is very large and quite large for the carba-analogue. The obtained results had been confirmed by NMR characterization of synthesized compounds, on the base of the comparison between the experimental and theoretical vicinal coupling constants. These results showed that the replacement of the pyranose or the anomeric oxygen with a methylene group does not significantly influence the geometrical properties of the analogues, compared to the natural MenA.

Moreover, the group of Professor Barbero studied the conformational behaviour of carba-analogue and natural MenA monomers through a combination of theoretical calculations and NMR experiments[88]. Despite the carba-analogue showed higher conformational flexibility than the natural structure, their results were consistent with the analogue's capability to act as conformational mimic of the natural structure. Indeed, they showed that one of the analogue existing geometries corresponds to the one of the natural monomer.

MenA Carba-analogue

In Men A carba-analogues (*Figure 9a*) the endocyclic oxygen of mannosamine is replaced by an isosteric methylene group: with this strategy, the acetalic nature of the phosphodiester bond is lost and the analogue gains in stability.

In 2012, the group of professor Lay[7] synthesized short chain length oligomers of c*arba N*-acetylmannosamine α-(1→6) phosphodiester up to the trimer. The carba moiety was created through sigmatropic Claisen rearrangement and the elongation was performed through the hydrogen-phosphonate method. The obtained fragments were conjugated to the carrier protein CRM_{197} and tested through ELISA assays. Only the trimer showed promising results in terms of antigenicity and immunogenicity and, even if the immune response was far lower than the one induced by the natural CPS, it was found a correlation between immune response and chain length.

Longer chains of the carba-analogue glycoconjugate oligomers had been synthetized by Lay's group, up to the octamer (DP8). This structure was able to compete with the natural CPS for binding an anti-MenA functional monoclonal antibody. However, even the octamer showed to be too poorly immunogenic[89].

In 2002, Berry and coworkers[90] showed that the acetylation of the natural MenA CPS structure (75 to 90% at position 3 and up to 20% in position 4) has a fundamental role in its immunogenicity. According to these results, Enotarpi et al[6] published in 2020 the synthesis of the random 3-O and 4-O acetylated DP8 carba-analogue, conjugated to CRM_{197} protein. This new structure showed to be able to elicit high level of anti-MenA antibodies with activity comparable to the one of the existing vaccines.

MenA Triazolyl-analogue

In 2018 Vangala et al.[8] published the first synthesis of a triazolyl-analogue of MenA CPS fragments (*Figure 9b*), in which the labile phosphate bridge of the natural CPS unit was

replaced by a triazolyl group, by the use of click chemistry. The strategy proceeded through the preparation of a 1-azido-N-acetyl mannosamine derivative and its conversion into 1,4-disubstituted 1,2,3-triazole linked mono-, di- and trisaccharide analogues. Unfortunately, no immunogenicity studies have been performed so far.

MenA-Phosphono analogue

The synthesis of the phosphono-analogue (*Figure 9c*) of MenA disaccharide had been reported for the first time by the group of Professor Lay in 2005[4].

In 2007[91], the same authors published the synthesis of the analogue up to the trisaccharide.

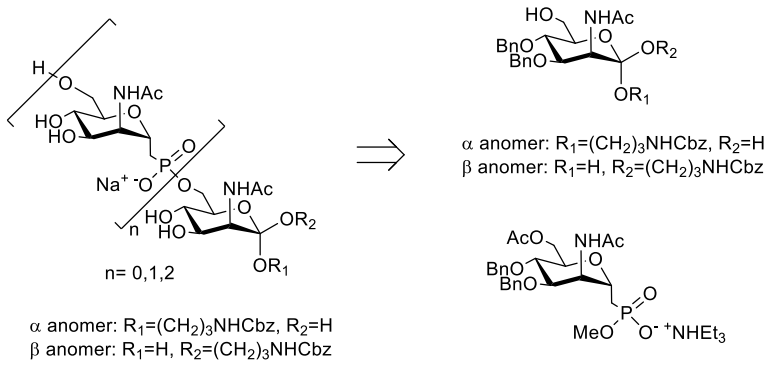

Scheme 1. Retrosynthetic approach to the phosphono-analogue oligosaccharides[4,91]

The synthetic monomer consisted in a mannoside unit, bearing an aminopropyl linker in anomeric position (both in α and β configuration), suitable for protein or nanoparticles conjugation.

In order to achieve the dimer and the trimer, a phosphonate moiety was synthesized.

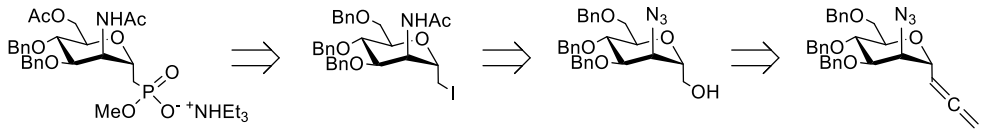

Scheme 2. Lay's retrosynthetic approach to the phosphonate fragment [4,91]

The key steps envisioned by the authors to achieve the phosphonate fragment were the introduction of a C-allenyl group on a masked, protected mannosamine, followed by ozonolysis, substitution of the obtained alcohol with iodine and Arbuzov reaction to give the

phoshonate (*Scheme 2*). Mitsunobu reaction was used to couple the mannoside to the phosphonate fragment to give the dimer and, likewise, to couple the dimer to give the trimer. In 2006, Oscarson *et al.*[92] published an alternative synthesis of phosphono-analogues oligomers up to the tetramer.

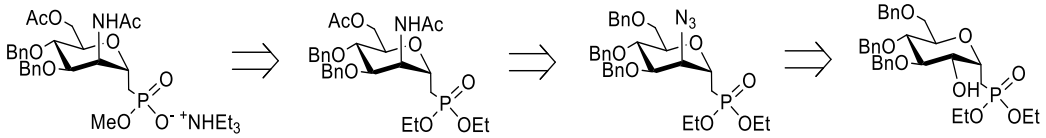

Scheme 3. Oscarson's retrosynthetic approach to the phosphonate fragment[92].

The phosphonate was introduced on a glucose moiety in the first steps of the synthesis as diethyl phosphonodiester by the use of a modified version of the procedure published in 1996 from Casero et al.[93], followed by gluco-manno epimerization through azide introduction, reduction and conversion of the ethyl phosphonodiester to methyl phosphonoester (*Scheme 3*).

Some biological studies have been performed on the phosphono-analogue oligomers. Competitive ELISA studies performed by Lay *et al.*[91] on the oligomers up to the trimer demonstrated that the MenA serum can recognize both the phosphono analogues and the mannoside monomer. Moreover, they showed that the ability of the compounds to compete with the binding of natural MenA polysaccharide to specific antibodies, depends on the chain length of the oligomers but not on the anomeric configuration (*Table 2*).

Substrate	**EC_{50} [mg mL^{-1}]**	**Maximum inhibition [%]***
Natural Men A	$6.6x10^{-6}$	100
Natural Men Y (negative control)	-	-
Trimer (β configuration)	$2.6x10^{-3}$	60
Dimer (β configuration)	$4.0x10^{-3}$	40
Dimer (α configuration)	$2.4x10^{-3}$	40
Monomer (β configuration)	$5.9x10^{-4}$	48
Monomer (α configuration)	$4.9x10^{-3}$	48

*(measured at 10^{-1} mg mL^{-1})

Table 2. Results of competitive ELISA assay by Lay et al. [91].

In 2008, phosphonoester-linked monomer, dimer and trimer were conjugated to gold nanoparticles (AuNPs) by Manea *et al*.[94] attempting to improve their immunogenicity by exploiting multivalent presentation. MenA oligomers conjugated to AuNPs, demonstrated to bind stronger to MenA polyclonal human antibodies than the unconjugated oligomers, showing more than two orders of magnitude higher binding affinity.

In 2015, Fallarini *et al.* conjugated phosphono-analogue monomer, dimer and trimer to the immunogenic carrier protein HSA[95] and they tested them for their ability to induce immune response *in vitro* and *in vivo*. They showed that the conjugates were able to induce *in vitro* T cell activation and IgG production *in vivo*. They moreover noticed that the loading of the sugar (*i.e.*, the sugar-protein ratio) seemed to be important for B cell activation (with half loading giving better results when compared to the full sugar loading compounds), while the oligomers chain length does not appear relevant for the anti-MenA titres. In addition, they observed interesting results regarding the unconjugated disaccharide: due to its zwitterionic nature (with a positive charge on the amino-linker and a negative charge on the phosphonate), the disaccharide showed to be able to trigger *in vitro* T cell activation, even if the same compound was not capable of inducing anti-MenA IgG antibodies *in vivo*.

2.2 Aim of the project

Despite MenA infections drastically decreased in the last years thanks to the introduction of new glycoconjugate vaccines (especially MenAfriVac), the WHO highlights the importance of persisting with a strict vaccination schedule.

Since the shelf-life of MenA vaccines is significantly reduced by the instability of MenA CPS, the production of a more stable vaccine is object of interest; indeed, this could lead not only to the production of a long-lasting vaccine, but it could also make possible to distribute the vaccine in fully liquid formulation, which is more convenient in comparison to the current lyophilized form. In order to increase CPS and consequently vaccine's stability, three different analogues had been synthetized: the carba-, the triazolyl- and the phosphono-analogue.

Focusing on the phosphono-analogue, interesting results had been obtained, showing that these compounds are able to induce *in vitro* T cell activation and IgG production *in vivo*. However, they revealed to be poorly immunogenic, when compared to the vaccines currently licenced.

To move to the production of more immunogenic compounds, the studies of Berry and coworkers[90] could be crucial. Indeed, they demonstrated the important role of the O-acetylation pattern in MenA CPS for its immunogenicity. Furthermore, a recent study published in 2020 by Henriques et al.[96], identified MenA's epitope as the trisaccharide, anchoring the antibody via the O- and N-acetyl groups through CH-π or H-bonding interactions. Moreover, their in-silico docking studies showed the importance of the 3-O acetylation of the upstream fragment for antibody binding, while, regarding the other two residues, the O-acetyl moiety could be equally accommodated in position 3 or 4.

For this reason, this project deals with the synthesis of 3-O acetylated phosphono-analogues up to the trimer (*Figure 10*), containing a C-3 amino linker which could be used for the conjugation to an immunogenic carrier protein as well as for the conjugation to AuNPs.

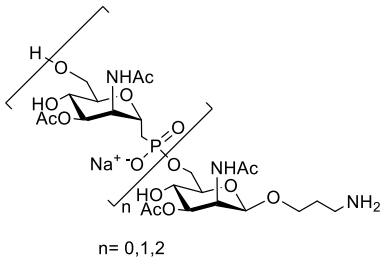

Figure 10. Structure of the synthetic targets.

The biological activity of the produced glycoconjugate will be tested to understand whether the acetylated analogues are suitable for the development of a glycoconjugate vaccine targeting MenA.

2.3 Results and discussion

2.3.1 Retrosynthetic approach

Despite the structural similarities between our target molecules and the non-acetylated structures published in 2005 and 2007 by the group of Prof. Lay[4,91], the need to selectively introduce an acetyl group in position 3 of each unit required important changes in the synthetic strategy. However, similar building blocks have been identified: a mannoside and a phosphonate, which could be coupled via Mitsunobu reaction to provide the target dimer and trimer.

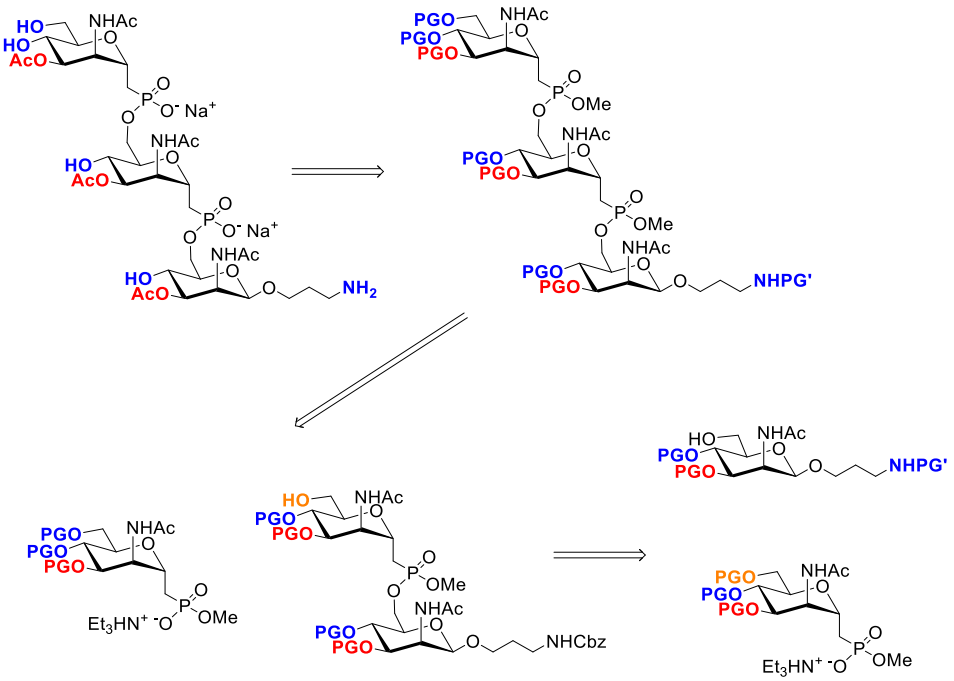

Scheme 4. Retrosynthetic approach to the dimer and the trimer.

The choice of the correct protective groups, both on the mannoside and on the phosphonate moieties, was crucial.

The groups coloured in blue must be permanent protecting groups: they need to be stable during all the synthesis, to be cleaved in the last step (*Scheme 4*).

Position 3 of all residues (in red) must be functionalized with an acetyl group or protected by a temporary protective group, which is selectively removed to be replaced by the acetyl

ester.

Moreover, the group coloured in orange must be orthogonal to all the others, making it possible its selective cleavage after the first coupling reaction to perform chain elongation.

*Figure 11. Structure of the designed mannoside (**1**) and phosphonate (**2**) fragments.*

Mannoside **1** (*Figure 11*) was designed with benzyl and benzyloxycarbonyl (Cbz) as permanent protective groups for the hydroxyl and the amino groups respectively, while 3-OH was acetylated.

Regarding the phosphonate fragment, in our first approach, position 3 was functionalized with an acetyl group and positions 4 and 6 were protected with a benzylidene acetal (*Figure 11*). The benzylidene protective group was chosen for its versatility: it could be removed by hydrogenolysis in the last step of the synthetic sequence, together with benzyls and Cbz, or it could be selectively opened to deliver 6-OH to allow chain elongation.

2.3.2 Synthesis of the mannoside fragment

The synthesis of mannoside **1** was already settled in our group.

The first step was the glycosylation of N-Cbz protected amino propanol with the commercially available glucose penta-acetate (*Scheme 5*). The reaction, performed using $BF_3{\cdot}Et_2O$ as a Lewis acid[97], led to the formation of a complex mixture, containing the desired product, its α isomer and the 2-O deacetylated products, together with unreacted starting material.

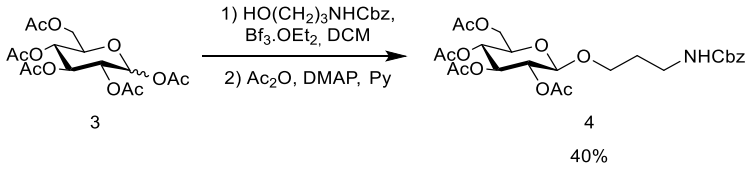

Scheme 5. Introduction of the N-Cbz protected aminopropyl linker

In order to facilitate the purification of the desired compound, it was decided to acetylate the crude. After acetylation, product **4** could be isolated in 40% yield.

Compound **4** was deacetylated under Zemplen conditions and selectively protected in positions 4 and 6 with a benzylidene acetal, giving diol **5** in 70% yield (*Scheme 6*).

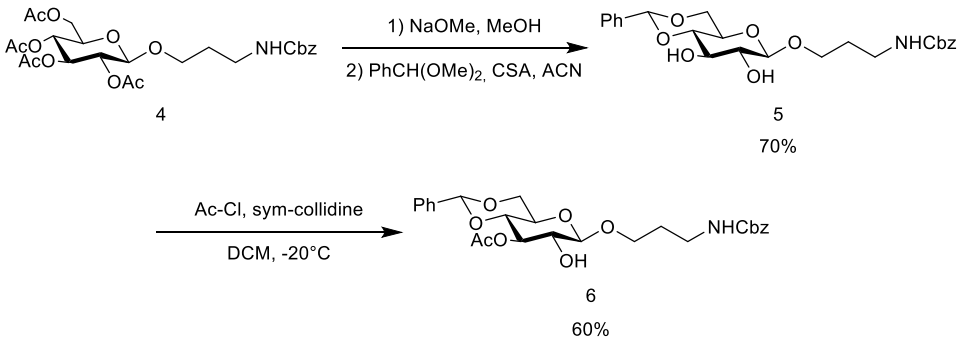

*Scheme 6. Synthesis of intermediate **6***

Regioselective acetylation was carried out to functionalize position 3. A protocol described in the literature[98], involving a hindered amine (sym-collidine) as a base and acetyl chloride as acylating agent, was used. The reaction proceeded in 60% yield, with the formation of a small amount of 2-O acetylated product (<5%) and around 20% of the 2,3-diacetylated glucoside, together with <20% of unreacted starting material. The by-products could be deacetylated and the selective acetylation reaction repeated, leading to an overall yield of 80% over three steps (acetylation-deacetylation-acetylation).

The free hydroxyl group in position 2 of compound **6** was then activated as a triflate, a good leaving group for a S_N2 substitution. After reaction with sodium azide and subsequent inversion of configuration from the *gluco*- to *manno*- form, mannoside **7** was isolated in 84% yield over two steps (*Scheme 7*). The C-2 inversion of configuration was confirmed by NMR (change of $J_{1,2}$ from 7.7 Hz to 3.7 Hz), while the presence of the azide was confirmed by IR (stretching signal at 2106 cm^{-1}).

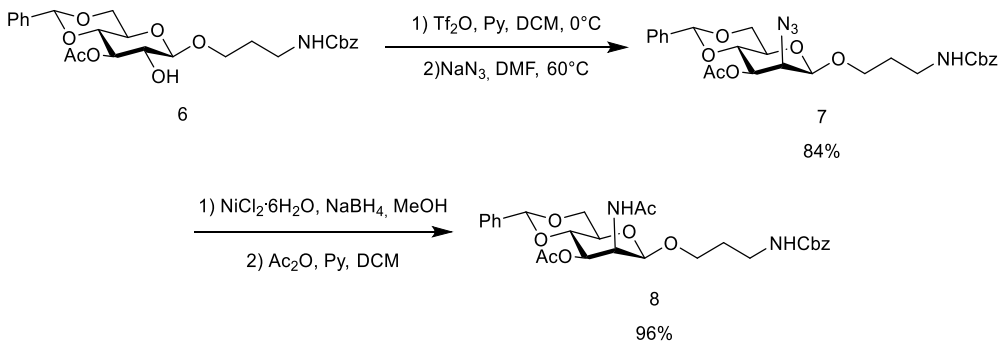

*Scheme 7. Synthesis of intermediate **8***

Azide reduction led to the formation of a mixture of the desired 3-OAc mannosamine **8** and 3-OH N-acetyl mannosamine, produced by the migration of the acetyl group from the position 3 to the free amine. After acetylation of the crude, compound **8** was isolated in 96% yield.

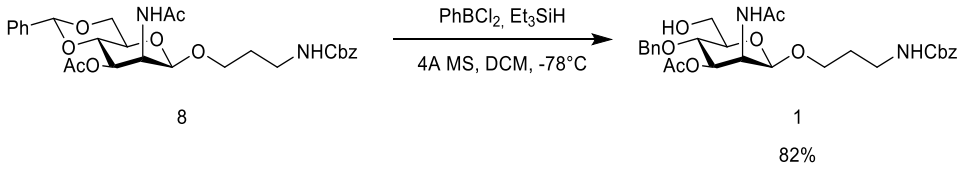

*Scheme 8. Synthesis of mannoside fragment **1***

The benzylidene ring was eventually opened using $PhBCl_2$ as Lewis acid and Et_3SiH as reducing agent at -78°C in rigorously dry conditions, giving mannoside **1** in 82% yield with high regioselectivity (*Scheme 8*).

2.3.3 First approach to the synthesis of the phosphonate fragment

Starting from commercially available methyl α-D-glucopyranoside, compound **13** was achieved through a four steps reaction sequence followed by a single purification step (*Scheme 9*).

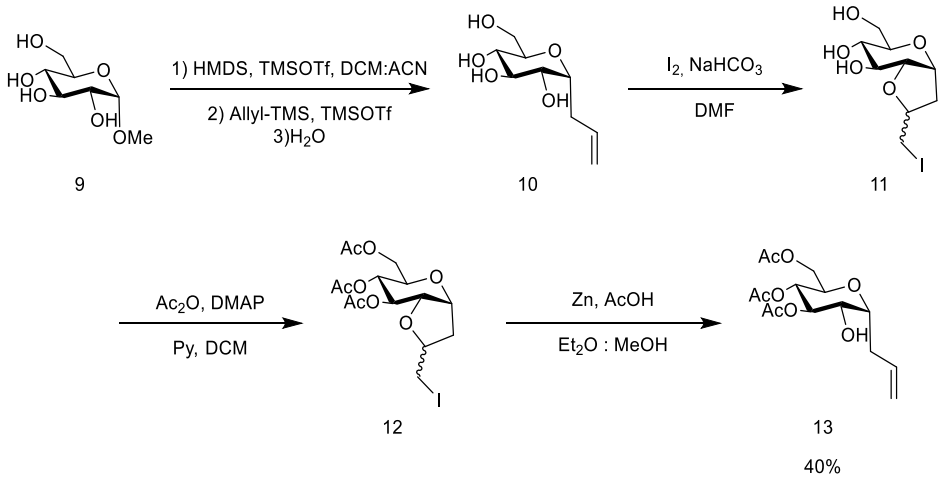

*Scheme 9. Synthesis of intermediate **13***

The first reaction consisted in the one-pot O-silylation[99] of the starting material, followed by 1-C-allylation and silyl ethers cleavage[100]. The reaction proceeded with high selectivity for the product in α configuration **10**. Iodocyclization was then carried out in order to selectively protect the hydroxyl group in position 2, leading to the formation of the bicyclic compound **11** as a mixture of diastereomers, whose acetylation followed by reductive elimination and consequent cycle opening, allowed to obtain compound **13** in 40% overall yield.

The free hydroxyl group in position 2 of **13** was converted into a good leaving group by treatment with triflic anhydride. Due to the high tendency of the triflate to undergo elimination, it was necessary to work at low temperatures and to immediately perform the next step, involving nucleophilic substitution reaction with sodium azide. The use of 15-crown-5 to increase N_3^- ion nucleophilicity by coordinating Na^+ counter-ion resulted to be crucial to obtain compound **14** in good yields. The S_N2 type reaction led to the desired change of configuration from *gluco-* to *manno-* form (*Scheme 10*).

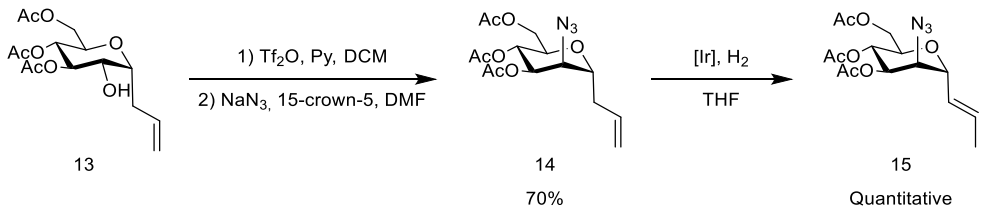

*Scheme 10. Synthesis of intermediate **15***

The introduction of azide and the change of configuration were confirmed through NMR and IR spectroscopy (presence of the stretching signal at 2094 cm^{-1}). Derivative **14** was obtained in 70% yield.

The allyl to propenyl isomerization was carried out using 0.1 eq. of (1,5-cyclooctadiene) bis(methyldiphenylphosphine)Iriudim(I) hexafluorophospate catalyst ([Ir])[101]. The reaction led to isomer **15** in quantitative yields (*Scheme 10*).

Intermediate **15** was deacetylated under Zemplen conditions and positions 4 and 6 regioselectively protected as benzylidene acetal, giving compound **16** in 70% yield.

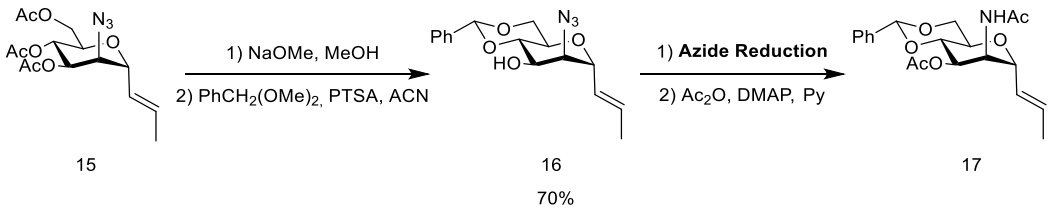

15 16 17

70%

*Scheme 11. Synthesis of intermediate **17***

Azide reduction, followed by acetylation of both the free amine and 3-OH led to compound **17** (*Scheme 11*). Different conditions were screened for the reduction of the azide (*Table 3*).

Entry	Reduction conditions	Yield*
1	Zn, Ac_2O, AcOH, THF	40%
2	1)PPh_3, THF; 2) H_2O	60%
3	PDT, DIPEA, MeOH	94%

*After acetylation

Table 3. Screening of different conditions for azide reduction

The best yield was achieved by using 1,3-propandithiol (PDT) as reducing agent (*Entry 3*).

With compound **17** in our hands, we decided to focus on the optimization of the previous reaction steps in order to make it possible the production of intermediate **17** on a larger scale.

In particular, the high cost of the [Ir] catalyst used for isomerization prompted us to explore alternative strategies. Pd(II) catalysts (Pd(II) chloride diacetonitrile complex and $PdCl_2$) have been screened. Despite different reaction conditions were tested, no starting material conversion was observed. Therefore, it was decided to go back to compound **14** and modify the reaction sequence in order to study the best isomerization conditions on a more advanced substrate (*Scheme 12*).

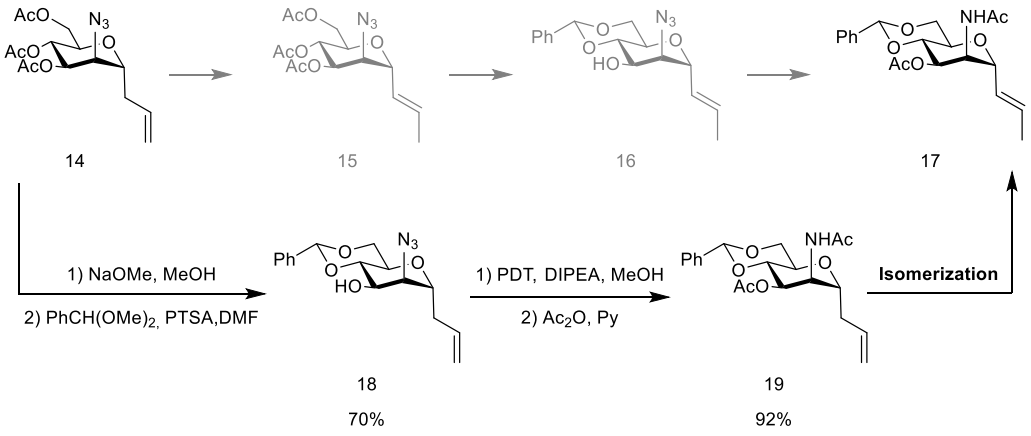

*Scheme 12. Alternative strategy towards intermediate **17***

Hence, we proceeded with deacetylation of compound **14**, followed by benzylidene introduction, azide reduction and acetylation to give acetamide **19**.

Different allyl isomerization conditions have been screened using **19** as starting material (*Table 4*).

Entry	Catalyst	Solvent	Temperature	Reaction time	Yield
1	$PdCl_2$ (0.2 eq.)	THF	Reflux	48h	15%
2	$PdCl_2$ (0.1 eq.)	Toluene	Reflux	48h	33%
3	$PdCl_2$ (0.2 eq.)	Toluene	Reflux	48h	35%
4	Pd(II) chloride diacetonitrile complex (0.05 eq.)	Toluene	Reflux	24h	35%

Entry	Catalyst	Solvent	Temperature	Reaction time	Yield
5	Pd(II) chloride diacetonitrile complex (0.1 eq.)	Toluene	Reflux	72h	40%
6	[Ir] (0.1 eq.)	THF	RT	1h	Quant.

Table 4. Screening of different conditions for allyl group isomerization

Even if the use of Pd(II) chloride diacetonitrile complex as catalysts led to the desired isomerization reaction with yields up to 40% (*Entry 5*), separation of isomers **17** and **19** resulted to be challenging. Therefore, the use of the iridium catalyst resulted once again the best option for this reaction.

The achieved propenyl C-glycoside **17** was subjected to oxidative cleavage, followed by aldehyde reduction (*Scheme 12*). Several reaction conditions were screened (*Table 5*).

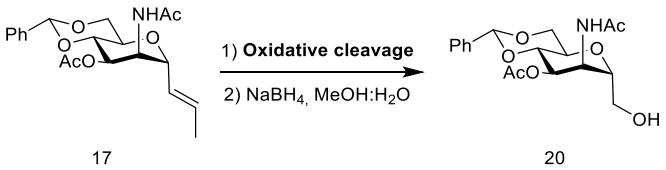

17 20

Scheme 12. Propenyl C-glycoside oxidative cleavage and reduction

Entry	Reagents	Solvent	Temperature	Yield
1[102]	1) OsO_4, TMAO 2) $NaIO_4$	1) DCM 2) THF : phosphate buffer	RT	30%
2[103]	$RuCl_3$, $NaIO_4$	ACN : H_2O 6:1	RT	25%
3[104]	$KMnO_4$, alumina	DCM : H_2O 50:1	RT	N.R.
4[102]	1) OsO_4, TMAO; 2) Na_2CO_3, $Pb(OAc)_4$	1) DCM 2) Chloroform	RT	N.R.
5	O_3	DCM	-78°C	60%
6	O_3, Me_2S	DCM	-78°C	50%

Table 5. Screening of oxidative cleavage conditions

Ozonolysis reaction (*Entry 5*), which resulted to be the most efficient method among the ones screened, led to the desired compound **20** in 60% yield.

Alcohol 20 was activated as a mesylate and reacted with sodium iodide to give compound **22** (*Scheme 13*).

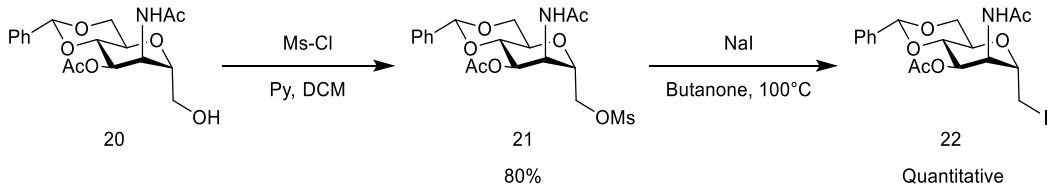

*Scheme 13. Conversion of alcohol **20** into iodide **22***

Different approaches were screened for phosphonate synthesis (*Scheme 14*), starting from both alcohol **20** and iodide **22** (*Table 6*).

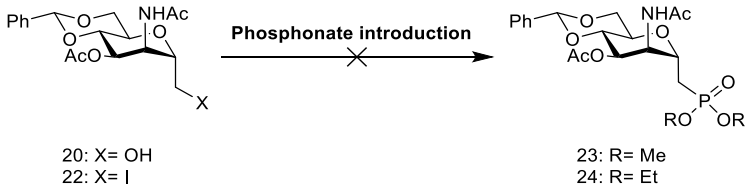

Scheme 14. Approaches to phosphonate synthesis

Entry	X	R	Conditions	Yield
1	I	Me	$P(OMe)_3$, 100°C, 300 mmHg	N.R.
2	I	Me	$P(OMe)_3$, 120°C, 300 mmHg	N.R.
3[105]	I	Me	$PH(OMe)_2$, Cs_2CO_3, DMF	N.R.
4[106]	OH	Me	$P(OMe)_3$, TBAI, 100°C	N.R.
5[106]	OH	Et	$P(OEt)_3$, TBAI, 100°C	N.R.

Table 6. Screening of different conditions for the synthesis of the phosphonate

Our first approach consisted in the conversion of iodide **22** into phosphonate **23** through Arbuzov reaction. However, no reaction was observed at 100°C (*Entry 1*), even after long reaction time, while only degradation products were observed at higher temperatures (*Entry 2*).

Treatment of alcohol **22** under Michaelis-Arbuzov conditions (*Entry 4*), led to full conversion of the starting material into by-product **25** (*Scheme 15*).

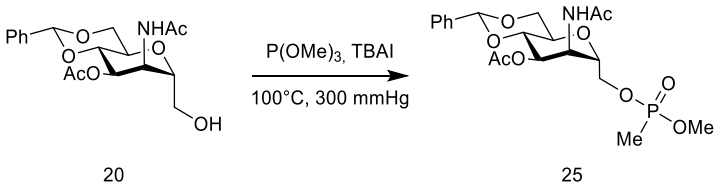

20 25

*Scheme 15. Conversion of intermediate **20** into by-product **25***

Indeed, the attack of the iodide anion on the methyl group is extremely favoured compared to the one on the secondary carbon of the sugar, leading to the formation of the undesired by-product **25** (*Scheme 16)*.

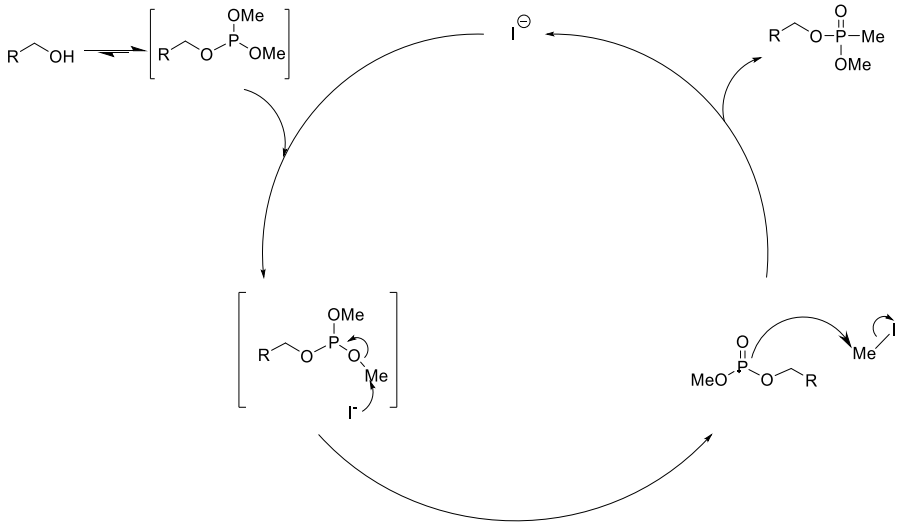

*Scheme 16. Mechanism of conversion of **22** into by-product **25***

The same reaction was performed with $P(OEt)_3$ instead of $P(OMe)_3$, assuming that the attack of the iodide ion to the secondary carbon of the sugar could be competitive with the one on the secondary carbon of the ethyl phosphite. However, only the undesired isomer was obtained.

We did not try the reaction of substrate **22** with $P(OiPr)_3$, even if the attack of iodide anion to a tertiary carbon should be very unlikely, as the subsequent selective monohydrolysis of the isopropyl phosphodiester was expected to be highly problematic.

While the formation of the undesired isomer **25** was rather predictable, the lack of reactivity of substrate **22** under classical Arbuzov conditions was completely unexpected.

Indeed, the same reaction, performed on a similar substrate (**26**)[4], proceeded in good yields (*Scheme 17*).

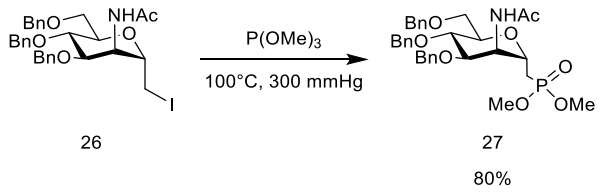

*Scheme 17. Synthesis of phosphonate **27***

The lack of reactivity of compound **22** was attributed to the high conformational rigidity of the bicyclic system, due to the presence of the benzylidene acetal. Accordingly, it was necessary to change protective groups in positions 4 and 6.

2.3.4 Second approach to the synthesis of the phosphonate fragment

Phosphonate **28** (*Figure 12*), in which positions 4 and 6 were protected as benzyl ethers, was chosen as upstream fragment for its similarity to **27**.

However, position 6 cannot be selectively deprotected, making **28** unsuitable for the synthesis of the trimer. Therefore, phosphonate **29** (*Figure 12*) was selected as elongation fragment, in which position 6 is protected with an orthogonal protective group, such as a silyl ether.

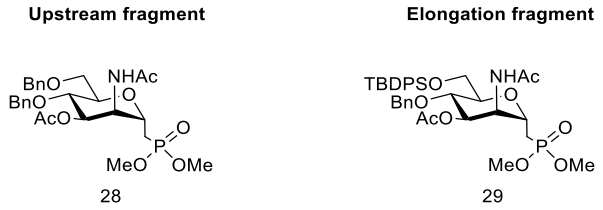

*Figure 12. Upstream (**28**) and elongation (**29**) phosphonate fragments.*

In order to achieve compounds **28** and **29**, we proceeded through acetylation, benzylidene reductive opening and subsequent benzylation of the previously synthesized intermediate **18** (*Scheme 18*).

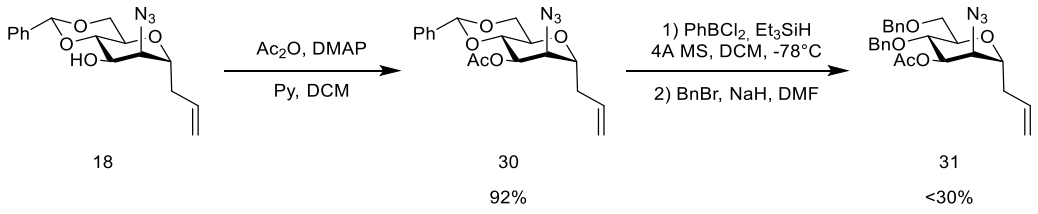

*Scheme 18. Synthesis of intermediate **31***

Unfortunately, **31** was never isolated as a pure compound. A mixture of 3-, 4-, and 6-O acetylated, di-benzylated and 3, 4, 6-tri-benzylated compounds was obtained, due to acetyl group migration. To avoid migration, it was decided to replace the acetyl group in position 3 with a temporary protective group such as p-methoxybenzyl ether (PMB).

Starting from intermediate **18**, position 3 was protected as PMB ether. The use of TBAI revealed to be crucial for the success of the etherification reaction. Indeed, no conversion was observed without its addition to the reaction mixture. The benzylidene acetal of **32** was then opened and the crude was benzylated, leading to compound **33** in 50% yield over two steps (*Scheme 19*).

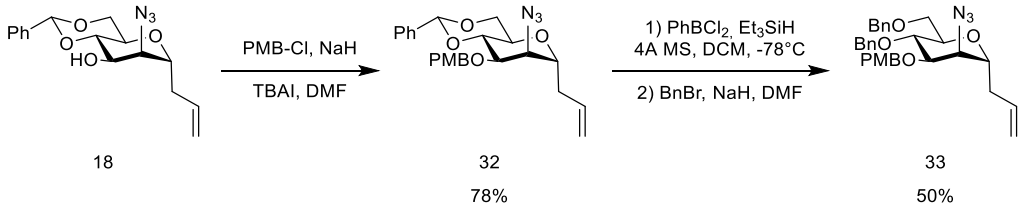

18 32 78% 33 50%

*Scheme 19. Synthesis of intermediate **33***

The low yield of compound **33** could be attributed to the low stability of PMB- group in acidic conditions. Therefore, non-acidic reaction conditions have been tested, using DIBAL-H as reducing agent. Despite the selectivity of the reaction resulted to be very high, without the detection of any by-product, the conversion of the starting material was poor, with more than 70% of recovered starting material even after long reaction time (up to 48 hours) and with the use of 10 equivalents of reducing agent.

Further conditions for benzylidene deprotection (*Scheme 20*), which led to the full hydrolysis of the acetal, were screened (*Table 7*).

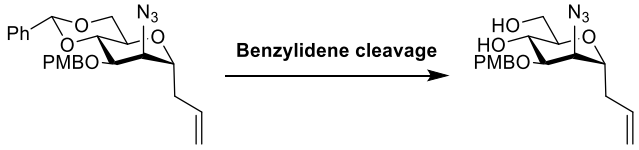

32 34

Scheme 20. Benzylidene cleavage.

Entry	Conditions	Yield
1	80%aq AcOH, 80°C	Up to 90%
2	EtSH, PTSA, DCM	70%

Table 7. Benzylidene acetal cleavage conditions.

Although the best yield was achieved by the treatment of **32** with acetic acid (*Entry 1*), the method revealed to be poorly reproducible, with yields ranging from 30 to 90%. For this

reason, the more reliable reaction with ethanthiol and PTSA as acid catalyst was preferred (*Entry 2*).

Compound **34** was used as common intermediate in the synthesis of both upstream and elongation phosphonate fragments (**28** and **29**).

Synthesis of the upstream fragment

For the synthesis of the upstream phosphonate **28**, compound **34** was di-benzylated and the azide group was reduced and acetylated to give acetamide **35**. Allyl isomerization, oxidative cleavage and reduction gave alcohol **37**.

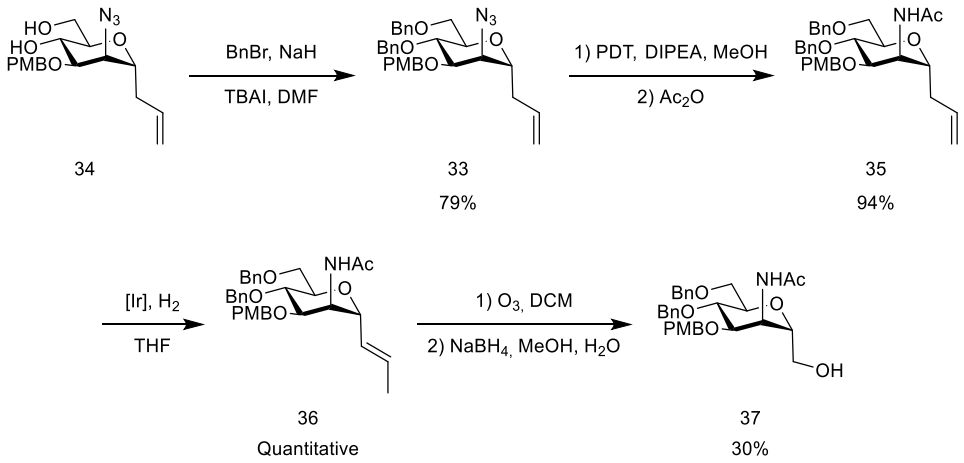

*Scheme 21. Synthesis of intermediate **37***

The oxidative cleavage, carried out following the synthetic protocol described above, led to the desired product **37** in low yield, probably due to the high polarity of the starting material (*Scheme 21*). Accordingly, it was decided to perform isomerization and ozonolysis reactions on substrate **33** by postponing the conversion of the azido group into acetamide **37** to a later stage of the synthesis (*Scheme 22*).

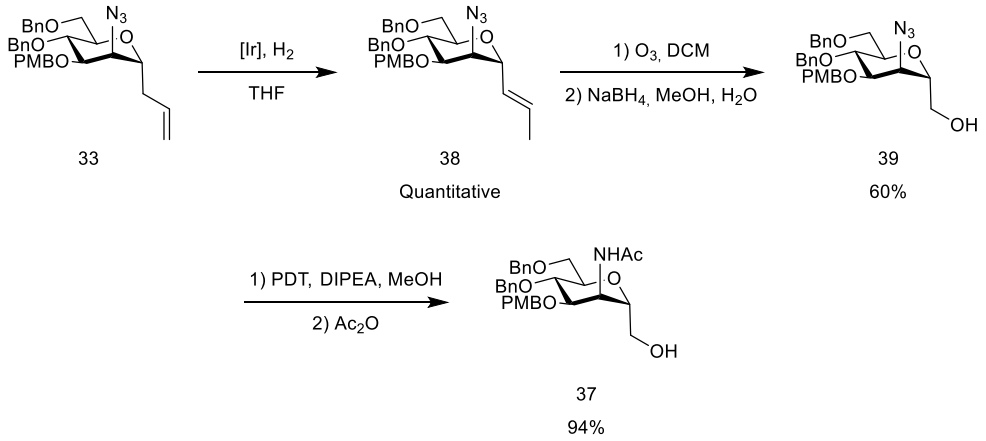

*Scheme 22. Alternative synthesis of intermediate **37***

This strategy allowed to improve the yield of the oxidative cleavage reaction from 30% to 60%.

The next steps toward the synthesis of the desired phosphonate were the activation of the primary hydroxyl group as a mesylate and its conversion into iodide **41**, used as substrate for the following Arbuzov reaction.

As expected, compound **41** showed a reactivity similar to the 3-O benzylated model substrate **26**, leading to phosphonate **42** in good yields.

PMB removal was achieved by the treatment with 2,3-Dichloro-5,6-dicyano-p-benzoquinone (DDQ) in a H_2O/DCM mixture, followed by acetylation of the obtained free hydroxyl group in position 3 to give **44**, which was eventually subjected to selective monohydrolysis to afford the desired upstream fragment **45** (*Scheme 23*).

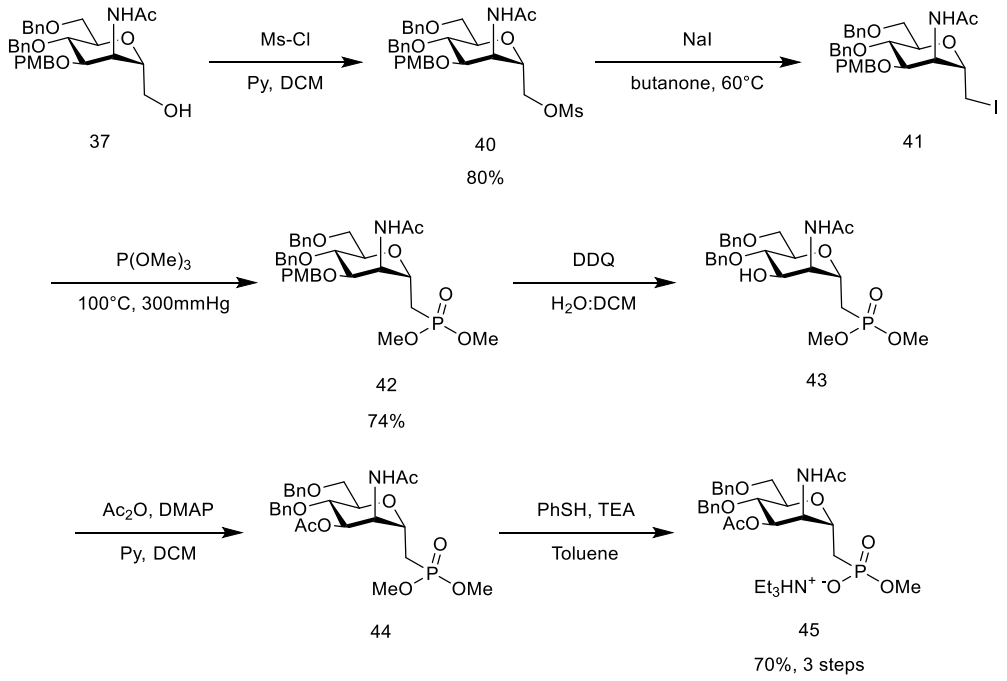

*Scheme 23. Synthesis of phosphonate upstream fragment**45***

It was decided to synthesize also the 3-O-PMB protected phosphonate fragment **46** through selective monohydrolysis of the phosphonoester **42** (*Scheme 24*).

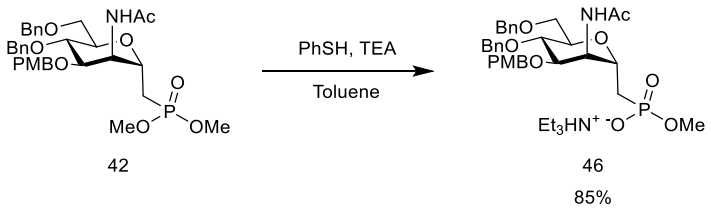

*Scheme 24. Synthesis of alternative phosphonate upstream fragment **46***

Synthesis of the elongation fragment

Intermediate **34** was used as a starting material for the synthesis of the elongation fragment. Selective protection of the primary hydroxyl group was achieved using the sterically hindered tert-butyldiphenylsilyl chloride to give alcohol **47**, which was 4-O-benzylated to furnish **48** in 77% yield over two steps (*Scheme 25*).

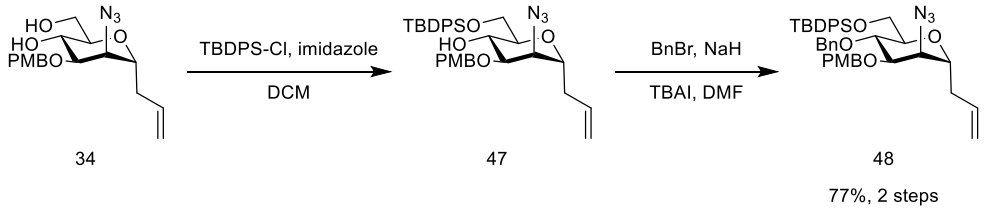

*Scheme 25. Synthesis of intermediate **48***

Intermediate **48** was then converted into the desired phosphonate **55** using the same synthetic approach reported for the synthesis of the upstream fragment (*Scheme 26*).

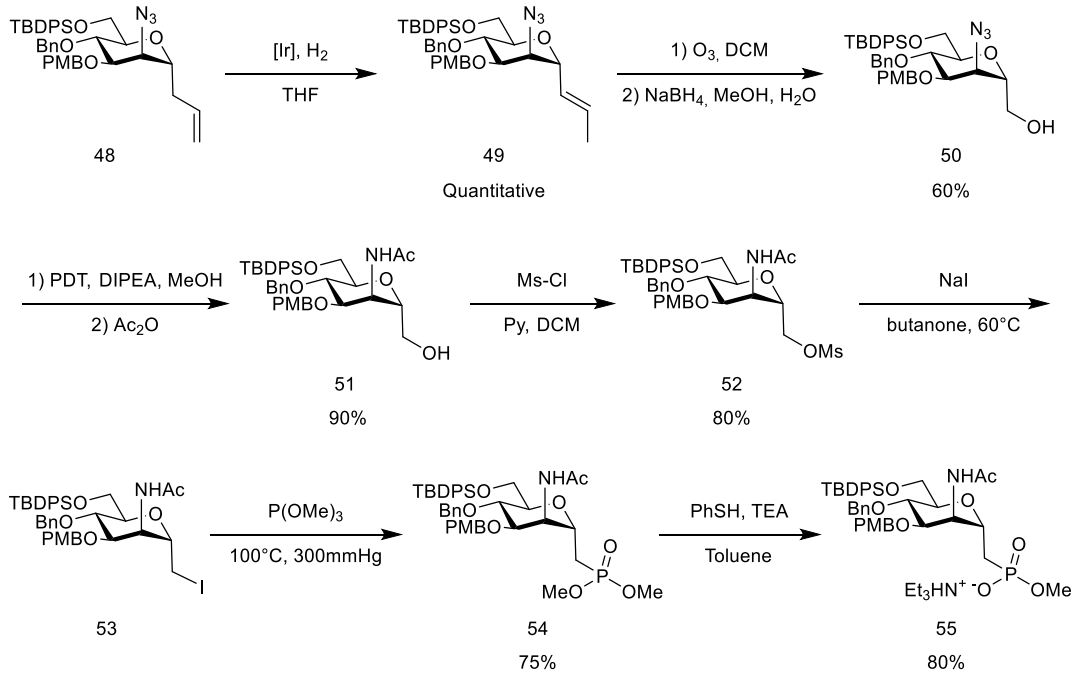

*Scheme 26. Synthesis of phosphonate elongation fragment **55***

Compound **55** was obtained in 26% yield over 7 steps.

2.3.5 Synthesis of the dimer

Having both the mannoside and the phosphonate fragments in our hands, the two phosphonate building blocks **45** and **46** were coupled to the mannoside fragment **1** under classical Mitsunobu conditions, as previously reported for the synthesis of the non-acetylated phosphono-analogues[4].

The 3-OAc phosphonate **45** was coupled to compound **1** to give phosphono-disaccharide **56** in 45% yield (*Scheme 27*).

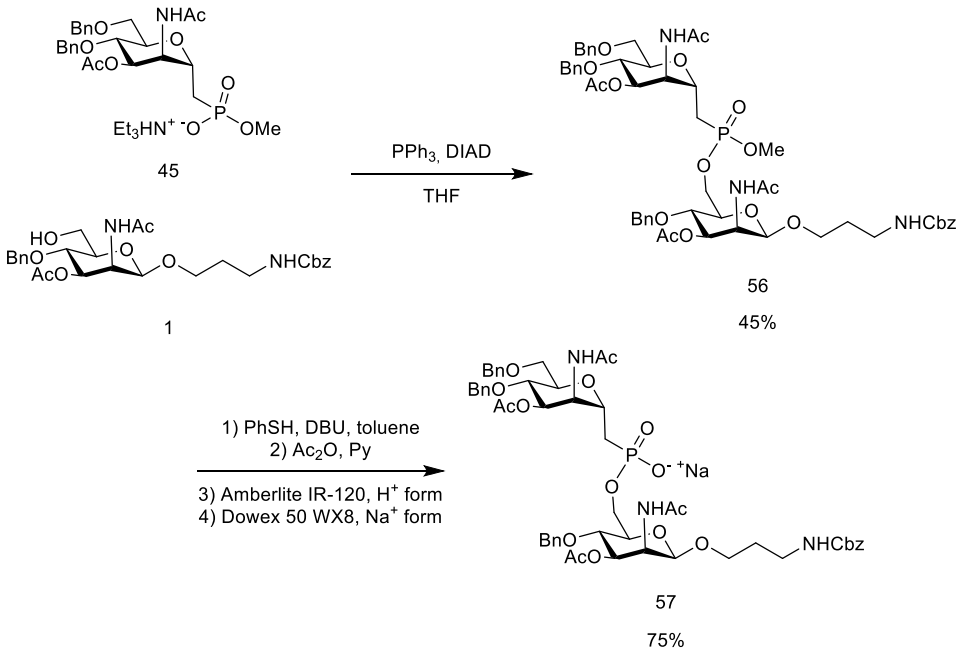

*Scheme 27. Synthesis of dimer **57***

Phosphonate monohydrolysis was carried out under the conditions reported for the synthesis of the non-acetylated phosphono-analogue[4]. However, due to the alkaline conditions required, partial 3-O-deacetylation was observed, making it necessary to carry out acetylation of the crude. The following purification and double ion exchange gave the sodium salt **57** in 75% yield (*Scheme 27*). Moreover, it was observed that treatment of **56** with PhSH and TEA instead of DBU as a base prevented 3-O-deacetylation, giving the desired compound **57** in 75% yield without the need of the additional acetylation step (*Scheme 28*).

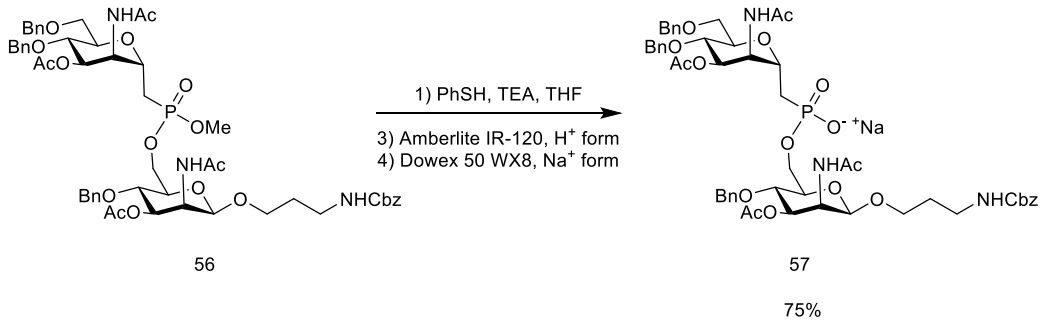

Scheme 28. Selective phosphonate monohydrolysis

Disaccharide **57** was also synthesized starting from the 3-O-PMB protected phosphonate **46** and mannoside **1**. First, the Mitsunobu reaction led to disaccharide **58** in 70% yield. The oxidative cleavage of the PMB group, followed by phosphonoester hydrolysis, acetylation and ion exchange provided phosphonodisaccharide **57** in 78% yield over three steps (*Scheme 29*).

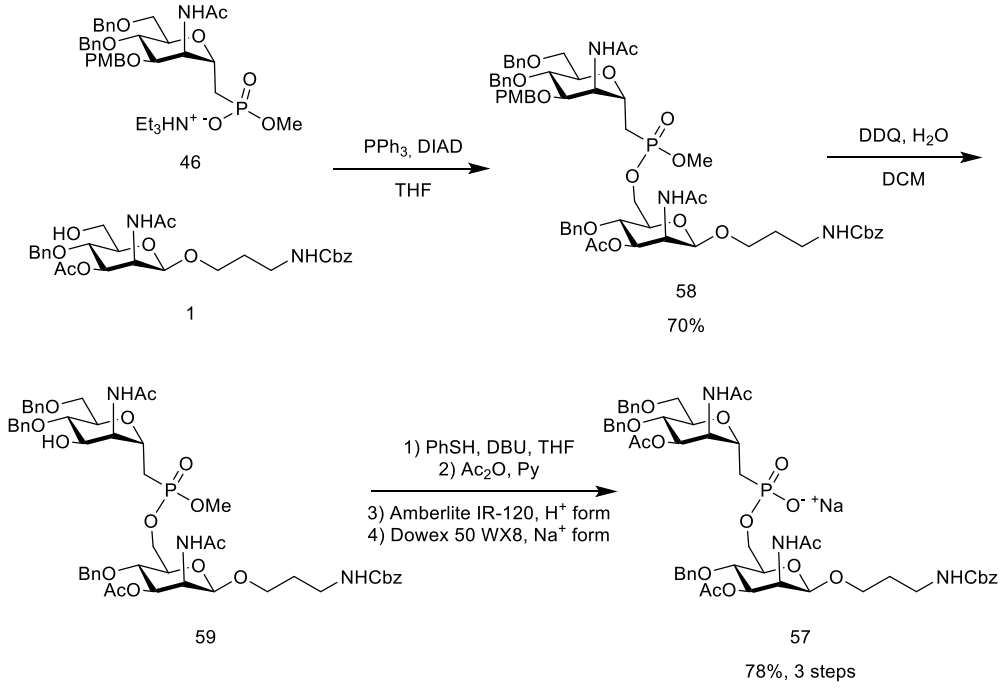

*Scheme 29. Alternative synthesis of dimer **57***

2.3.6 Synthesis of the trimer

To achieve the target trimer, a dimer containing the elongation fragment was synthesized in the same conditions described before, starting from phosphonate **55** and mannoside **1**. First, the Mitsunobu coupling gave phosphonodisaccharide **60** in 76% yield. The silyl ether was then cleaved with TBAF to afford the 6-O-deprotected dimer **61** in 94% yield (*Scheme 30*).

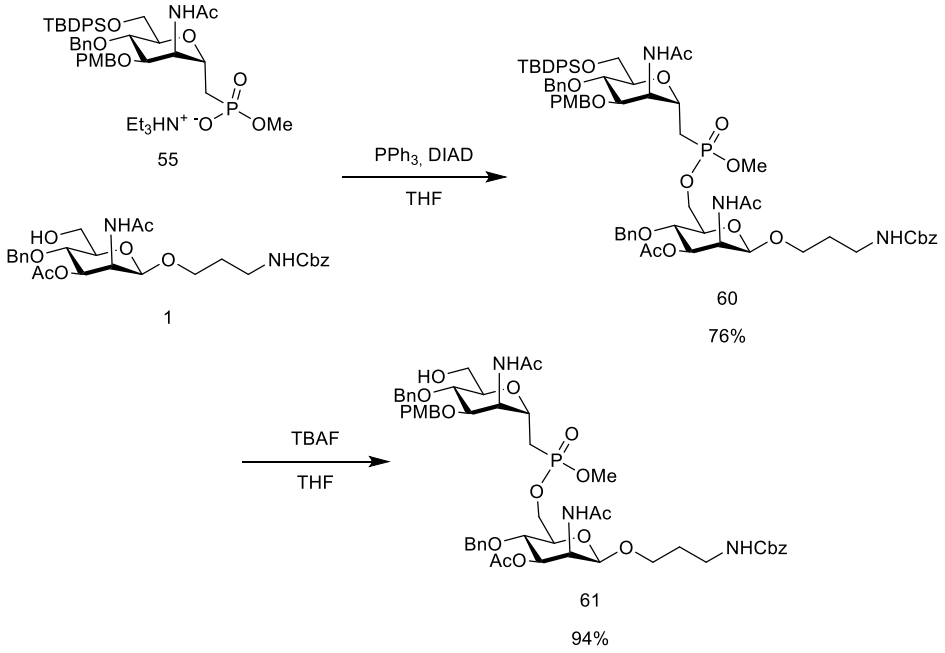

*Scheme 30. Synthesis of dimer **61***

The subsequent Mitsunobu coupling with phosphonate **46** led to trimer **62** in 64% yield (*Scheme 31*).

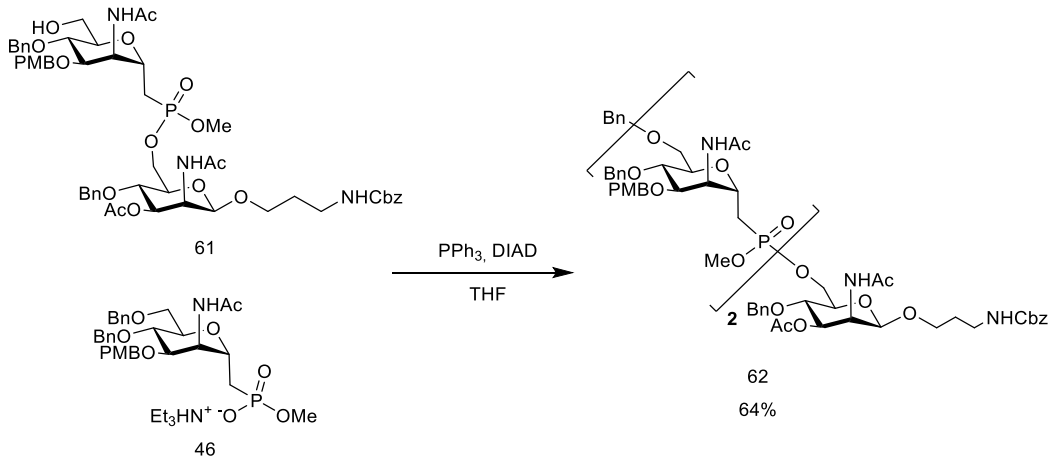

*Scheme 31. Synthesis of trimer **62***

The deprotection sequence, including PMB cleavage, phosphonoester hydrolysis and 3-O acetylation, followed by ionic exchange was expected to give trimer **65** as sodium salt (*Scheme 32*).

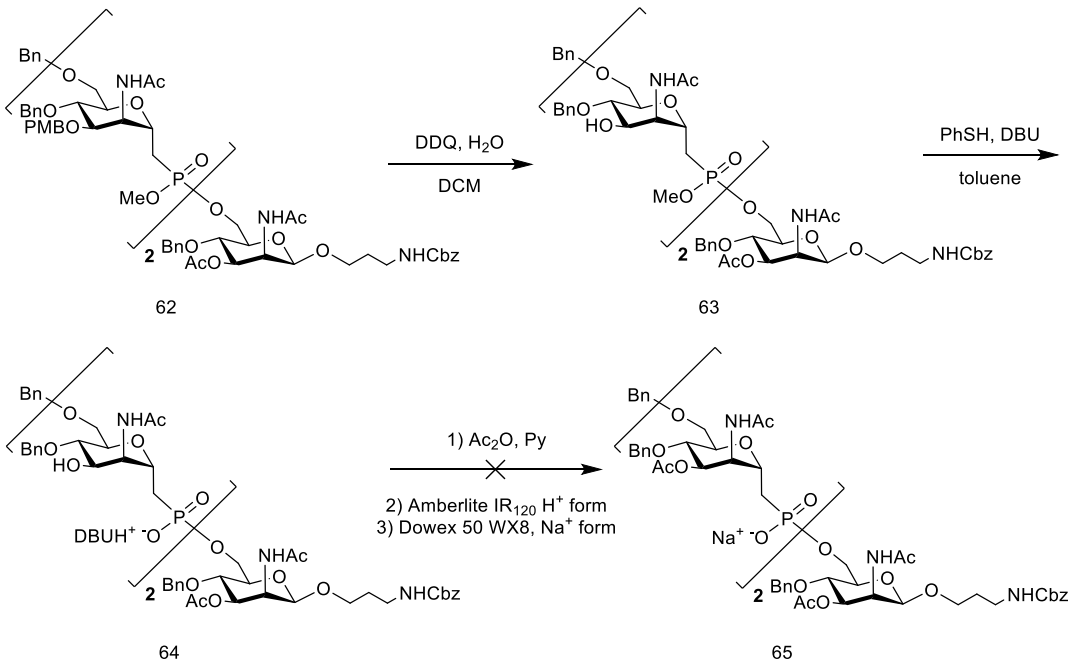

*Scheme 32. Approaches towards trimer **65***

However, the NMR analysis of the product obtained after acetylation showed unexpected signals probably due to the formation of the mixed aceto-phosphonic anhydride.
In order to achieve the desired compound **65**, acetylation was performed right after PMB removal, followed by phosphonate hydrolysis. In the latter step, to avoid the deprotection of the acetyl groups in position 3 observed in the synthesis of the disaccharide (*Chapter 2.3.5*), TEA was used as a base instead of DBU (*Scheme 33*).

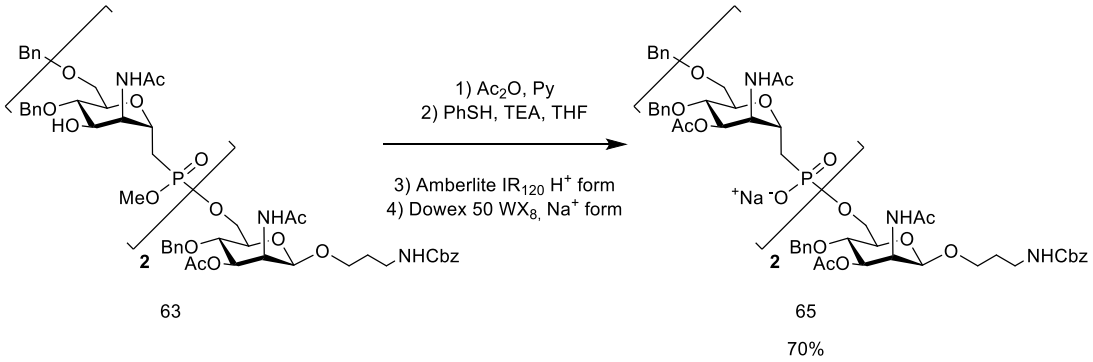

*Scheme 33. Effective synthesis of trimer **65***

Purification of crude **65** is currently in progress.

2.3.7 Towards synthesis optimization

Due to the high number of steps needed to achieve the desired disaccharide and trisaccharide, and in particular to obtain the phosphonate fragments, some alternative strategies have been screened to optimize the synthesis.

First strategy

The first strategy involved the protection of positions 4 and 6 in the early stages of the synthesis. 1–C-allylation was performed on α-methyl-D-glucopyranoside leading to compound **10**, and positions 4 and 6 were protected as a benzylidene acetal giving compound **66** in 45% yield over two steps (*Scheme 34*).

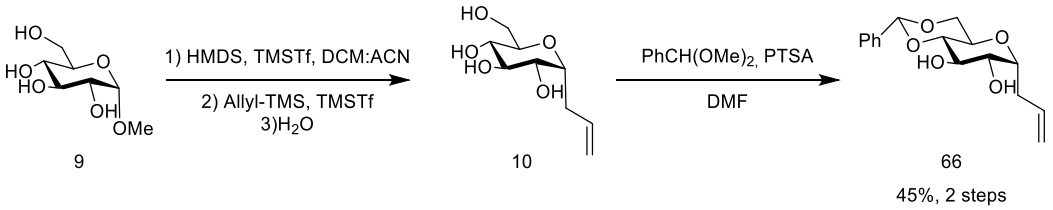

Scheme 34. Synthesis of intermediate ***66***

Regioselective azide introduction at position 2, reported in the literature for the synthesis of 2-azido-2-deoxy-D-manno derivatives[107], was tested on substrate **66** (*Scheme 35*).

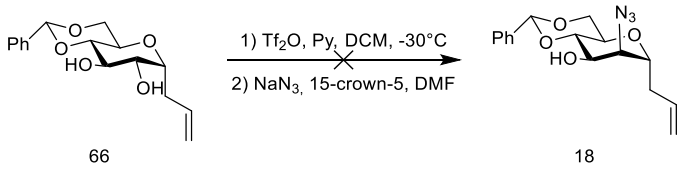

Scheme 35. Attempt of regioselective azide introduction

However, TLC and crude NMR analysis showed that the first reaction step (introduction of the triflate) occurred with poor regioselectivity. In addition the second step, consisting in the S_N2 reaction with sodium azide, led to a mixture of unidentified products, different from both the desired **18** and its 3-azido-3-deoxy regioisomer, both at low (-20°C) and high (70°C) temperature.

A second attempt to differentiate positions 2 and 3 on diol **66** was carried out using the same regioselective acetylation protocol reported in *Chapter 2.3.2* for the synthesis of the mannoside fragment (*Scheme 36*).

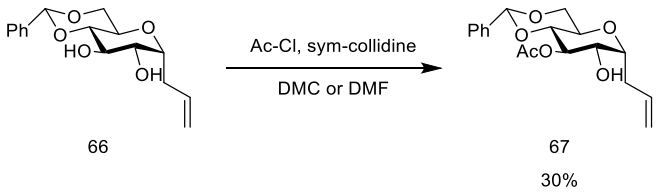

Scheme 36. Regioselective acetylation of intermediate ***66***

Although the higher reactivity at position 3 of compound **66** in comparison to position 2, (with only about 5% of 2-O-acetylated product isolated compared to 30% of the desired product **67**), the monoacetylated products were proven to be more reactive than substrate **66**. As a result, low conversion was observed (about 30% of starting material recovered), together with the formation of about 30% of the 2,3-di-O-acetylated product when 1 equivalent of acetylating agent was used. We speculated that this could be due to the higher solubility in DCM (the solvent typically used for acetylation reaction) of the monoacetylated compounds. The same reaction was therefore performed in a more polar solvent, such as DMF. Unfortunately, no better results were achieved.
The reaction by-products were deacetylated and the monoacetylation was repeated, leading to 50% yield over three steps (acetylation, deacetylation, acetylation) and two purifications.

We then proceeded with the azide introduction (*Scheme 37*).

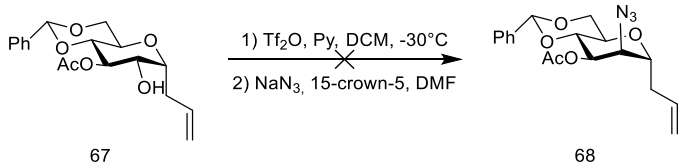

67 68

Scheme 37. Attempt of azide introduction

Once again, the formation of an unidentified product took place both at -20°C and 70°C and the desired product **68** could not be obtained.
We reasoned that the azide introduction was successfully carried out in our first strategy on a substrate containing the 1-C-allyl group but without the benzylidene ring, while examples of the same reaction, performed on glucose moieties containing a benzylidene group but not a 1-C allyl group are literature reported by Alex *et al.*[107]. We therefore hypothesized that-the simultaneous presence of the two functional groups on the glucose substrate could impair the substrate reactivity. Accordingly, it was decided to open the benzylidene ring before performing the azide introduction reaction.

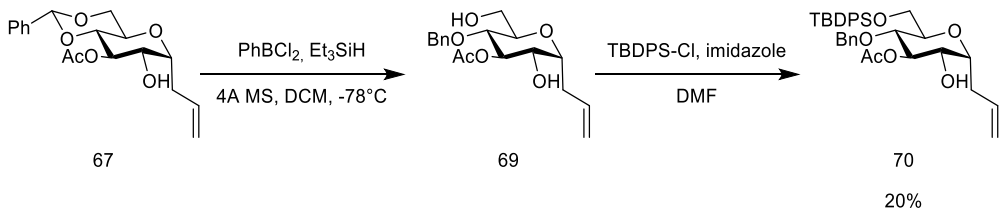

67 69 70

20%

*Scheme 38. Synthesis of intermediate **70***

Benzylidene ring opening on alcohol **67** was followed by selective protection of the 6-OH as a tert-butyldiphenylsilyl ether, leading to compound **70** in 20% yield over two steps (*Scheme 38*). The low yield resulted to be mainly due to the poor selectivity achieved in the benzylidene ring opening reaction and to acetyl group migration.

Intermediate **70** was converted into the azido derivative **71** in 60% yield over 2 steps (*Scheme 39*).

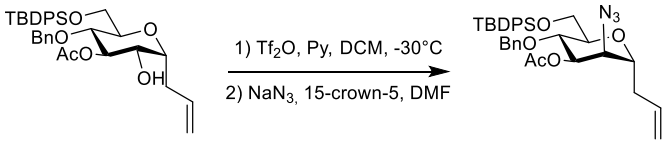

70 71

60%

*Scheme 39. Synthesis of intermediate **71***

The intermediate **71** could be employed in the previously described reaction sequence to give the desired phosphonate fragments.

Second strategy

The second strategy involved the protection of positions 4 and 6 in the early stages of the synthesis, together with the 3-OH protection with as a PMB ether.

One-pot silylation and 1-C allylation has been performed on methyl α-D-glucopyranoside leading to the TMS protected intermediate **72**. The following one-pot sequence comprising benzylidene introduction, regioselective installation at 3-OH of PMB ether and desilylation gave compound **73** with 45% yield (*Scheme 40*).

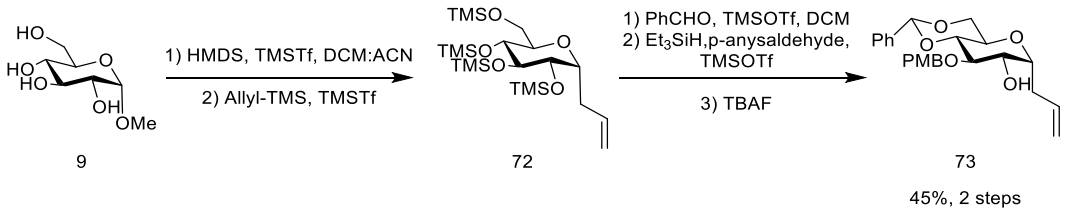

*Scheme 40. Regioselective synthesis of intermediate **73***

The main by-products observed consisted in C-mannosides containing the benzylidene ring in positions 4 and 6, and one benzyl and one PMB group or two PMB groups in positions 2 and 3. The actual position of the PMB group in compound **73** has been confirmed through acetylation of a little amount of product. NMR analysis of the acetylated compound made possible to identify the proton in position 2 as the one adjacent to the acetylated hydroxyl group, confirming that position 3 was the one protected as a PMB ether.

Activation of 2-OH and subsequent nucleophilic substitution with sodium azide were expected to lead to the azido derivative **32** (*Scheme 41*). Unfortunately, once again, only an unidentified by-product was obtained even changing the N_3^- ion source and the reaction conditions (*Table 8*).

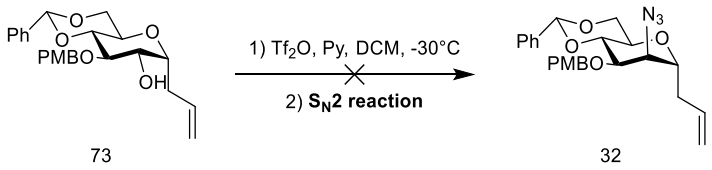

Scheme 41. Azide introduction reaciton

Entry	S_N2 reaction conditions	Temperature	Yield
1	NaN_3, 15-crown-5, DMF	-20°C to RT	N.R.
2	Bu_4NN_3, toluene	50°C	N.R.
3	NaN_3, HMPT	70°C	N.R.

*Table 8. Screening of different conditions for the synthesis of **32***

^{1}H NMR of the isolated by-product is reported below (*Figure 13*), in comparison with the NMR spectra of the starting material, the triflate derivative and the desired product **32**, achieved with the synthetic strategy described in *Chapter 2.3.4.* It was possible to observe a low-field shift of the proton in the pseudo-anomeric position (1) in the spectrum of the compound isolated when compared to both the triflate intermediate and the desired product. Moreover, from its HSQC analysis, it was found that the carbon bringing the proton 1 has a shift of 100 ppm, classically attributed to anomeric carbons. Furthermore, ESI analysis revealed m/z picks for the isolated by-product of 599, way higher than the 437 expected for the product and the 544 of the triflate, excluding the possibility of an elimination reaction. The analytical results suggest that an unexpected rearrangement took place.

However, it was decided not to further investigate on the nature of the byproduct and to perform benzylidene ring opening before the introduction of the azido group, in order to try to avoid the by-product formation.

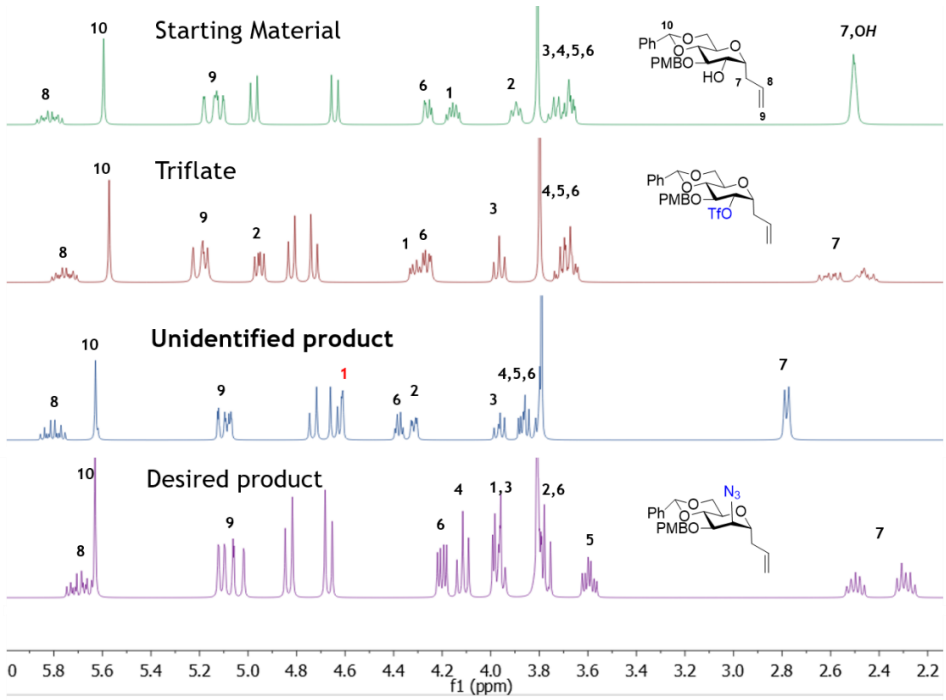

Figure 13. Comparison between ^{1}H NMRs of the starting material, the triflate derivative, the unidentified isolated product and the desired product

Different conditions were screened for benzylidene ring reductive opening (*Scheme 42*, *Table 9*).

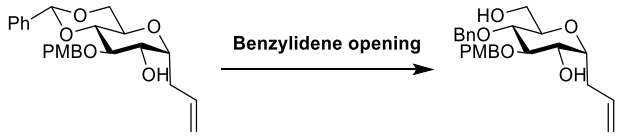

73 74

Scheme 42. Benzylidene opening reaction

Entry	Conditions	Yield
1	BH_3·THF, Bu_2BOTf, DCM	15%
2	DIBAL-H, DCM or toluene, 0 °C to RT	10% (≈90% SM recovered)
3	DIBAL-H, THF, 0 °C to RT	N.R. (≈100% SM recovered)
4	$PhBCl_2$, Et_3SiH -78 °C	Up to 45%

Table 9. Screening of benzylidene reductive opening conditions

Unfortunately, all the reaction conditions tested led to the desired compound **74** in low yields. While low starting material conversion has been observed using DIBAL-H as reducing agent, the acidic conditions generated by the use of a combination of $PhBCl_2$ and Et_3SiH, caused the formation of the 3-O deprotected product, due to the lability of the PMB ether in acidic conditions. The desired product could be achieved in yields ranging from 15 to 45%.

Compound **74** was treated with tert-butyldiphenylsilyl chloride to achieve selective 6-O protection. Eventually the free hydroxyl group in position 2 was activated as triflate and converted into azide **48** in 60% yield over two steps (together with the formation of a by-product, with spectroscopic characteristics similar to the ones reported in *Figure 13*) (*Scheme 43*).

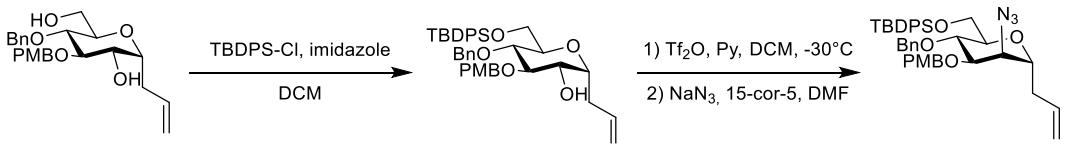

74 75 48

76% 60%

*Scheme 43. Alternative synthesis of intermediate **48**.*

Compound **48** could be used as intermediate for the synthesis of the phosphonate fragment.

2.4 Conclusions and future perspectives

Dimer **57** and trimer **65** were successfully synthesized.

Purification of crude **65** and hydrogenolysis of the permanent protective groups on both dimer **57** and trimer **65** will lead to the final, deprotected target molecules (*Scheme 44*).

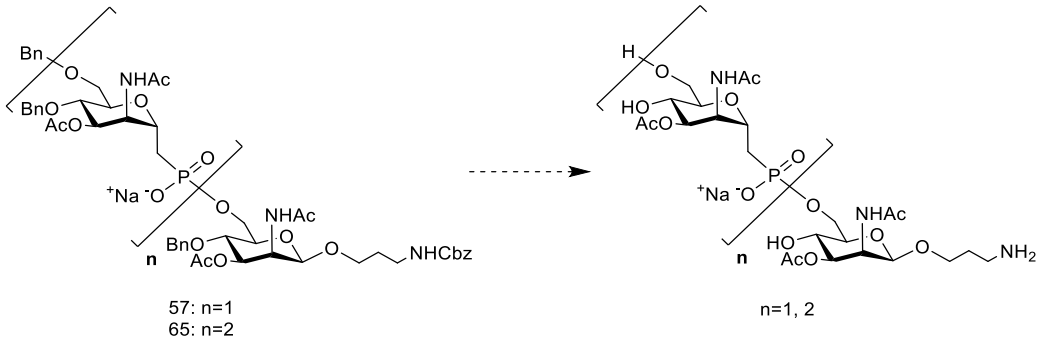

Scheme 44. Synthesis of the target phosphonoester-linked oligomers

Due to the high number of reactions needed to achieve the target compounds, some alternative strategies were explored. However, the new and shorter strategies explored (*Chapter 2.3.7*) presents some drawbacks, mainly related to the low yields achieved for the benzylidene opening reaction (*Scheme 45*).

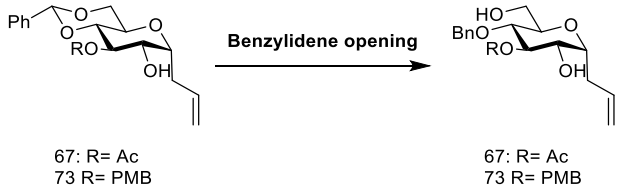

Scheme 45. Benzylidene opening reaction

Screening of different conditions for the benzylidene opening reaction could lead to an improvement of the whole phosphono-analogue synthetic strategy.

Synthesis of Bacteroides fragilis lipid A moieties for structure-activity relationship studies

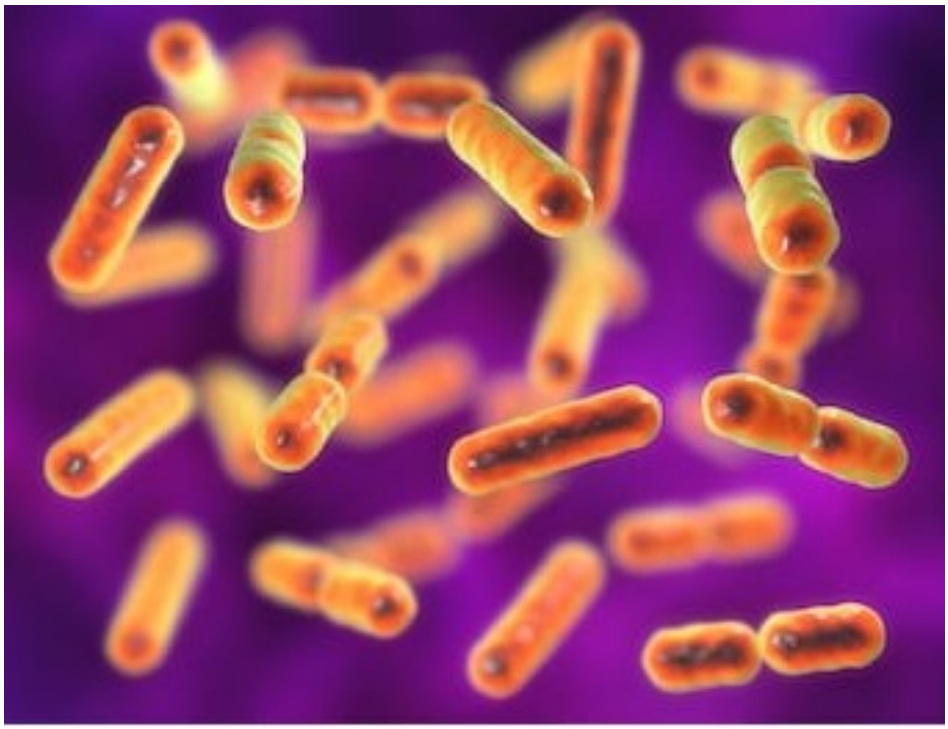

3.1 Introduction to bacterial lipid A

As described in *Chapter 1.1.1*, Gram-negative bacteria outer membrane exposes the LPS, anchored to the OM through its lipophilic part: the lipid A.

The lipid A domain is responsible for much of the toxicity of Gram-negative bacteria. When bacterial cells are lysed by the immune system, fragments of membrane containing lipid A are released into the circulation, causing fever, diarrhoea, and possible fatal endotoxic shock (also called septic shock)[10]. Indeed, the Lipid A can stimulate the Toll-like receptor 4 (TLR4), a receptor present on the surface of immune cells like monocytes, neutrophils, dendritic cells and macrophages[108], which is able to activate other intracellular adapter molecules starting a cascade that results in a strong inflammatory response, which strictly depends on the Lipid A/LPS structure and concentration. On the other hand, in low concentration, some LPSs can induce a non-specific resistance to the invading microbe[17].

Structure-activity relationship studies on lipid A derivatives and analogues have shown that the endotoxicity of lipid A is mainly due to its phosphorylation degree and to the number, length and distribution of the acyl chains[109]. Furthermore, it has been shown that some over or under acylated lipid A behave as TLR4-antagonists[110]. Therefore, lipid A structure can be modulated to work as immunomodulator and used to regulate the innate immune response. Specific lipid A structures can be used for vaccines and in particular adjuvants development and for the treatment of several diseases such as neuro-inflammation, cancer and allergies[111].

3.1.1 Lipid A as vaccine adjuvant

As reported in *Chapter 1.3.2*, many subunit vaccines may require the co-administration of adjuvants to enhance strength and duration of the induced immune response[112].

In particular, *immune potentiator* adjuvants act by activating the innate immune system through stimulation of PRRs such as TLRs.

Most of the lipid A are known to be potent stimulants of the innate immune system, mainly through activation of TLR4. As mentioned above, however, most of them are highly toxic for humans. In order to uncouple the toxicity of lipid A from its ability to activate the innate immune response, an interesting property for adjuvants development, Masihi et al[11] developed in 1986 monophosphoryl lipid A (MPLA).

MPLA consists in the lipid A portion of *Salmonella Minnesota* R595, from which an acyl chain and a phosphate group have been removed by controlled hydrolysis (*Figure 14*). These

structural modifications lead to a compound with 100-fold less toxicity compared to the natural lipid A, leaving the immunostimulatory properties unaffected.

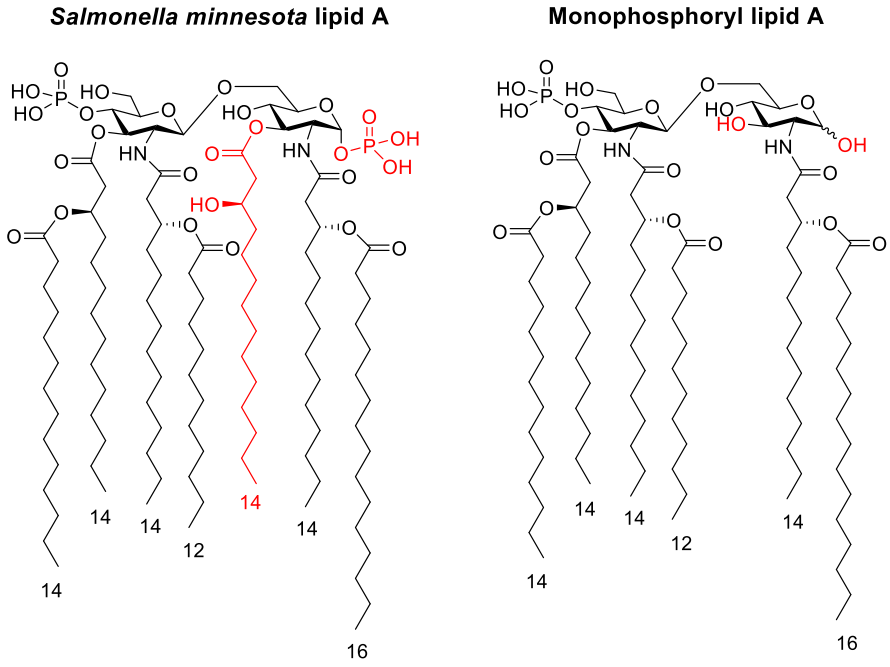

Figure 14: Structures of Salmonella Minnesota R595 *lipid A and MPLA*

MPLA acts as TLR4 agonist, promoting the maturation of dendritic cells[113] and the production of Th1 CD4+ T cells, resulting in an enhanced immune response to co-administered antigens[12] .

MPL®, a MPLA-based adjuvant, is the only TLR4 ligand licensed in human vaccines. In particular, MPLA, combined with alum, is contained in two licensed vaccines targeting human papilloma virus and Hepatitis B virus (Cervarix®, and Fendrix®, by GSK)[12] .

3.2 Bacteroides fragilis

The human intestine is inhabited by up to 100 trillion microbes, most of them symbionts, essential to human health. A balanced healthy human microbiota (HMb) depends on the host's immune system ability to discriminate between pathogens and symbionts. Indeed, a tolerogenic mechanism must be developed by the host's immune system through the elaboration of specific signals emitted by the microbes.

Among all the different bacteria phyla that compose a HMb, *Firmicutes*, *Bacteroidetes*, *Actinobacteria*, *Proteobacteria*, *Fusobacteria*, and *Verrucomicrobia* are the most abundant ones, representing 90% of gut microbiota[114,115].

Bacteroides fragilis is a Gram-negative obligate bacterium inhabiting the gastrointestinal tract of humans. It has important immunomodulatory effects on the immune system through its polysaccharide A (PSA), such as: protection from infections, stimulation of immune system development, protection from intestinal inflammatory diseases and from systemic immune-mediated diseases. Such abilities made the PSA of *Bacteroides fragilis* the model symbiotic immunomodulatory molecule[116–118].

Polysaccharide A, the most abundant carbohydrate in *B. fragilis* capsule complex, is anchored to the outer membrane through a modified lipid A structure. Even if this lipopolysaccharide is considered as part of the lipid A family, some structural characteristics distinguish them from the classical Gram-negative bacteria lipid A structures, e.g. *E. coli*'s. While *E. coli* LPS is typically hexaacylated with 14-C straight chains and diphosphorylated, the lipid component of *B. fragilis* shows high structural variability in acylation (number, position, length and structure of the chains) and phosphorylation[13]. The diverse structures could explain the discrepancies found in TLR2/TLR4-mediated responses to *B. fragilis* lipid A when compared to other symbionts[119].

In 2019, Kasper group[13] reported that the lipid A anchoring PSA moiety of *B. fragilis* has a key immunomodulatory role. They showed how the combination of TLR1-TLR2 heterodimer activation by the lipidic part of PSA and Dectin1-dependent activation by the polysaccharide moiety leads to the activation of specific genes essential for PSA processing and presentation to CD4+T cells by APCs. These genes activation is crucial for MHCII mediated processing and presentation of the saccharide portion of PSA to regulatory T cells (T_{regs}) and so to produce Interleukin 10 (IL-10), the main anti-inflammatory molecule

associated with PSA immune stimulation. The above pathway was not initiated by stimulation with the de-lipidated PSA, underlying the importance of the lipid moiety.

3.2.1 Bacteroides fragilis lipid A

Kasper group first identified the structural characteristics of the lipid A present on PSA of *B. fragilis*[13]. While measuring the average molecular size of *B. fragilis* PSA through size exclusion chromatography, they observed discrepancies in the results obtained when a detergent-containing and a detergent-free buffer solution were used for elution. The higher size values obtained in the second condition suggested the presence of hydrophobic lipid moieties, able to form micellar-like structures, which are broken by the detergent. To study more in-depth the nature of their discovery, they proceeded with a chloroform/methanol extraction and they observed no lipid in the organic phase, suggesting that the lipid structure should be covalently linked to the PS. Treatment of PSA with phospholipase A2 was then performed to check whether the structure contained a phospholipid moiety, a common anchoring moiety for CPS of other organisms[13, 70]. However, no change in the micelle aggregates was found, implying that the lipid found was not a phospholipid. However, the acid hydrolysis of the PSA led to the release of a low molecular weight compound, found in the organic phase after chloroform/methanol extraction and consisting in around 1% of the dry mass of the PSA. The ^{1}H NMR of the remaining PSA showed no significant modification, suggesting that this moiety is minimal compared to the high molecular-weight repeating unit structure of PSA. LC-MS/MS studies have then been performed on the isolated, low molecular weight fragment: di-glucosamine was identified with different degrees of acylation with linear acyl chain, with chain lengths from C15 to C17. The studies revealed some variability in the bacterium lipid A, with different acylation and phosphorylation patterns, showing a prevalence of the penta-acylated, unphosphorylated structure (44.5%), followed by the penta-acylated, monophosphorylated (33.6%) and by other non and monophosphorylated tri and tetraacylated compounds[13].

3.3 Aim of the project

The lipid A of *B. fragilis* PSA presents promising biological properties in relation to its immunomodulatory abilities. Since the discovery and isolation of these compounds is quite recent, information about their actual structures is missing. For this reason and considering the great interest in performing structure-biological activity relationship studies, we decided, in the context of a collaboration with Professor Kasper, to synthesize some of the possible structures of *B. fragilis* lipid A.

The structures reported in *Figure 15* have been identified as initial targets of the investigation.

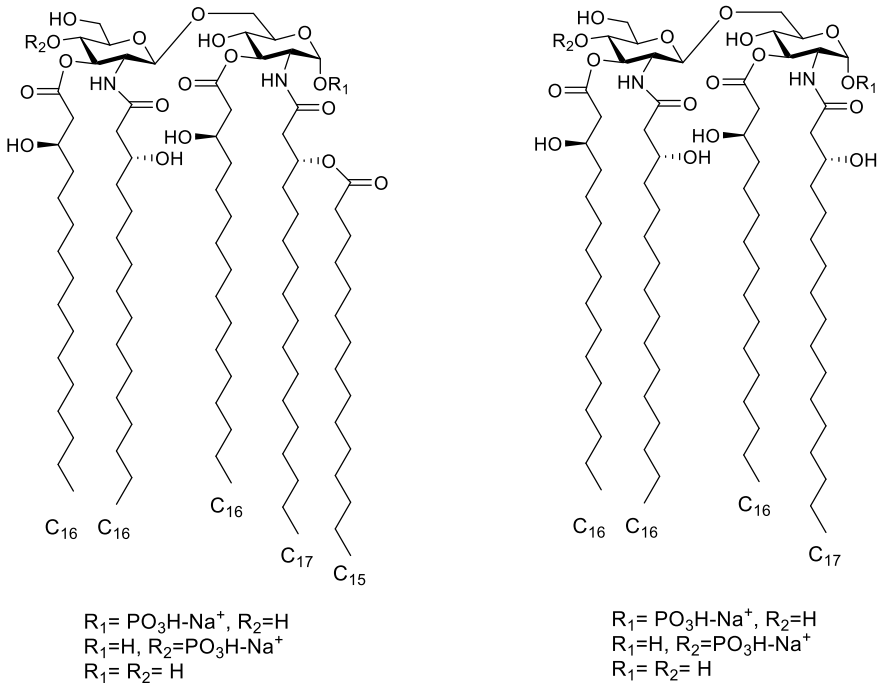

Figure 15. Synthetic targets of the project.

3.4 Results and discussion

3.4.1 Retrosynthetic approach

For the synthesis of the lipid A library, we envisaged four common building blocks: a suitably protected di-glucosamine and three different fatty acid chains (*Scheme 46*).

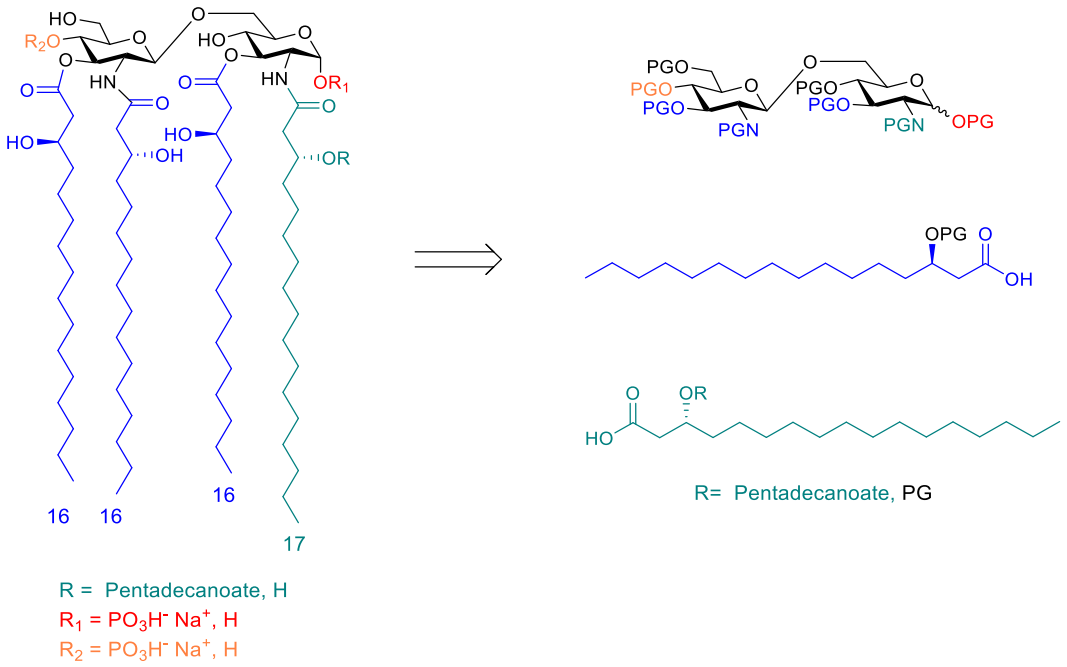

Scheme 46. Building blocks for lipid A library's assembly.

In our first approach, di-glucosamine **76** was designed as carbohydrate building block (*Scheme 47*). Indeed, we planned the regioselective glycosylation of donor **80** with diol acceptor **78**, relying on the higher nucleophilicity of primary 6-OH in comparison to secondary 3-OH. As it will be detailed below, however, 3-OH and 6-OH showed similar reactivity under glycosylation conditions, leading to mixtures of β(1→3) and β(1→6) disaccharides. 3-O acetylated acceptor **79** was therefore employed to achieve β(1→6) di-glucosamine **77**.

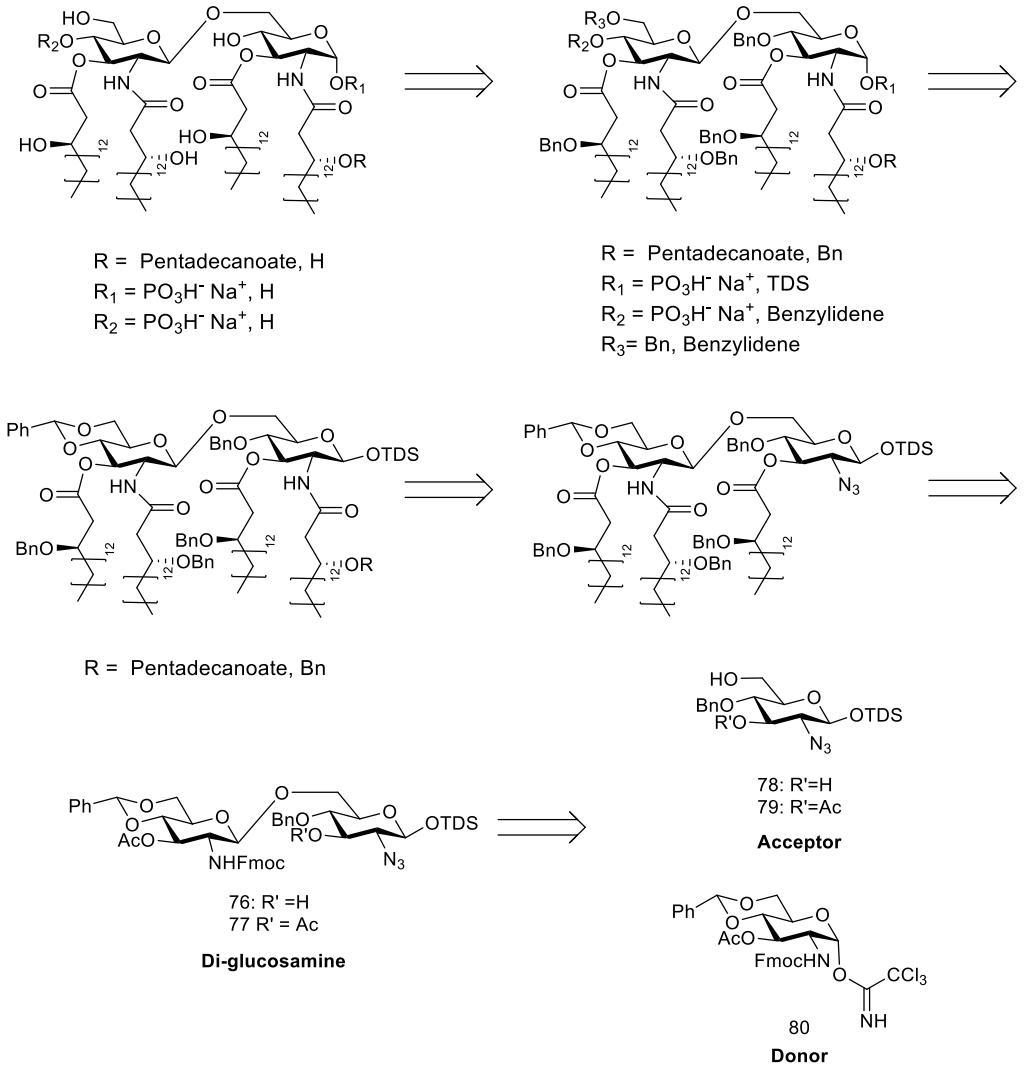

Scheme 47. Retrosynthetic approach to the lipid A library

In order to assemble the full library, we anticipated the introduction of the 16-C atom chains at positions 3, 2', and 3' of the di-glucosamine (blue) as a first stage of our endeavour. Accordingly, Fmoc and acetyl ester (both removable in basic conditions) were chosen as protective groups for the amine in position 2' and the hydroxyl in position 3', respectively, while position 3 was initially left unprotected.

The second step would be the introduction of the 17-C atom chain (which, in turn, could be O-acylated with a pentadecanoic acid chain in the synthesis of the penta-acylated target

structures) in position 2. The amino group in position 2 was masked as an azide, which selective reduction would give the desired amine, used to synthesize the amide with the 17-C atoms fatty acid chains.

Position 1 was protected as a silyl ether, cleavable by F^- sources to allow phosphate introduction, while position 4' and 6' were protected as benzylidene acetal, which could be selectively opened to allow phosphate introduction in position 4', or cleaved in the last step of the synthesis, together with the permanent benzyl groups used to protect position 4 of the di-glucosamine and the hydroxy groups of the fatty acid chains.

3.4.1 Synthesis of the acceptor

The first approach to acceptor synthesis started from D-glucosamine hydrochloride. After diazotransfer reaction with imidazole-1-sulfonyl azide hydrogen sulfate **82**[120], which led to the azido compound **83**, selective protection of positions 4 and 6 with a benzylidene acetal and protection of the anomeric position as a silyl ether were carried out without any purification (*Scheme 48*).

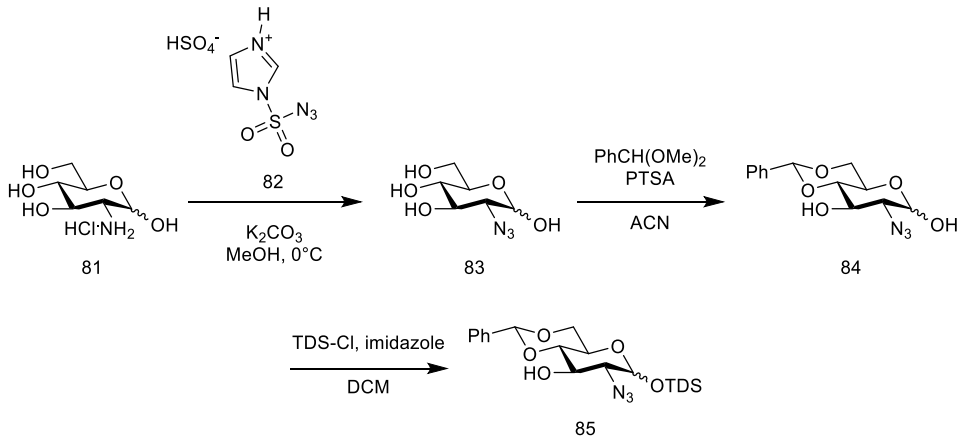

*Scheme 48. First strategy of synthesis of **85***

However, the reaction mixture was extremely complex and the isolation of the desired product **85** resulted to be tricky. Due to the purification problems encountered, a longer but more reliable procedure was adopted for the synthesis of the acceptor.

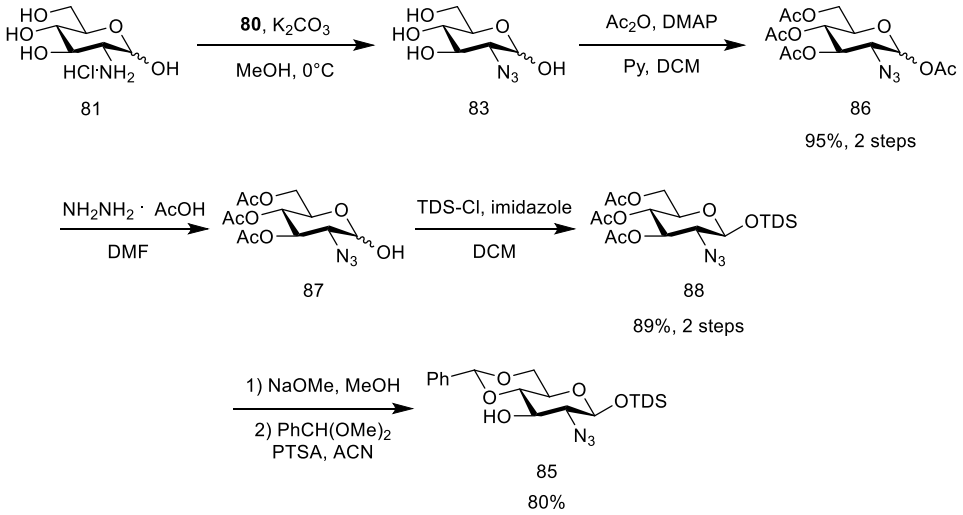

*Scheme 49. Synthesis of intermediate **85**.*

Glucosamine hydrochloride was converted into azide **83** as previously described. Peracetylation of **83** gave compound **86**, which could be easily isolated from the reaction mixture. The acetyl group in anomeric position was selectively removed by treatment with hydrazine acetate to be replaced by a bulky silyl ether, leading to compound **88** as a single β-anomer. The following deacetylation and introduction of the benzylidene acetal led to compound **85** in 80% yield (*Scheme 49*).

Different conditions were screened to achieve regioselective reductive opening of the benzylidene ring (*Scheme 50, Table 10*).

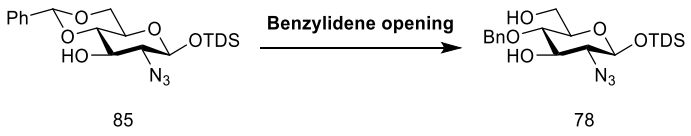

Scheme 50. Benzylidene opening reaction.

Entry	Conditions	Yield
1	DIBAL-H, DCM, 0°C to RT	10%
2	BH_3·THF, DiBuBTf, DCM, 0°C	35%
3	$PhBCl_2$, Et_3SiH -78 °C	30%

Table 10. Screening of benzylidene opening conditions

Unfortunately, the best yield achieved for the synthesis of **78** (*Entry 2*) was only 35% (mainly due to full benzylidene cleavage), while treatment of **85** with DIBAL-H (*Entry 1*) led to low conversion (with 90% SM recovered).

3.4.2 Synthesis of the donor

First, the synthesis of the glycosyl donor was attempted by using a strategy similar to the one initially employed for the preparation of acceptor **78**. The three-steps synthesis of intermediate **91**, however, resulted once more in a complex mixture of compounds (*Scheme 51*).

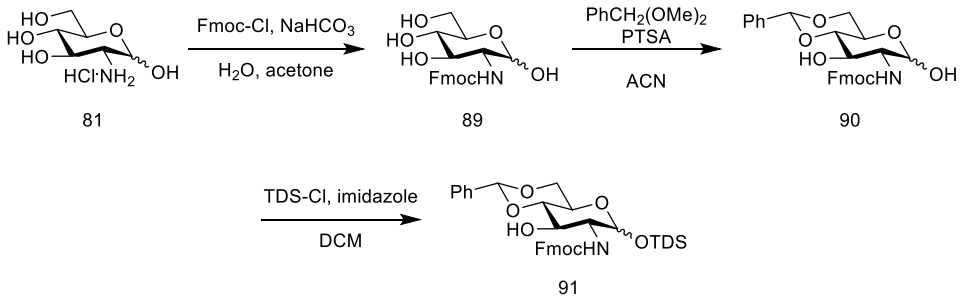

*Scheme 51. First approach to the synthesis of intermediate **91**.*

It was decided to move to a longer synthetic strategy.

Glucosamine hydrochloride was protected as Fmoc carbamate **89** and peracetylated to give compound **92**, which could be purified through acidic work-up. The acetyl group in anomeric position was then removed by treatment with hydrazine acetate to be silylated, leading to compound **94** as a single anomer (*Scheme 52*).

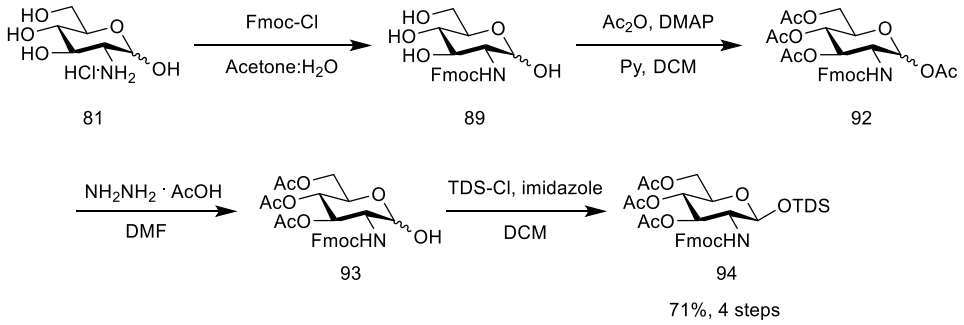

*Scheme 52. Synthesis of intermediate **94**.*

Compound **94** was converted into **95** in a three-steps reaction sequence comprising deacetylation, protection of positions 4 and 6 as benzylidene acetal and acetylation of free hydroxyl group at position 3 (*Scheme 53*).

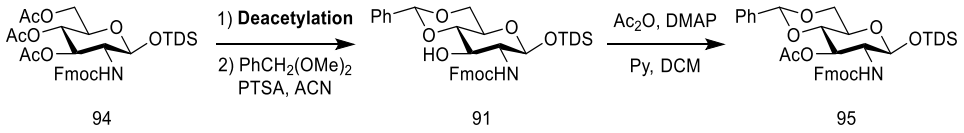

*Scheme 53. Synthesis of intermediate **95**.*

However, the similar reactivity of Fmoc and acetyl esters, which is beneficial during the deprotection step, resulted to be quite problematic at this stage: the basic reaction conditions required for deacetylation of compound **94** led to partial carbamate removal, due to the acidity of the proton labelled in red in *Scheme 54*.

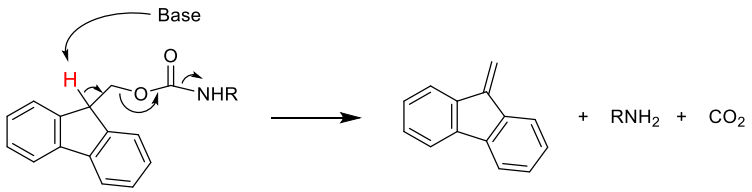

Scheme 54. Mechanism of N-Fmoc cleavage[121]

Different conditions were tested for the chemoselective deacetylation reaction (*Table 11*).

Entry	Deacetylation conditions	Yield*
1	NaOMe (0.1 eq.), MeOH, RT	Up to 66%
2	K_2CO_3 (0.1 eq.), MeOH, RT	15%
3[122]	4Å MS, MeOH, reflux	0%
4	Guanidine, EtOH	15%

*Over 3 steps (after isolation of **95**)

Table 11. Screening of different deacetylation conditions

Deacetylation in classical Zemplen conditions (*Entry 1*) led to compound **95** in non-reproducible yields, ranging from 35% to 66%, while almost full deprotection of the Fmoc group was observed in the conditions reported in *Entries 2*, *3 and 4*.

Alternatively, **95** could be achieved starting from **85**, an intermediate in the acceptor synthesis.

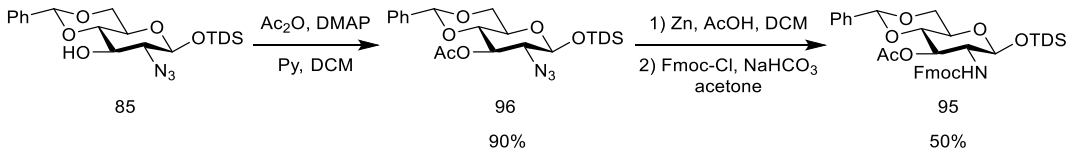

85 96 90% 95 50%

*Scheme 55. Alternative synthesis of intermediate **95**.*

The 3-OH group of **85** was acetylated. The azide reduction and amine protection as Fmoc-carbamate gave **95** in 50% yield (*Scheme 55*).
Since the low yield is probably due to acetyl group migration to give the corresponding acetamide, conversion of azide **96** into N-Fmoc carbamate should be achieved in higher yields by performing the 3-O-acetylation step after azide reduction and introduction of the carbamate.

Anomeric deprotection and treatment with trichloroacetonitrile in the presence of Cs_2CO_3 provided trichloroacetimidate **80**, achieved as a single α-anomer due to the formation of hydrogen bond between the carbamate and the acetimidate (*Scheme 56*).

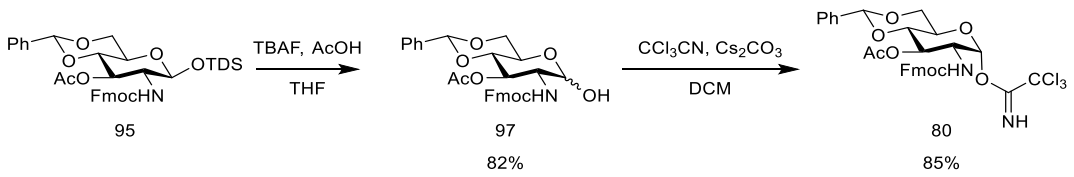

*Scheme 56. Synthesis of donor **80**.*

3.4.3 Synthesis of the disaccharide

Glycosylation reaction, catalysed by triflic acid, was carried out in order to couple the two glucosamine units (*Scheme 57*).

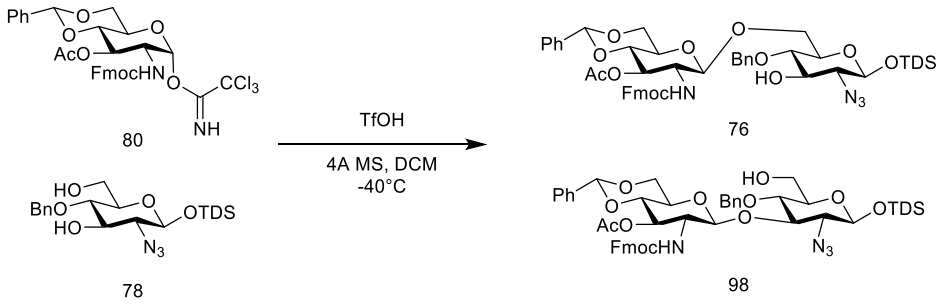

*Scheme 57. Glycosylation of acceptor **78** and donor **80**.*

However, a 1:2 mixture of β 1→6 (compound **76**) and β 1→3 (compound **98**) disaccharides was obtained. The reasons for the higher reactivity of the secondary 3-OH compared to the primary 6-OH are not clear, but they are probably related to the presence of an azido group in position 2 of the acceptor.

To avoid the formation of the β 1→3 isomer, position 3 of the acceptor was protected with an acetyl group to give **96** in 90% yield.

Eventually, the benzylidene acetal was selectively opened to give the new acceptor **79**. Acetylation of the hydroxy group at position 3 also allowed to dramatically increase the yield of the benzylidene reductive opening from 35% to 93% yield (*Scheme 58*).

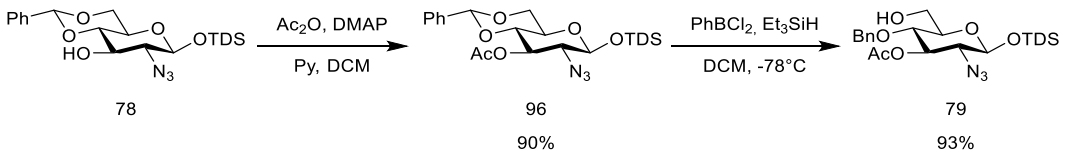

*Scheme 58. Synthesis of acceptor **79**.*

Glycosylation reaction between donor **80** and the new acceptor **79** led to the desired disaccharide **77** (*Scheme 59*), as a single anomer, in up to 67% yield (Table 12, entry 2).

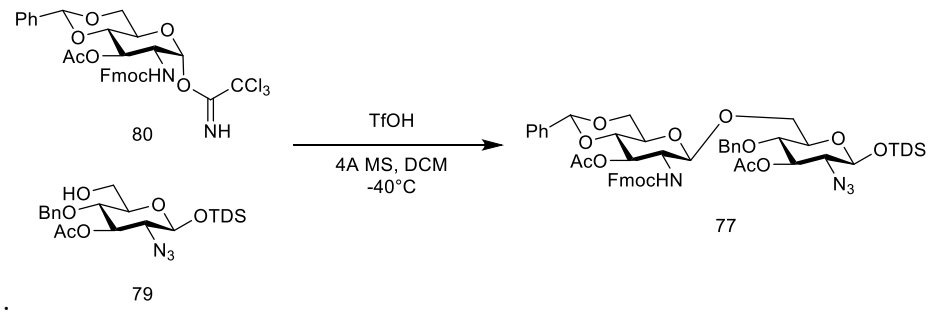

Scheme 59. Synthesis of di-glucosamine 77.

Entry	Eq. of TfOH	Donor : Acceptor ratio	Temperature	Yield
1	0.5	1.05	-40°C to -10°C	30% (40% of **79** recovered)
2	0.15	1.3	-45° to -25°C	67% (10% of **79** recovered)

Table 12. Glycosylation conditions

3.4.4 Synthesis of the fatty acid chains

To achieve the desired 16 and 17-C atoms fatty acid chains, a protocol described by Oikawa *et al.*[123] for the synthesis of similar substrates was followed.

It was decided to use tetradecanol and pentadecanol as starting material instead of the corresponding, more expensive aldehydes. Indeed, the first step of the synthesis consisted in alcohol oxidation (*Scheme 60*).

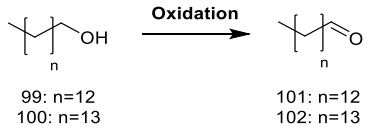

Scheme 60. Oxidation reactions.

Entry	Reaction conditions	Yield
1	IBX (3 eq.), DCM	30% (70% SM)
2	IBX (10 eq.), DCM	Quantitative
3	DMP (2 eq.), DCM	Quantitative

Table 13. Oxidation conditions.

Oxidation with the cheap, freshly prepared IBX[124] was screened (*Table 13*). However, due to large amount of oxidant needed to obtain full conversion of the alcohols **99** and **100** into the desired aldehydes **101** and **102**, respectively (*Entry 2*), Dess-Martin periodinane (DMP) was chosen as the best oxidizing agent.

Wittig olefination of **101** and **102** with freshly prepared, stabilized ylide **103** gave the 16-C and 17-C α,β-unsaturated esters **104** and **105** respectively, both in about 95:5 E:Z ratio and in 90% yield for the pure E isomer (*Scheme 61*).

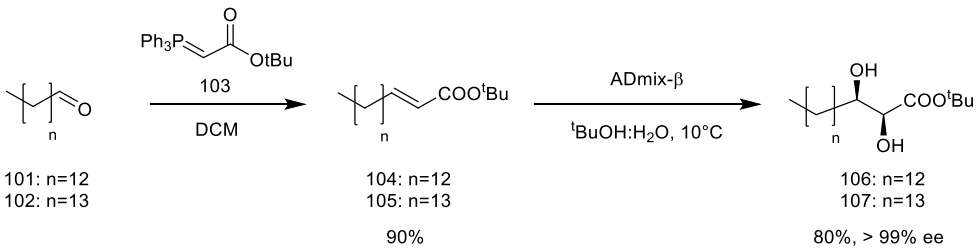

*Scheme 61. Synthesis of diols **106** and **107**.*

The isolated E isomers were then subjected to asymmetric dihydroxylation[125] to give diols **106** and **107**, both in 80% yield and >99% e.e. (*Scheme 61*).

The enantiomeric excess was determined by ^{1}H-NMR spectra of the corresponding Mosher's bis-(S)-α-methoxy-(α-(tfifluoromethyl)phenylacetic acid (MTPA) esters[126,127].

However, absolute configuration determination of 1,2-diols from the corresponding Mosher's esters is often not accurate[128]. For this reason, absolute configuration assignment has been postponed to a more advanced stage, when a single hydroxyl group is present on the molecule. However, $[\alpha]_D$ values calculated for **106** and **107** were in line with the ones reported by Oikawa and Kusumoto[129] for *tert*-butyl (2S,3R)-2,3-dihydroxytetradecanoate, confirming, with a good degree of accuracy, that the desired isomers were achieved.
Due to time issues, the next synthetic steps were performed only on the 16-C atoms chain. However, the same synthetic strategy could be applied on the 17-C atoms chain.

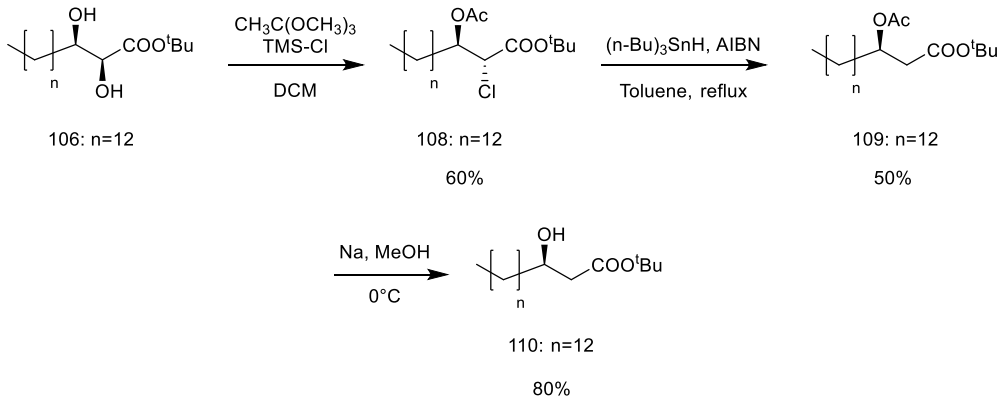

*Scheme 62. Synthesis of compound **110**.*

Diol **106** was treated with TMS-Cl and trimethylorthoacetate to achieve a regioselective S_N2-type substitution at the electronically activated C_2 position, which occurred in 60% yield (with around 20% SM recovered). After radicalic dechlorination, 3-O-deacetylation was performed at low temperature to avoid t-butyl ester migration, which was observed in some extent (around 10%), making it necessary to quench the reaction before full starting material conversion. In this way around 10% of the starting material has been recovered. Compound **110** was isolated in 80% yield (*Scheme 62*).
According to Oikawa and Kusumoto[123] synthetic strategy, hydroxyl group benzylation (or acylation) and t-butyl ester hydrolysis will be performed in order to achieve the desired fatty acid chains.

3.5 Conclusions and future perspectives

Di-glucosamine **77** (*Figure 16*) has been synthetized as first building block for lipid A library assembly.

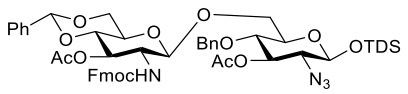

77

*Figure 16. Structure of the synthesized di-glucosamine **77**.*

Compounds **106** and **110** were synthesized as precursors of the 17-C atoms and 16-C atoms fatty acid chains, respectively (*Figure 17*).

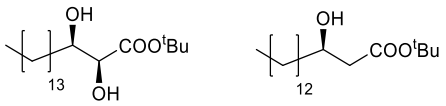

106 110

*Figure 17. Structure of the synthesized intermediates **106** and **110**.*

Fatty acid building blocks synthesis has to be completed either by protection of the hydroxyl group as benzyl ether (to give the linear chains) or by acylation with pentadecanoic acid (*Scheme 62*).

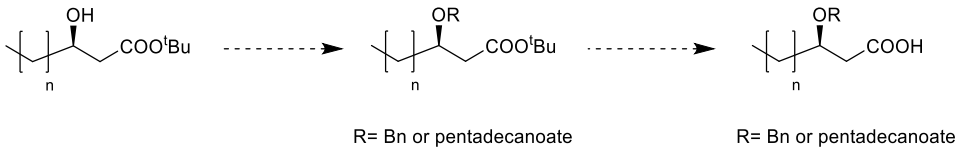

Scheme 62. Missing steps for the synthesis of the fatty acid chains.

Once the fatty acid chains synthesis will be completed, they will be used to functionalize the sugar moiety at positions 2, 3, 2' and 3', after proper deprotection/acylation steps.
Selective deprotection of positions 1 or 4' and subsequent phosphorylation, followed by di-glucosamine global deprotection will lead to the desired lipid A library.

The synthetic lipid A derivatives will be then used to clarify the structure of the lipid A structures newly isolated by the group of Kasper[70] and to perform structure-activity relationship studies to better understand their biological and immunomodulatory properties.

In particular, according to the preliminary studies published in 2019[70], the group of Professor Kasper will investigate, by means of different knockout cell lines or mice, on the type of TLR the new lipid A structures could activate. Moreover, the potential production of IL (specially IL-10, typical of *B. fragilis* lipid A-induced response) will be evaluated through DC-T cell co-cultures.

Experimental session

4.1 General experimental methods

Thin Layer Chromatography (TLC) analyses were performed on glass support Merck $60F_{254}$ (0.25mm thickness) and *High-Performance Thin Layer Chromatography (HPTLC) analyses* were performed on Kiesgel $60F_{254}$.

Reactions were always followed by TLC. Compounds were visualized, when appropriate by UV light (254nm), and always by spraying with one or more of the following stains:

- molybdic solution (21g of $(NH_4)_6Mo_7O_{24}$, 1g of $Ce(SO_4)_2$, 31mL of H_2SO_4 98%, 970mL H_2O)

- sulfuric acid solution (50mL of H_2SO_4 98%, 450mL of MeOH, 450mL H_2O)

- ninhydrin (2.7g of 2,2-dihydroxyindane-1,3-dione, 27mL of AcOH, 900mL of EtOH)

- permanganate solution (1.5g of $KMnO_4$, 10g K_2CO_3 and 1.25mL 10% NaOH in 200mL H_2O)

with detection by charring at 300°C.

Flash chromatography: according to Still procedure[130], compounds were purified by flash chromatography using Silica gel (SiO_2, high-purity Merck grade, pore size 60Å, 230-400 mesh particle size from Sigma-Aldrich). Otherwise it was also used a flash purification system, Biotage SP1. Normal phase Biotage SNAP cartridges (sizes from 5g to 50g, standard 50µm silica) were used to purify the compounds.

NMR Analysis: NMR spectra were recorded on a Bruker AMX 400 instrument (400, 162 and 100.6MHz for ^{1}H, ^{31}P and ^{13}C respectively). All NMR were run at room temperature.

The samples were prepared using deuterated solvents ($CDCl_3$, D_2O, CD_3OD and acetone-d6 from Eurisotop). Chemical shifts (δ) are reported in ppm and the coupling constants (*J*) in Hz. Chemical shifts were referenced to the residual proton in the solvent according to Gottlieb and Nudelman[131]. Multiplicities are abbreviated as: br (broad or Brownian), s (singlet), d (doublet), t (triplet), q (quadruplet), m (multiplet) or their combinations. Bidimensional experiments (COSY, HSQC and HMBC) were used to better assign peaks to the structure.

Carbons and protons were numbered according to their position as shown in *Figure 18.*

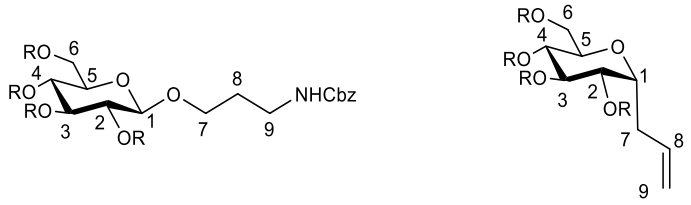

Figure 18. Carbon and bound proton numeration used in ^{1}H and ^{13}C NMR spectra assignment.

Mass Analysis: low resolution mass analyses were recorded in negative or positive mode on a Thermo Finnigan LCQ Advantage equipped with an ESI source. High resolution mass analyses were recorded on a Waters Micromass Q-Tof micro equipped with a LockSpray ESI source or on a Bruker Daltonics ICR-FTMS APEX II at C.I.G.A, University of Milan.

Anhydrous environment: Unless otherwise described, all the reactions were conducted under dry nitrogen atmosphere. When stirred overnight, reactions were put under anhydrous atmosphere by an Argon-balloon.

Solvents: unless otherwise described, all the reactions were performed using dry solvents. DCM, Et_2O, MeOH, DMF, EtOAc, Py, Tol, DMF, ACN and THF were purchased from Sigma-Aldrich and used without further purifications.

.

4.2 General procedures

*General procedure **A**: acetylation*

The SM (1 eq.) was dissolved in DCM (0.2 M), then Py (4 eq. per OH or NH_2), Ac_2O (2 eq. per OH or NH_2) and DMAP (catalytic amount, when required) were added.

The reaction progress was monitored by TLC and, after completion, the reaction mixture was diluted with DCM and washed with 3x HCl 5%, 1x $NaHCO_3$ (saturated aqueous solution) and 1x H_2O. The organic phase was dried over Na_2SO_4, filtered and the solvent was removed under reduced pressure.

*General procedure **B**: deacetylation*

The SM (1 eq.) was dissolved in MeOH (0.1 M). NaOMe (0.1 eq. per OH) was added and the mixture was stirred at RT until full SM conversion was detected by TLC.

The reaction was quenched by addition of an excess of Amberlite IR-120 resin, H^+ form. After removal of the resin by filtration, the solvent was evaporated under reduced pressure.

*General procedure **C**: synthesis of benzylidene acetal*

To a solution of SM (1 eq.) in the proper solvent (0.1 M - indicated in the specific procedure), benzaldehyde dimethyl acetal (2.2 eq.) and the proper acid catalyst (0.2 eq. - indicated in the specific procedure) were added. The mixture was stirred at RT until complete SM conversion (detected by TLC).

The reaction was quenched by addition of TEA till neutral pH and the solvent was removed under reduced pressure.

*General procedure **D**: benzylidene reductive opening*

Freshly activated 4Å MS were added to the SM (1 eq.) under Ar atmosphere. DCM (0.05 M) was added and the mixture was stirred for 1 h at -78°C before Et_3SiH (3.5 eq) addition. The mixture was stirred for additional 15', then $PhBCl_2$ (1.1 eq) was added. The reaction progress was monitored by TLC.

When the reaction was completed, it was quenched by addition of TEA and MeOH. The MS were removed by filtration over Celite, the organic phase was washed 1x $NaHCO_3$ (saturated aqueous solution), 1x H_2O, 1x brine and dried over Na_2SO_4. After filtration, the crude was concentrated in vacuo.

*General procedure **E**: Two steps azide introduction via O-triflate*

To a solution of the SM (1 eq.) in DCM (0.1 M), Py (4 eq.) and Tf_2O (1.2 eq.) were added at the proper temperature (as indicated in the specific procedures).

When the TLC showed the full SM conversion, the mixture was diluted with DCM and washed with cold HCl 5% and cold $NaHCO_3$ (saturated aqueous solution), dried over Na_2SO_4, filtered and concentrated in vacuo.

The crude triflate was dissolved in DMF (0.2 M), then NaN_3 (5 eq.) and 15-crown-5 (0.1 eq) were added. The reaction mixture was stirred at the proper temperature (as indicated in the specific procedures) until full conversion of the triflate into a new compound.

The reaction mixture was diluted with Et_2O and washed 3x H_2O and 1x brine. The organic phase was dried over Na_2SO_4, filtered and concentrated in vacuo.

*General procedure **F**: azide reduction*

The SM (1 eq.) was dissolved in MeOH (0.2 M), then DIPEA (6 eq.) and PDT (6 eq.) were added and the reaction mixture was stirred until complete SM conversion (TLC).

The solvent was removed under reduced pressure.

*General procedure **G**: allyl to propenyl isomerization*

The SM (1 eq.) was dissolved in THF (0.05 M) under Ar atmosphere. The solution was degassed three times by freezing it in a liquid N_2 bath under Ar and allowed to warm up to RT under vacuum, in order to remove Ar and O_2. [Ir] catalyst was added (0.1 eq.) and the solution was degassed once again. The [Ir] catalyst was then activated using a H_2 balloon. The catalyst activation was confirmed by the change of the solution color from red to pale-yellow/colorless. The excess of H_2 was immediately removed through vacuum/Ar cycles in order to prevent alkene hydrogenation. If the color of the solution turned back to red, H_2-vacuo-Ar cycles were repeated until the pale-yellow color became persistent.

The reaction progress was monitored by ^1H NMR. After SM full conversion, the solvent was removed under reduced pressure.

*General procedure **H**: ozonolysis and aldehyde reduction*

The SM (1 eq.) was dissolved in DCM (0.02 M). The solution was cooled down to -78°C and O_3 was bubbled until the color of the solution turned to blue or, anyway, until the HPTLC

showed the full conversion of the SM. N_2 was then bubbled in order to remove the excess of O_3.

A solution of $NaBH_4$ (6 eq.) in MeOH:H_2O 7:3 was added and the mixture was allowed to warm to RT and stirred until full reduction of the aldehyde was achieved (TLC).

The solution was washed with H_2O and brine and the organic phase was dried over Na_2SO_4, filtered and concentrated under reduced pressure.

*General procedure **I**: mesylation*

The SM (1 eq.) was dissolved into dry DCM (0.1 M). The solution was cooled to 0°C and Py (6 eq.) and Ms-Cl (5 eq.) were added.

When the TLC showed the full conversion of the SM, the solution was washed with 2x HCl 5%, 1x $NaHCO_3$ (saturated aqueous solution) and the organic phase was dried over Na_2SO_4 and filtered. The solvent was evaporated under reduced pressure.

*General procedure **J**: iodide introduction*

To a solution of the SM (1 eq.) in butanone (0.1 M), NaI (5 eq.) was added. The mixture was stirred at 60°C until full SM conversion was detected by TLC.

The solvent was removed under reduced pressure, the crude was dissolved in chloroform and the solution washed with aq. $NaHSO_3$ 10% and H_2O. The organic phase was dried over Na_2SO_4, filtered and the solvent was removed under reduced pressure.

*General procedure **K**: Arbuzov reaction*

The SM (1 eq.) was dissolved in $P(OMe)_3$ (10 mL/mmol SM). The solution was stirred at 100°C and 300 mmHg. When full conversion of the SM was observed, the phosphite was removed under reduced pressure.

*General procedure **L**: O-alkylation with Bn-Br or PMB-Cl*

The SM (1 eq.) was dissolved in DMF (0.2 M). Bn-Br or PMB-Cl (1.2 eq. per OH) and TBAI (0.1 eq. per OH, when required) were added, followed by slow addition of NaH (60% in mineral oil, 1.5 eq per OH).

When the reaction was completed (TLC), the excess of NaH was quenched by slow and careful addition of MeOH and the mixture was diluted with Et_2O. The solution was washed

3x H_2O and 1x brine and the organic phase was dried over Na_2SO_4. After salt filtration, the solvent was removed under reduced pressure.

*General procedure **M**: PMB deprotection*

The SM (1 eq.) was dissolved in a mixture DCM:H_2O (0.1 M). DDQ (2.2 eq. per PMB) was added and the reaction was stirred at RT until full SM conversion was achieved (TLC).
The mixture was diluted with DCM and washed with $NaHCO_3$ (saturated aqueous solution), H_2O and brine. The organic layer was dried over Na_2SO_4, filtered and the solvent was removed under reduced pressure.

*General procedure **N**: phosphonoester monohydrolysis*

To a solution of the SM in the proper solvent (0.1 M, indicated in the specific procedure), PhSH (5 eq. per OH) and the proper base (5 eq. per OH, indicated in the specific procedure) were added. The mixture was stirred at RT until full SM conversion into a more polar compound was achieved (TLC). The reaction mixture was concentrated under reduced pressure.

*General procedure **O**: silylation*

The SM (1 eq.) was dissolved in DCM (0.1 M). Imidazole (2.2eq.) was added and the solution was stirred for 10' at RT. The solution was cooled to 0°C and the proper silyl-chloride (1.2 eq., as reported in the specific procedure) was added.
When the reaction was completed (TLC), the reaction mixture was washed with H_2O and brine. The organic phase was dried over Na_2SO_4, filtered and the solvent was removed under reduced pressure.

*General procedure **P**: silyl ether cleavage*

TBAF (1M in THF, 2 eq.) was added to a solution of SM (1 eq.) in THF (0.1M) at 0°C. When TLC showed full SM conversion, the solvent was removed under reduced pressure.

*General procedure **Q**: selective deacetylation*

Hydrazine hydrate (1.8 eq.) was dissolved in MeOH (1 M). AcOH (1.5 eq.) was slowly added at 0°C and the solution was stirred for 20 min to give hydrazine acetate.

The freshly prepared hydrazine acetate solution was slowly added to a solution of the SM (1 eq.) in DMF (0.5M).

When the reaction was completed (TLC), the reaction mixture was diluted with Et_2O and washed 1x H_2O and 1x brine. The organic phase was dried over Na_2SO_4, filtered and the solvent was removed under reduced pressure.

*General procedure **R**: Mitsunobu reaction*

Phosphonate and alcohol fragments (in the proper molar ratio, as indicated in the specific procedure) and freshly crystallized PPh_3 (2.2 eq.) were dissolved in dry THF (0.05M). DIAD (2.2 eq.) was added dropwise at 0°C and the solution was stirred at RT for approximately 12 h. After reaction completion (TLC), the solvent was removed under reduced pressure.

4.3 Synthesis of MenA CPS phosphono-analogues

4.3.1 Synthesis of the mannoside fragment

*N-(benzyloxycarbonyl)aminopropyl 2,3,4,6-tetra-O-acetyl-β-D-glucopyranoside (**4**)*

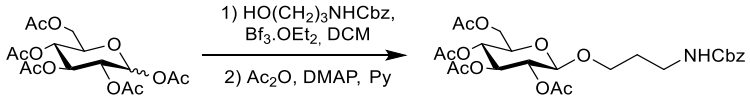

3 4

40%

1,2,3,4,6-penta-O-acetyl-D-glucopyranose **3** (4.96 g, 12.7 mmol) and benzyl N-(3-hydroxypropyl)carbamate (5.27 g, 25.2 mmol) were dissolved in DCM (130 mL). The solution was cooled to 0°C and $BF_3{\cdot}OEt_2$ (3.16 mL, 25.6 mmol) was added dropwise. The temperature was allowed to increase to RT and the reaction progress was monitored by TLC (Hex:EtOAc 1:1).

After 72 h, Py (7.2 mL, 88.5 mmol), Ac_2O (3.6 mL, 38.4 mmol) and DMAP (catalytic amount) were added and the mixture was stirred for additional 3 h, after which the TLC (Tol:EtOAc 6:4) showed the total disappearance of the starting material.

The solution was diluted with DCM and washed 3xHCl 5% and 1x$NaHCO_3$ (saturated aqueous solution). The organic phase was dried over Na_2SO_4, filtered and concentrated in vacuo.

The crude was purified by flash chromatography (Hex:EtOAc 6:4 to 1:1) to give compound **4** in 40% yield (2.77 g, 5.08 mmol).

Characterization

The spectroscopic data were in agreement with those reported in literature[97].

*N-(benzyloxycarbonyl)aminopropyl 4,6-O-benzylidene-β-D glucopyranoside (**5**)*

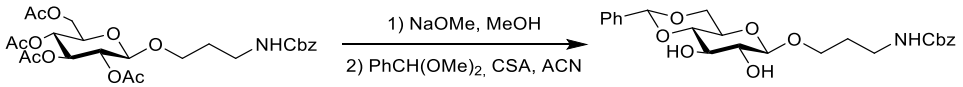

4 5

70%

Deacetylation of compound **4** (2.29g, 4.24 mmol) was carried out following *General procedure **B***.

The deacetylated mannoside was then converted into compound **5** through *General procedure **C***.

Reaction mixture purification by flash chromatography (Hex:EtOAc 3:7) led to compound **5** (1.34 g, 2.97 mmol) in 70% yield.

Characterization

^{1}H NMR (400 MHz, $CDCl_3$) δ 7.55 – 7.30 (m, 10H, H-Arom), 5.56 (s, 1H, C*H* benzylidene), 5.16 – 5.02 (m, 3H, N*H*, CH_2Ph), 4.42 – 4.32 (m, 2H, H-1, H-6a), 4.05 – 3.96 (m, 1H, H-7a), 3.89 – 3.75 (m, 2H, H-3, H-6b), 3.70 – 3.42 (m, 5H, H-2, H-4, H-5, H-7b, H-9a), 3.33 – 3.22 (m, 1H, H-9b), 1.96 – 1.72 ppm (m, 2H, H-8a,b).

^{13}C NMR (101 MHz, $CDCl_3$) δ 157.01 (*C*O), 137.18-136.65-129.89-129.37-129.15-128.69-128.45-128.31-126.44 (C-Arom), 103.49 (C-1), 102.02 (C-C*H* benzylidene), 80.62 (C-4), 74.74 (C-2), 73.53 (C-3), 68.81 (C-6), 67.49 (C-7), 67.00 (*C*H_2Ph), 66.59 (C-5), 37.87 (C-9), 29.89 ppm (C-8).

MS (ESI+) *m/z* calculated $[M+Na]^+$=482.2; found=482.2 (20%);

m/z calculated $[2M+Na]^+$=940.4; found=940.8 (100%)

N-(benzyloxycarbonyl)aminopropyl 3-O-acetyl-4,6-O-benzylidene-β-D glucopyranoside ***(6)***

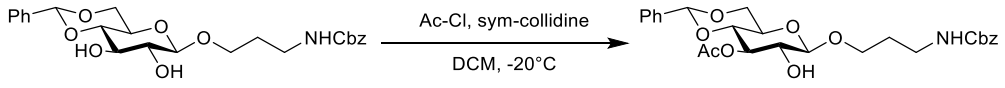

5 6

60%

5 (2.30 g, 5.0 mmol) was dissolved in DCM (75 mL, 0.07 M). Sym-collidine (3.31 mL, 25 mmol) was added and the solution was cooled to -20°C. After 5', acetyl chloride (0.93 mL, 6.0 mmol) was added dropwise and the reaction progress was monitored by TLC (Hex:EtOAc 3:7).

After 24h, the reaction mixture was diluted with H_2O and washed 2xHCl 5% and 1x $NaHCO_3$ (saturated aqueous solution). The organic phase was dried over Na_2SO_4, filtered and the solvent was removed under reduced pressure.

The crude was purified by flash chromatography (Hex:EtOAc 1:1 to 3:7) to give compound **6** (1.51 g, 3.02 mmol) in 60% yield.

Characterization

^{1}H NMR (400 MHz, $CDCl_3$) δ 7.51 – 7.31 (m, 10H, H-Arom), 5.51 (s, 1H, C*H* benzylidene), 5.24 (t, *J*= 9.4 Hz, 1H, H-3), 5.18 – 5.02 (m, 3H, CH_2Ph, N*H*), 4.43 (d, *J*= 7.7 Hz, 1H, H-1), 4.36 (dd, *J* = 10.5, 4.9 Hz, 1H, H-6a), 4.06 – 3.96 (m, 1H, H-7a), 3.79 (t, *J* = 10.2 Hz, 1H, H-6b), 3.71 – 3.47 (m, 5H, H-2, H-4, H-5, H-7b, H-9a), 3.33 – 3.22 (m, 1H, H-9b), 2.16 (s, 3H, CH_3CO), 1.94 – 1.70 ppm (m, 2H, H-8a,b).

^{13}C NMR (101 MHz, $CDCl_3$) δ 170.78-156.97 (*C*O), 137.12-136.68-129.21-128.69-128.37-128.31-126.29 (C-Arom), 103.89 (C-1), 101.62 (*C*H benzylidene), 78.65 (C-4), 73.84 (C-3), 73.49 (C-2), 68.78 (C-6), 67.68 (C-7), 67.01 (*C*H_2Ph), 66.66 (C-5), 37.82 (C-9), 29.85 (C-8), 21.15 ppm (*C*H_3CO).

MS(ESI+) *m/z* calculated $[M+Na]^+$=524.2; found=524.4 (30%)

N-(benzyloxycarbonyl)aminopropyl 3-O-acetyl-2-azido-4,6-O-benzylidene-2-deoxy-β-D mannopyranoside (7)

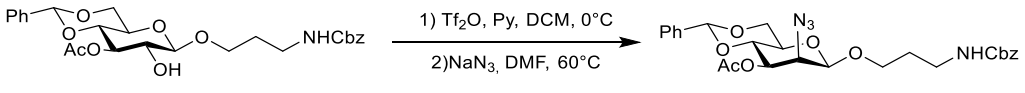

6 7

84%

Compound **6** (1.25 g, 2.59 mmol) was converted into the azido derivative **7** as described in *General Procedure **E***.

The crude was purified by flash chromatography (Hex:EtOAc 2:1) to give **7** (1.1 g, 2.10 mmol) in 84% yield.

Characterization

^{1}H NMR (400 MHz, $CDCl_3$) δ 7.50 – 7.31 (m, 10H, H-Arom), 5.55 (s, 1H, C*H* benzylidene), 5.25 – 4.98 (m, 4H, CH_2Ph, N*H*, H-3), 4.73 (br. s, 1H, H-1), 4.34 (dd, *J* = 10.5, 4.9 Hz, 1H, H-6a), 4.28 – 4.19 (m, 1H, H-2), 4.05 – 3.92 (m, 2H, H-4, H-7a), 3.87 (t, *J* = 10.3 Hz, 1H, H-6b), 3.71 – 3.62 (m, 1H, H-7b), 3.49 – 3.26 (m, 3H, H-5, H-9a,b), 2.17 (s, 3H, CH_3CO), 1.95 – 1.80 ppm (m, 2H, H-8a,b).

^{13}C NMR (101 MHz, $CDCl_3$) δ 170.40-(*C*O), 137.06-129.35-128.66-128.44-128.24-126.30 (C-Arom), 102.04 (*C*H benzylidene), 100.29 (C-1), 75.54 (C-4), 71.15 (C-3), 68.49 (C-6), 68.03 (C-7), 67.59 (C-5), 66.78 (*C*H_2Ph), 62.58 (C-2), 38.30 (C-9), 29.83 (C-8), 20.93 ppm (*C*H_3CO).

MS (ESI+) *m/z* calculated $[M+Na]^+$=549.2; found=549.5 (100%)

*N-(benzyloxycarbonyl)aminopropyl 2-acetamido-3-O-acetyl-4,6-O-benzylidene-2-deoxy-β-D mannopyranoside (**8**)*

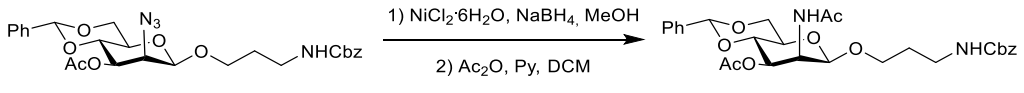

7 8 96%

$NiCl_2 \cdot 6H_2O$ (150 mg, 0.06 mmol) was added to a solution of **7** in MeOH (6 mL, 0.1 M). The solution was cooled to 0°C and $NaBH_4$ (30 mg, 0.79 mmol) was added. After 15', the TLC (Tol:Acetone 3:1) showed complete SM conversion and the solvent was removed in vacuo. The crude amine was converted into compound **8** according to *General procedure **A***. Purification by flash chromatography (Tol:Acetone 3:1) led to compound **8** (313 mg, 0.58 mmol) in 96% yield.

Characterization

^{1}H NMR (400 MHz, $CDCl_3$) δ 7.51 – 7.31 (m, 10H, H-Arom), 5.90 (d, *J* = 8.0 Hz, 1H, N*H*), 5.56 (s, 1H, C*H* benzylidene), 5.22 – 4.97 (m, 4H, H-3, CH_2Ph, N*H*), 4.85 – 4.77 (m, 1H, H-2), 4.73 (br s, 1H, H-1), 4.35 (dd, *J* = 10.5, 4.8 Hz, 1H, H-6a), 3.96 – 3.87 (m, 1H, H-7a), 3.79 (t, *J* = 10.2 Hz, 2H, H-4, H-6b), 3.73 – 3.59 (m, 1H, H-7b), 3.57 – 3.46 (m, 1H, H-5), 3.43 – 3.22 (m, 2H, H-9a,b), 2.12 – 2.00 (m, 6H, 2x CH_3CO), 1.89 – 1.74 ppm (m, 2H, H-8a,b).

^{13}C NMR (101 MHz, $CDCl_3$) δ 171.00 (*C*O), 170.45 (CO), 136.80-136.41-128.57-128.33-128.22-126.19 (C-Arom), 102.05 (*C*H benzylidene), 99.58 (C-1), 76.30 (C-4), 70.76 (C-3), 68.50 (C-6), 67.46 (C-5), 66.84 (C-7), 66.71 (*C*H_2Ph), 51.10 (C-2) , 38.31 (C-9), 29.58 (C-8), 23.11 (*C*H_3CO), 20.96 ppm (*C*H_3CO).

MS (Q-TOF) *m/z* calculated $[M+Na]^+$=565.2162; found=565.2493 (100%).

*N-(benzyloxycarbonyl)aminopropyl 2-acetamido-3-O-acetyl-4-O-benzyl-2-deoxy-β-D mannopyranoside (**1**)*

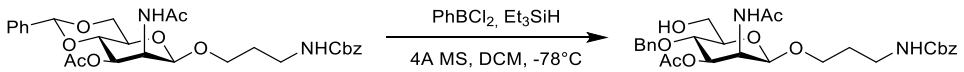

8 1

82%

Compound **8** (300 mg, 0.55mmol) was converted into alcohol **1** according to *General procedure **D***.

The crude was purified by flash chromatography (EtOAc) to give 1 (250 mg, 0.46 mmol) in 82% yield.

Characterization

^{1}H NMR (400 MHz, $CDCl_3$) δ 7.43 – 7.29 (m, 10H, H-Arom), 5.63 (d, *J* = 8.6 Hz, 1H, N*H*), 5.28 – 5.07 (m, 3H, N*H*, CH_2Ph), 5.00 (dd, *J* = 9.7, 3.8 Hz, 1H, H-3), 4.84 – 4.63 (m, 4H, H-1, H-2, CH_2Ph), 3.95 – 3.74 (m, 4H, H-4, H-7a, H-6a,b), 3.73 – 3.61 (m, 1H, H-7b), 3.48 – 3.36 (m, 2H, H-5, H-9a), 3.35 – 3.18 (m, 1H, H-9b), 2.13 – 1.95 (m, 6H, 2x CH_3CO), 1.86 – 1.72 ppm (m, 2H, H-8a,b).

^{13}C NMR (101 MHz, $CDCl_3$) δ 171.13-170.47 (*C*O), 128.71-128.65-128.38-128.13-127.89 (C-Arom), 98.97 (C-1), 75.99 (C-5), 75.09 (*C*H_2Ph), 74.81 (C-3), 72.51 (C-4), 67.03 (*C*H_2Ph, C-7), 61.50 (C-6), 51.05 (C-2), 29.83 (C-8), 23.28 (*C*H_3CO), 21.12 ppm (*C*H_3CO).

MS (Q-TOF) *m/z* calculated $[M+Na]^+$=567.2319; found=567.2095 (100%);

4.3.2 Synthesis of the phosphonate fragments

*Iodoether **12***

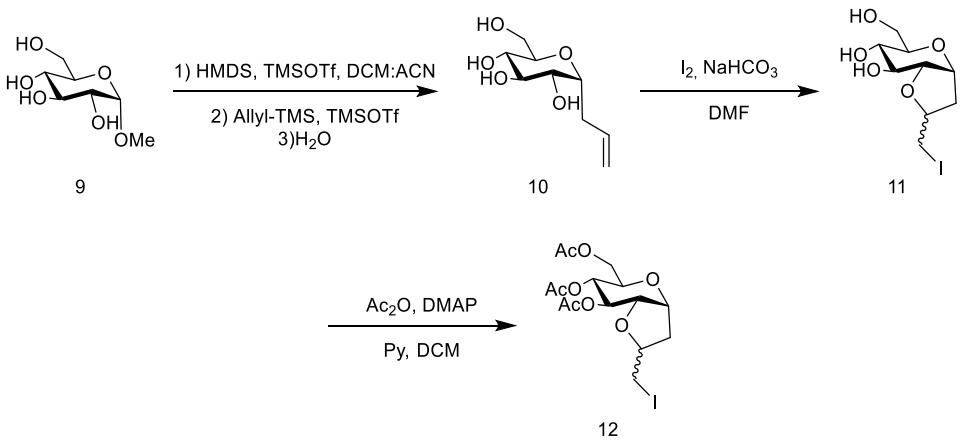

Methyl α-D glucopyranoside **9** (15 g, 77.50 mmol) was suspended in DCM:ACN 1:1 (250 mL, 0.3 M). HMDS (35.6 mL, 170.50 mmol) and TMSOTf (1.4 mL, 7.75 mmol) were added. The mixture was stirred at RT for about 30', until TLC (DCM:MeOH 8:2) showed the full conversion of **9**. The generated NH_3 was removed in vacuo for 2 h.

Allyl-TMS (24.7 mL, 155.0 mmol) was added, followed by the slow addition of TMSOTf (14.0 mL, 77.50 mmol). After 20h (TLC DCM:MeOH 8:2), cold H_2O (4.2 mL, 232.5 mmol) was added and the mixture was stirred for additional 30', after which it was quenched with TEA. The solvent was removed under reduced pressure and several co-evaporations with toluene were performed in order to remove H_2O traces.

The crude **10** was dissolved in DMF (500 mL, 0.15 M) and $NaHCO_3$ (25.04 g, 298,05 mmol) and I_2 (38.0 g, 150.82 mmol) were added. After 1 h, when the TLC (DCM:MeOH 9:1) showed the full conversion of **10**, $Na_2S_2O_3 \cdot 5H_2O$ was added to reduce the excess of I_2. The mixture was stirred until the color of the mixture turned from black to yellow and then the insoluble solids were filtered over Celite and the solvent was removed in vacuo.

The crude **11** was then converted into **12** as described in *General procedure **A***.

The crude **12** (achieved as a mixture of diastereomers) was used in the next reaction step without further purification. However a little amount of compound was purified by flash chromatography (Hex:EtOAc 8:2) for characterization.

Characterization

^{1}H NMR (400 MHz, $CDCl_3$) δ 5.17 (dd, *J* = 7.1, 5.2 Hz, 1H, H-3), 4.84 – 4.77 (m, 1H, H-4), 4.60 – 4.49 (m, H-1, H-1*), 4.39 – 4.29 (m, H-6a, H-6*a), 4.21 – 3.95 (m, H-2*, H-5, H-6b, H-6*b, H-8, H-8*), 3.95 – 3.86 (m, 1H, H-2), 3.36 – 3.13 (m, H-9a,b, H-9*a,b), 2.31 (ddd, *J* = 13.9, 7.3, 6.6 Hz, 1H, H-7a), 2.26 – 2.17 (m, 1H, H-7*a), 2.06 – 1.93 (m, 3xCH_3CO, H-7b), 1.89 – 1.79 ppm (m, 1H, H-7*b).

^{13}C NMR (101 MHz, $CDCl_3$) δ 170.69 (*C*O), 169.87 (*C*O), 169.47 (*C*O), 79.76 (C-2*), 79.01 (C-2), 78.64 (C-8), 73.70 (C-1*), 73.00 (C-1), 72.53, 72.00 (C-5), 71.24 (C-3), 70.74, 67.20, 67.09 (C-4), 62.00 (C-6*), 61.63 (C-6), 38.22 (C-7*), 36.99 (C-7), 20.87 (*C*H_3CO), 10.03 (C-9*), 9.06 ppm (C-9).

MS (Q-TOF) *m/z* calculated $[M+Na]^+$=479.0179; found: 479.0948 (100%)

*1-C-(3,4,6-tri-O-acetyl-α-D-glucopyranosyl)-3-prop-1-ene (**13**)*

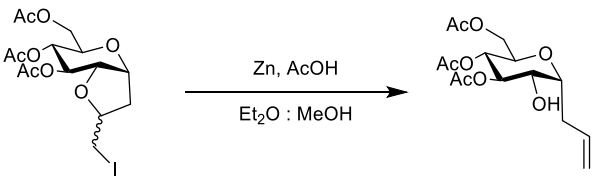

12 13

40%

Crude **12** was dissolved in Et_2O:MeOH (500 mL, 0.15 M). AcOH (8.4 mL, 147.0 mmol) and Zn (45.03 g, 689.0 mmol) were added and the mixture was stirred for 24 h, after which TLC (Hex:EtOAc 6:4) showed the SM full conversion. The insoluble residue was filtered over Celite and the solvent was removed under reduced pressure.

The crude was purified by flash chromatography (Hex:EtOAc 6:4) to give **13** (10.09 g, 30.50 mmol) in 40% yield over 4 steps.

Characterization

^{1}H NMR (400 MHz, CDCl3) δ 5.74 (ddt, *J* = 16.9, 10.2, 6.8 Hz, 1H, H-8), 5.14 – 5.01 (m, 3H, H3/H-4, H-9a,b), 4.85 (t, *J* = 8.1 Hz, 1H, H-3/H-4), 4.21 (dd, *J* = 12.1, 6.0 Hz, 1H, H-6a), 4.11 – 3.98 (m, 2H, H-1, H-6b), 3.83 (m, 2H, H-2, H-5), 2.48 – 2.38 (m, 2H, H-7a,b), 2.08 – 1.94 ppm (m, 9H, 3x C*H*$_3$CO).

^{13}C NMR (101 MHz, CDCl3) δ 171.05-170.75-169.62 (*C*O), 133.69 (C-8), 117.57 (C9), 73.79 (C-1), 73.18 (C-3/C-4), 69.59 (C-5/C-2), 69.51 (C-5/C-2), 68.44 (C-3/C-4), 62.06 (C-6), 30.32 (C-7), 20.90 (*C*H_3CO), 20.75 ppm (*C*H_3CO).

MS (Q-TOF) *m/z* calculated $[M+Na]^+$=353.1212; found: 378.3146 (100%)

*1-C-(3,4,6-tri-O-acetyl-2-azido-2-deoxy-α-D-mannopyranosyl)-3-prop-1-ene (**14**)*

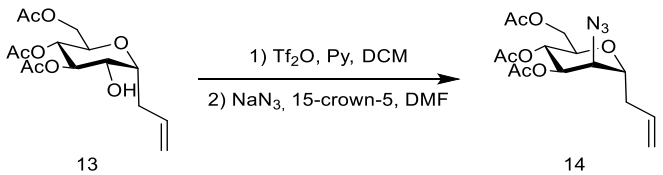

13 14

70%

Compound **13** (5.00 g, 15.38 mmol) was converted into **14** according to *General procedure **E***.

The crude was purified by flash chromatography (Hex:EtOAc 8:2) to give **14** (3.87 g, 10.77 mmol) in 70% yield.

Characterization

^{1}H NMR (400 MHz, $CDCl_3$) δ 5.86 – 5.72 (m, 1H, H-8), 5.30 (dd, *J* = 8.0, 3.5 Hz, 1H, H-3), 5.25 – 5.12 (m, 3H, H-4, H-9a,b), 4.31 (dd, *J* = 12.1, 6.3 Hz, 1H, H-6a), 4.15 – 3.98 (m, 2H, H-1, H-6b), 3.89 (m, 1H, H-5), 3.83 (br t, *J* = 3.7 Hz, 1H, H-2), 2.48 (qt, *J* = 14.1, 7.1 Hz, 2H, H-7a,b), 2.15 – 2.05 ppm (m, 9H, 3x C*H*$_3$CO).

^{13}C NMR (101 MHz, $CDCl_3$) δ 170.69-169.91-169.46 (*C*O), 132.48 (C-8), 118.61 (C-9), 73.39 (C-1), 70.96 (C-5), 70.19 (C-3), 66.75 (C-4), 61.89 (C-6), 60.45 (C-2), 34.46 (C-7), 20.72 (*C*H$_3$CO), 20.59 ppm (*C*H$_3$CO).

MS (Q-TOF) *m/z* calculated $[M+Na]^+$=378,1277; found: 378,3146 (100%)

*1-C-(2-azido-4,6-O-benzylidene-2-deoxy-α-D-mannopyranosyl)-3-prop-1-ene (**18**)*

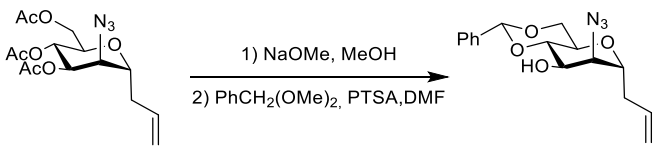

14 18

70%

14 (3.87 g, 10.77 mmol) was fully deacetylated according to *General procedure **B*** and converted into **18** through *General procedure **C***.

The crude was purified by flash chromatography (Hex:EtOAc 8:2) to give **18** (2.40g, 7.53 mmol) in 70% yield.

Characterization

^{1}H NMR (400 MHz, $CDCl_3$) δ 7.56 – 7.29 (m, 5H, H-Arom), 5.77 (m, 1H, H-8), 5.59 (s, 1H, C*H* benzylidene), 5.23 – 5.12 (m, 2H, H-9), 4.27 – 4.13 (m, 2H, H-3, H-6a), 4.05 (t, *J* = 7.8 Hz, 1H, H-1), 3.96 – 3.86 (m, 2H, H-2, H-4), 3.76 (t, *J* = 10.1 Hz, 1H, H-6b), 3.61 (td, *J* = 9.6, 4.8 Hz, 1H, H-5), 2.65 – 2.53 (m, 2H, O*H*, H-7a), 2.44 – 2.32 ppm (m, 1H, H-7b).

^{13}C NMR (101 MHz, $CDCl_3$) δ 137.17 (C-Arom), 132.91 (C-8)-129.47-128.53-126.34 (C-Arom), 118.77 (C- 9), 102.39 (*C*H benzylidene), 79.67 (C-4), 76.93 (C-1), 69.18 (C-3), 69.09 (C-6), 65.10 (C-5), 63.72 (C-2), 34.38 ppm (C- 2).

MS (ESI+) *m/z* calculated $[M+Na]^+$=340.14; found=340.39 (100%)

*1-C-[2-azido-4,6-O-benzylidene-2-deoxy-3-O-(4-methoxybenzyl)-α-D-mannopyranosyl]-3-prop-1-ene (**32**)*

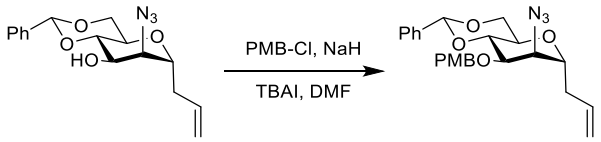

18 32

78%

18 (2.40g, 7.53 mmol) was converted into **32** as described in *General procedure **L***.
The crude was purified by flash chromatography (Hex:EtOAc 9:1 to 8:2) to give **32** (2.57g, 5.88 mmol) in 78% yield.

Characterization

^{1}H NMR (400 MHz, $CDCl_3$) δ 7.44 (ddd, *J* = 45.9, 5.5, 1.5 Hz, 5H, H-Arom), 7.30 (d, *J* = 8.6 Hz, 2H, H-Arom), 6.88 (d, *J* = 8.7 Hz, 2H, H-Arom), 5.79 – 5.64 (m, 1H, H-8), 5.64 (d, *J* = 5.6 Hz, 1H, C*H* benzylidene), 5.14 – 4.99 (m, 2H, H-9), 4.83 (d, *J* = 11.8 Hz, 1H, C*H*HPh) 4.67 (d, *J* = 11.9 Hz, 1H, C*H*HPh), 4.20 (dd, *J* = 10.3, 4.8 Hz, 1H, H-6a), 4.12 (dd, *J* = 12.9, 6.3 Hz, 1H, H-4), 4.00 – 3.89 (m, 2H, H-3, H-1), 3.85 – 3.72 (m, 5H, H-2, H-6b, OC*H*$_3$), 3.59 (td, *J* = 9.6, 4.7 Hz, 1H, H-5), 2.56 – 2.43 (m, 1H, H-7a), 2.34 – 2.23 ppm (m, 1H, H-7b).

^{13}C NMR (101 MHz, $CDCl_3$) δ 132.94 (C-8), 129.57 - 126.15 (C-Arom), 118.65 (C-9), 113.90 (C-Arom), 101.72 (*C*H benzylidene), 79.68 (C-4), 76.78 (C-1), 74.79 (C-3), 73.01 (*C*H$_2$Ph), 69.17 (C-6), 65.70 (C-5), 62.79 (O*C*H$_3$), 55.44 (C-2), 34.40 ppm (C-7).

MS (ESI+) *m/z* calculated $[M+Na]^+$=460.18; found=460.55 (100%)

*1-C-[2-azido-2-deoxy-3-O-(4-methoxybenzyl)-α-D-mannopyranosyl]-3-prop-1-ene (**34**)*

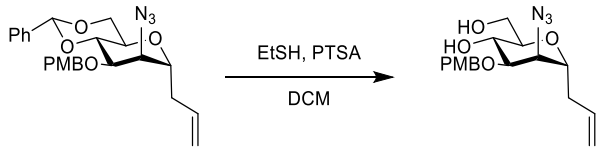

32 34

Compound **34** (2.57 g, 5.88 mmol) was dissolved in DCM (120 mL, 0.05M). EtSH (1.70 mL, 23.52 mmol) and PTSA (67 mg, 0.35 mmol) were added. After 30', TLC (Hex:EtOAc 8:2) showed that the reaction was completed. TEA was added till neutral pH and the solvent was removed under reduced pressure.

The crude could be used in the next step without purification.

Characterization

^{1}H NMR (400 MHz, $CDCl_3$) δ 7.29 (dd, *J* = 8.9, 6.2 Hz, 2H, H-Arom), 6.96 – 6.86 (m, 2H, H-Arom), 5.79 – 5.65 (m, 1H, H-8), 5.19 – 5.04 (m, 2H, H-9), 4.74 – 4.51 (m, 2H, C*H*$_2$Ph), 4.02 – 3.94 (m, 1H, H-1), 3.90 (t, *J* = 8.9 Hz, 1H, H-5), 3.85 – 3.68 (m, 7H, OC*H*$_3$, H-6a, H-2, H-6b, O*H*), 3.54 – 3.45 (m, 3H, H-4, H-3, O*H*), 2.48 (ddd, *J* = 14.6, 8.0, 6.7 Hz, 1H, H-7a), 2.25 ppm (dt, *J* = 24.8, 8.8 Hz, 1H, H-7b).

*1-C-[2-azido-4,6-O-dibenzyl-2-deoxy-3-O-(4-methoxybenzyl)-α-D-mannopyranosyl]-3-prop-1-ene (**33**)*

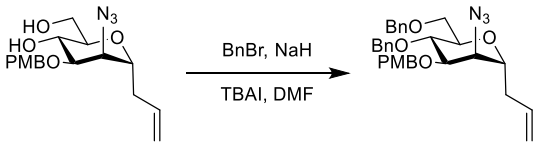

34 33

79%

34 (2.05g, 5.88 mmol) was converted into **33** according to *General procedure **L***.
The crude was purified by flash chromatography (Hex to Hex:EtOAc 8:2) to give **33** (2.46g, 4.65 mmol) in 79% yield.

Characterization

^{1}H NMR (400 MHz, $CDCl_3$) δ 7.38 – 7.25 (m, 10H, H-Arom), 7.23 – 7.16 (m, 2H, H-Arom), 6.84 (t, *J* = 9.4 Hz, 2H, H-Arom), 5.77 (ddt, *J* = 17.0, 10.4, 6.9 Hz, 1H, H-8), 5.16 – 5.01 (m, 2H, H-9), 4.76 – 4.47 (m, 6H, 3xCH_2Ph), 3.96 (dd, *J* = 11.6, 6.8 Hz, 1H, H-1), 3.91 – 3.84 (m, 1H, H-3), 3.83 – 3.76 (m, 4H, OCH_3, H-4), 3.74 – 3.58 (m, 4H, H-5, H-6, H-2), 2.46 – 2.27 ppm (m, 2H, H-7).

^{13}C NMR (101 MHz, $CDCl_3$) δ 159.65-138.39-138.12 (C-Arom), 133.55 (C- 8), 129.91-128.57-128.47-127.90 (C-Arom), 118.08 (C-9), 114.07 (C-Arom), 78.03 (C-3), 74.27 (C-6), 74.22 (C-1), 73.61 (C-5), 73.48 (CH$_2$Ph), 73.10 (C-4), 72.42 (CH$_2$Ph), 68.93 (CH$_2$Ph), 60.61 (C-2), 55.41 (OCH$_3$), 35.09 ppm (C-7).

MS (ESI+) *m/z* calculated $[M+Na]^+$=552.26; found=552.15 (100%)

*1-C-[2-azido-4,6-O-dibenzyl-2-deoxy-3-O-(4-methoxybenzyl)-α-D-mannopyranosyl]-1-propene (**38**)*

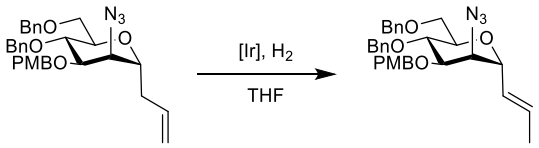

33 38

Quantitative

Isomerization of allyl **33** (2.46g, 4.65 mmol) to propenyl **38** was carried out according to *General procedure **G***.

The crude was purified by filtration on silica (Hex:EtOAc 7:3) to give 38 (2.46g, 4.65 mmol) in quantitative yield.

Characterization

^{1}H NMR (400 MHz, $CDCl_3$) δ 7.42 – 7.18 (m, 12H, H-Arom), 6.95 – 6.81 (m, 2H, H-Arom), 5.81 – 5.63 (m, 1H, H-8), 5.50 (ddt, *J* = 15.6, 5.7, 1.5 Hz, 1H, H-7), 4.82 – 4.48 (m, 6H, 3xC*H*$_2$Ph), 4.46 – 4.41 (m, 1H, H-1), 3.94 – 3.88-3.68 (m, 3H, H-3, H-4, H-5), 3.83 (s, 3H, OC*H*$_3$), 3.77 – 3.68 (m, 3H, H-2, H-6), -1.74 ppm (dt, *J* = 6.4, 1.4 Hz, 3H, H-9).

^{13}C NMR (101 MHz, $CDCl_3$) δ 130.92 (C-8), 129.77-128.38-128.03-127.79-127.55 (C-Arom), 126.80 (C-7), 113.91 (C-Arom), 78.39 (C-3), 74.45 (C-1), 74.34 (C-5), 74.17 (*C*H_2Ph), 73.66 (*C*H_2Ph), 73.39 (*C*H_2Ph), 72.34 (C-4), 68.97 (C-6), 61.73 (C-2), 55.28 (O*C*H_3), 18.08 ppm (C-9).

MS (ESI+) *m/z* calculated $[M+Na]^+$=552.26; found=552.15 (100%)

*C-[2-azido-4,6-O-dibenzyl-2-deoxy-3-O-(4-methoxybenzyl)-α-D-mannopyranosyl]-methanol (**39**)*

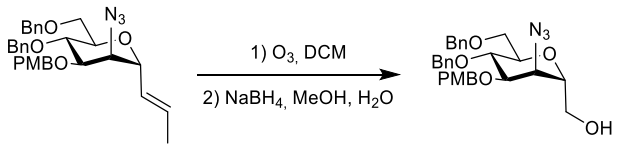

38 39

60%

Compound **38** (2.00 g, 3.77) mmol was converted into **39** according to *General procedure **H***.

The crude was purified by flash chromatography (6:4 to 5:5 Hex:EtOAc) to give compound **39** (1.18 g, 2.26 mmol) in 60% yield.

Characterization

^{1}H NMR (400 MHz, $CDCl_3$) δ 7.45 – 7.26 (m, 10H, H-Arom), 7.23 (d, *J* = 8.7 Hz, 2H, H-Arom), 6.88 (d, *J* = 8.8 Hz, 2H, H-Arom), 4.68 – 4.48 (m, 6H, 3xCH_2Ph), 4.08 (dt, *J* = 6.8, 4.6 Hz, 1H, H-1), 3.99 – 3.89 (m, 2H, H-3, H-4), 3.84 (s, 3H, OCH_3), 3.81 – 3.75 (m, 3H, H-6a, H-7), 3.75 – 3.64 (m, 3H, H-2, H-5, H-6b), 2.51 ppm (brs, 1H, O*H*).

^{13}C NMR (101 MHz, $CDCl_3$) δ 159.56-138.05-137.72-129.74- 129.37- 128.50-128.42-127.92-127.74-113.95 (C-Arom), 76.68 (C-3), 74.41 (C-1), 73.29 (C-5), 72.93-72.74-72.65 (CH_2Ph), 70.99 (C-4), 68.20 (C-6), 61.97 (C-7), 56.85 (C-2), 55.29 ppm (CH_3).

MS (ESI+) *m/z* calculated $[M+Na]^+$=542.24; found=542.23 (100%)

*C-[2-acetamido-4,6-O-dibenzyl-2-deoxy-3-O-(4-methoxybenzyl)-α-D-mannopyranosyl]-methanol (**37**)*

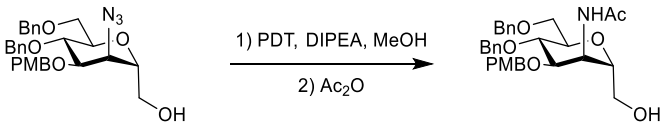

39 37

94%

Azide **39** (1.18 g, 2.26 mmol) was reduced to the corresponding amine according to *General procedure **F***.

Ac_2O (1.16 mL, 11.3 mmol) was added at 0°C to crude **37** and the mixture was stirred for additional 30'. The crude was purified through flash chromatography (Hex: EtOAc 4:6 to 2:8) to give **37** (1.14 g, 2.12 mmol) in 94% yield.

Characterization

^{1}H NMR (400 MHz, $CDCl_3$) δ 7.36 – 7.16 (m, 10H, H-Arom), 7.05 – 6.98 (m, 2H, H-Arom), 6.84 – 6.69 (m, 2H, H-Arom), 5.62 (d, *J* = 8.9 Hz, 1H, N*H*), 4.57 (d, *J* = 12.2 Hz, 1H, C*H*HPh), 4.50 – 4.40 (m, 3H, CH_2Ph, C*H*HPh), 4.36 (d, *J* = 11.6 Hz, 1H C*H*HPh), 4.22 (dt, *J* = 8.9, 3.5 Hz, 1H, H-2), 4.16 (m, 1H, H-5), 4.05 (d, *J* = 11.4 Hz, 1H, C*H*HPh), 3.73 (s, 3H, OCH_3), 3.71 – 3.60 (m, 3H, H-4, H-6a, H6-b), 3.60 – 3.49 (m, 3H, H-3, H-7), 3.45 (td, *J* = 10.5, 9.2, 3.5 Hz, 1H, H-1), 1.76 ppm (s, 3H, CH_3CO).

^{13}C NMR (101 MHz, $CDCl_3$) δ 170.77 (*C*O), 159.74-138.13-137.85-129.92-129.23-128.84-128.42-128.29-128.05-127.87-127.66-114.18 (C-Arom), 75.60 (C-3), 73.43 (C-5), 73.14-71.79-71.60 (*C*H_2Ph), 71.15 (C-1), 70.96 (C-4), 67.75 (C-6), 62.00 (C-7), 55.34 (O*C*H_3), 44.71(C-2), 23.13 ppm (CH_3CO).

MS (ESI+) *m/z* calculated $[M+Na]^+$=358.26; found=558.54 (100%)

*C-[2-acetamido-4,6-O-dibenzyl-2-deoxy-3-O-(4-methoxybenzyl)-α-D-mannopyranosyl]-methyl methanesulfonate (**40**)*

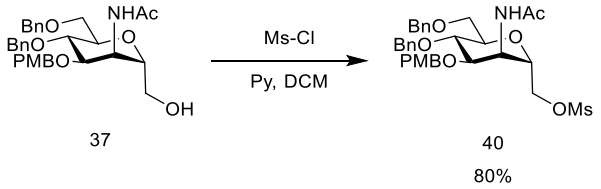

37 40

80%

37 (1.14 g, 2.12 mmol) was converted to **40** as reported in *General procedure **I***.

The crude was purified by flash chromatography (Hex:EtOAc 4:6 to 3:7) to give **40** (1.04 g, 1.70 mmol).

Characterization

^{1}H NMR (400 MHz, $CDCl_3$) δ 7.45-7.24 (m, 10H, H-Arom), 7.16-7.07 (m, 2H, H-Arom), 6.94-6.83 (m, 2H, H-Arom), 5.64 (d, *J* = 9.2 Hz, 1H, N*H*), 4.67-4.53 (m, 4H, 2x CH_2Ph), 4.46 (d, *J* = 11.4 Hz, 1H, C*H*HPh), 4.36 – 4.25 (m, 3H, H-2, H-7), 4.20 (d, *J* = 11.5 Hz, 1H, C*H*HPh), 4.16 (td, *J* = 6.2, 3.0 Hz, 1H. H-5), 3.99 – 3.89 (m, 1H, H-1), 3.83 (s, 3H, OCH_3), 3.80 (m, 1H, H-6a), 3.70 – 3.61 (m, 3H, H-3, H-4, H-6b), 3.02 (s, 3H, SO_2CH_3), 1.85 ppm (s, 3H CH_3CO).

^{13}C NMR (101 MHz, $CDCl_3$) δ 130.08-128.65-128.62-128.11-127.87-127.83-114.32 (C-Arom), 75.42 (C-3), 74.03 (C-5), 73.43 (C-7), 72.30-71.90-70.10 (CH_2Ph), 71.56 (C-4), 70.42 (C-1), 67.82 (C-6), 55.47 (OCH_3), 45.16 (C-2), 37.81 (SO_2CH_3), 23.39 ppm (CH_3CO).

MS (ESI+) *m/z* calculated $[M+Na]^+$=636.23; found=636.28 (100%)

*Dimethyl C-[2-acetamido-4,6-O-dibenzyl-2-deoxy-3-O-(4-methoxybenzyl)-α-D-mannopyranosyl]methanephosphonate (**42**)*

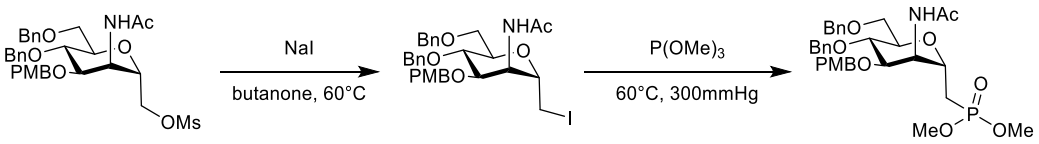

40 41 42

74%

40 (1.04 g, 1.70 mmol) was converted into iodide **41** according to *General procedure **J***. The crude iodide was treated with $P(OMe)_3$ according to *General procedure **K***.
Flash chromatography purification (EtoAc to EtOAc:MeOH 9:1) led to **42** (790 mg, 1.26mmol) in 74% yield over two steps.

Characterization

^{1}H NMR (400 MHz, $CDCl_3$) δ 7.41 – 7.25 (m, 10H, H-Arom), 7.14 (d, *J* = 8.7 Hz, 2H, H-Arom), 6.90 – 6.82 (d, *J* = 8.7 Hz, 2H, H-Arom), 5.82 (d, *J* = 9.3 Hz, 1H, N*H*), 4.66 (d, *J* = 11.9 Hz, 1H, C*H*HPh), 4.61 – 4.51 (m, 3H, CH_2Ph, C*H*HPh), 4.40 (d, *J* = 11.3 Hz, 1H, C*H*HPh), 4.37 – 4.33 (m, 1H, H-2), 4.30 (d, *J* = 11.4 Hz, 1H, C*H*HPh), 4.16 (m, 1H, H-1), 4.02 (dd, *J* = 5.0 Hz, 9.7 Hz, 1H, H-5), 3.91 – 3.85 (m, 1H, H-6a), 3.82 (s, 3H, OCH_3), 3.80-3.69 (m, 3H, H-3, H-4, H-6b), 3.75 (d, *J*= 12.6 Hz, 3H, POCH_3), 3.72 (d, *J*= 12.6 Hz, 3H, POCH_3), 2.21 – 2.00 (m, 2H, H-7), 1.89 ppm (s, 3H, CH_3CO).

^{13}C NMR (101 MHz, $CDCl_3$) δ 169.90 (*C*O), 159.57-138.05-137.89-129.95-129.40-128.40-127.97-127.84, 127.77-114.03 (C-Arom), 75.64 (C-3), 73.73 (C-5), 73.39-72.86 (*C*H_2Ph), 72.06 (C-4), 71.52 (C-1), 68.28 (C-6), 55.30 (O*C*H_3), 52.85 (d, *J*=5.9 Hz, PO*C*H_3), 52.21 (d, *J*=5.9 Hz, PO*C*H_3), 48.82 (d, *J*=13.2 Hz, C-2), 27.66 (d, *J*=145.2Hz, C-7), 23.39 ppm (*C*H_3CO).

^{31}P NMR (162 MHz, $CDCl_3$) δ 32.06 ppm.

MS (ESI+) m/z calculated $[M+Na]^+$=650.25; found=650.25 (100%).

*Methyl C-[2-acetamido-4,6-O-dibenzyl-2-deoxy-3-O-(4-methoxybenzyl)-α-D-mannopyranosyl]methanephosphonate triethylammonium salt(**46**)*

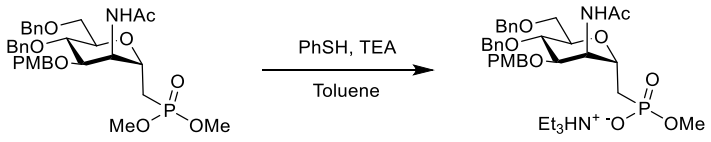

42 46

85%

42 (300 mg, 0.48 mmol) was converted into compound **46** as described in *General procedure **N***.

The crude was purified by flash chromatography (EtOAc to EtOAc:MeOH 8:2). The product, obtained as a mixture of acid and salts was passed through a column filled with Amberlite IR-120 resin, H^+ form. TEA was added in order to give compound **46** (292 mg, 0.41 mmol) as a single, trietylammonium salt in 85% yield over three steps.

Characterization

^{1}H NMR (400 MHz, $CDCl_3$) δ 7.33 – 7.04 (m, 12H, H-Arom), 6.79 – 6.70 (m, 2H, H-Arom), 6.29 (d, *J* = 9.0 Hz, 1H, N*H*), 4.73 – 4.61 (m, 2H, H-2, C*H*HPh), 4.59 – 4.27 (m, 5H, C*H*HPh, 2x CH_2Ph), 4.23 – 4.12 (m, 1H, H-1), 3.86 (dd, *J* = 7.5, 3.8 Hz, 1H, H-3), 3.78 – 3.67 (m, 2H, H-5, H-6a), 3.70 (s, 3H, OCH_3) 3.62 – 3.50 (m, 2H, H6-b, H-4) 3.54 (d, *J*=10.7 Hz, POCH_3), 2.98 (q, *J* = 7.3 Hz, 6H, 3xCH_2CH$_3$), 2.12 – 1.91 (m, 2H, H-7), 1.87 (s, 3H, CH_3CO), 1.23 ppm (t, *J* = 7.3 Hz, 9H, 3xCH$_2$CH_3).

^{13}C NMR (101 MHz, $CDCl_3$) δ 130.18-128.50-128.45-128.02-127.94-127.75-114.01 (C-Arom), 76.85(C-3), 73.93 (*C*H$_2$Ph), 73.79(*C*H$_2$Ph), 73.55 (C-4), 73.29 (C-5), 71.63 (*C*H$_2$Ph), 71.52 (C-1), 69.07 (C-6), 55.41 (O*C*H$_3$), 51.85 (PO*C*H$_3$), 49.65 (d, *J*≈5 Hz, C-2), 45.55 (*C*H$_2$CH$_3$), 28.44 (d, *J*=126 Hz, C-7), 23.64 (*C*H$_3$CO), 8.65 ppm (CH$_2$*C*H$_3$).

^{31}P NMR (162 MHz, $CDCl_3$) δ 22.85 ppm.

MS (ESI+) *m/z* calculated $[M+2Na]^+$=658.28; found=658.59 (100%)

*1-C allyl-2-azido-4-O-benzyl-6-O-(tert-butyl diphenysilyl)-2-deoxy-3-O-(4-methoxybenzyl)- α-D-mannopyranoside (**48**)*

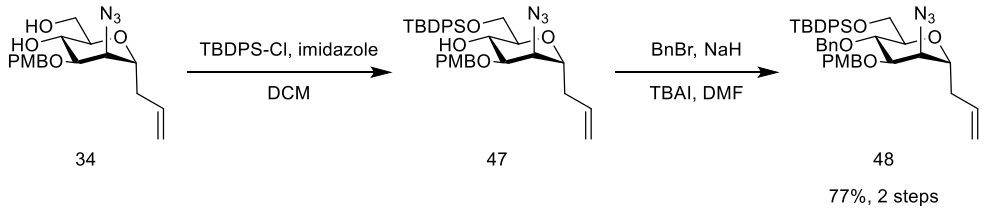

34 47 48

77%, 2 steps

34 (2.00 g, 5.88 mmol) was converted into **48** through the sequence of *General procedures* ***L*** and ***O***.

The crude was purified by flash chromatography (Hex to Hex:EtOAc 8:2) to give **48** (3.07 g, 4.53 mmol) in 77% yield.

Characterization

^{1}H NMR (400 MHz, $CDCl_3$) δ 7.59 (ddd, *J* = 8.1, 5.1, 1.4 Hz, 4H-Arom), 7.40 – 7.09 (m, 13H-Arom), 6.79 – 6.68 (m, 2H-Arom), 5.82 – 5.57 (m, 1H, H-8), 5.06 – 4.92 (m, 2H, H-9), 4.62 (d, *J* = 11.4 Hz, 1H, C*H*HPh), 4.53 – 4.45 (m, 3H, C*H*HPh, CH_2Ph), 3.92 – 3.75 (m, 5H, H-1, H-3, H-6, H-4), 3.72 (s, 3H, OCH_3), 3.69 – 3.63 (m, 1H, H-5), 3.49 (dd, *J* = 5.1, 2.9 Hz, 1H, H-2), 2.36 – 2.17 (m, 2H, H-7), 0.97 ppm (s, 9H, C(CH_3)$_3$).

^{13}C NMR (101 MHz, CDCl3) δ 138.05-135.74-135.58 (C-Arom), 134.79(C-8), 133.54-129.74-128.43-127.67-127.60 (C-Arom),117.69 (C-9), 113.89 (C-Arom), 77.60 (C-3), 74.95 (C-5), 73.80 (*C*H_2Ph), 73.58 (C-4), 72.25 (*C*H_2Ph), 72.08 (C-1), 62.69 (C-6), 60.39 (C-2), 55.28 (O*C*H_3), 35.25 (C-7), 26.82 ppm (C(*C*H_3)$_3$).

MS (ESI+) m/z calculated $[M+Na]^+$=700.32; found=700.37 (30%).

m/z calculated $[M+Na-N_2]^+$=682.32; found=682.46 (100%).

*1-C-[2-azido-4-O-benzyl-6-O-(tert-butyl diphenysilyl)-2-deoxy-3-O-(4-methoxybenzyl)-α-D-mannopyranosyl]-1-propene (**49**)*

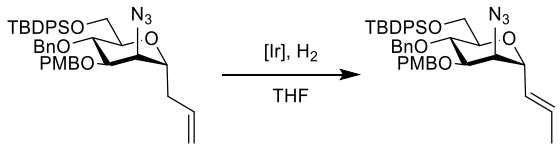

48 49

Quantitative

Isomerization of **48** (3.07 g, 4.53 mmol) to **49** was carried out according to *General procedure **G***.

The crude was purified by filtration on silica (Hex:EtOAc 7:3) to give **49** (3.07 g, 4.53 mmol) in quantitative yields.

Characterization

^{1}H NMR (400 MHz, $CDCl_3$) δ 7.71 – 7.00 (m, 17H, H-Arom), 6.82 – 6.69 (m, 2H, H-Arom), 5.71 – 5.59 (m, 1H, H-8), 5.36 (ddd, *J* = 15.5, 5.9, 1.7 Hz, 1H, H-7), 4.64 (d, *J* = 11.2 Hz, 1H, C*H*HPh), 4.55 – 4.44 (m, 3H, C*H*HPh, CH_2Ph), 4.36 – 4.26 (m, 1H, H-1), 3.93 – 3.77 (m, 4H, H-3, H-4, H-6), 3.73 (s, 3H, OCH_3), 3.71 – 3.64 (m, 1H, H-5), 3.56 (dd, *J* = 5.0, 3.2 Hz, 1H, H-2), 1.62 (dt, *J* = 6.5, 1.5 Hz, 3H, H-9), 0.98 ppm (s, 9H, C(CH_3)$_3$).

^{13}C NMR (101 MHz, $CDCl_3$) δ 135.93-135.79-130.95 (C-Arom), 129.92 (C-8), 128.57-128.09 (C-Arom), 127.82 (C-7), 127.74-127.34-114.03 (C-Arom), 78.11 (C-3), 75.18 (C-5), 74.11(*C*H_2Ph), 73.88 (C-4), 73.34 (C-1), 72.46 (*C*H_2Ph), 63.00 (C-6), 61.56 (C-2), 55.43 (O*C*H_3), 26.97 (C(*C*H_3)$_3$), 18.20 ppm (C-9).

MS (ESI+) m/z calculated $[M+Na]^+$=700.32; found=700.32 (80%).

m/z calculated $[M+Na-N_2]^+$=682.32; found=682.31 (100%).

*C-[2-azido-4-O-benzyl-6-O-(tert-butyl diphenysilyl)-2-deoxy-3-O-(4-methoxybenzyl)-α-D-mannopyranosyl]-methanol (**50**)*

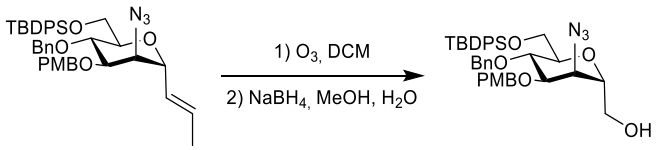

49 50

60%

Compound **49** (2.00 g, 2.95 mmol) was converted into **50** as described in *General procedure **H***.

The crude was purified by flash chromatography (Hex:EtOAc 7:3 to 6:4) to give compound **50** (1.18 g, 1.78 mmol) in 60% yield.

Characterization

^{1}H NMR (400 MHz, $CDCl_3$) δ 7.72 - 7.27 (m, 15H, H-Arom), 7.13 (d, *J*= 8.7 Hz, 2H, H-Arom), 6.78 (d, *J*= 8.7 Hz, 2H, H-Arom), 4.57-4.43 (m, 4H, 2x C*H*$_2$Ph), 3.98-3.84 (m, 4H, H-4, H-5, H-6), 3.79 (s, 3H, OC*H*$_3$), 3.78-3.73 (m, 2H, H-1, H-3), 3.69-3.65 (m, 2H, H-7), 3.61 (dd, *J*=8.6, 3.2 Hz, 1H, H-2), 1.93 (brs, 1H, O*H*), 1.04 ppm (s, 9H, (C(*CH*$_3$)$_3$)).

^{13}C NMR (101 MHz, CDCl3) δ 137.72-131.84-130.64-129.84-115.99 (C-Arom), 78.28 (C-5), 78.14 (C-4), 74.71-74.65 (*C*H$_2$Ph), 74.50 (C-1), 72.01 (C-3) , 64.41 (C-7), 64.06 (C-6), 58.53 (C-2), 57.39 (O*C*H$_3$) , 29.00 ppm (C(*CH*$_3$)$_3$).

MS (ESI+) m/z calculated $[M+Na]^+$=690.31; found=690.40 (100%).

*C-[2-acetamido-4-O-benzyl-6-O-(tert-butyl diphenysilyl)-2-deoxy-3-O-(4-methoxybenzyl)-α-D-mannopyranosyl]-methanol (**50**)*

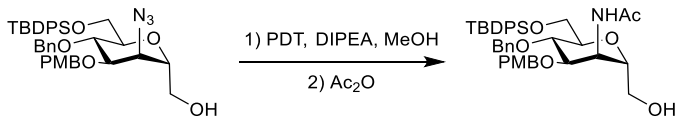

50 51

90%

Azide **50** (1.18 g, 1.78 mmol) was reduced to the corresponding amine according to *General procedure **F***.

After 24h, Ac_2O (1.16 mL, 11.3 mmol) was added at 0°C and the mixture was stirred for additional 30'. The crude was purified through flash chromatography (Hex: EtOAc 6:4 to 5:5) to give **51** (1.10 g, 1.60 mmol) in 90% yield.

Characterization

^{1}H NMR (400 MHz, $CDCl_3$) δ 7.56 - 7.15 (m, 15H, H-Arom), 6.91 (d, *J*= 8.7 Hz, 1H, H-Arom), 6.80 (d, *J*= 8.7 Hz, 1H, H-Arom), 5.56 (d, *J*= 9.0 Hz, 1H, N*H*), 4.54 (d, *J*= 12.5 Hz, 1H, C*H*HPh), 4.37 (d, *J*= 12.3 Hz, 1H, C*H*HPh), 4.32 (d, *J*= 11.5 Hz, 1H, C*H*HPh), 4.13 (td, *J*= 9.5, 9.0, 3.6 Hz, 1H, H-2), 4.01 (t, *J*= 7.0 Hz, 1H, H-5), 3.95 (d, *J*= 11.4 Hz, 1H, C*H*HPh), 3.85 (dd, *J*= 10.3, 7.6 Hz, 1H, H-6a), 3.78 (dd, *J*= 10.3, 6.5 Hz, 1H, H-6b), 3.75 - 3.71 (m, 1H, H-4), 3.67 (s, 3H, OC*H*$_3$), 3.55 - 3.49 (m, 1H, H-3), 3.46 - 3.32 (m, 2H, H-7), 3.25 (dt, *J* = 9.5, 2.9 Hz, 1H, H-1), 1.69 (s, 3H, C*H*$_3$CO), 0.92 ppm (d, *J* = 3.8 Hz, 9H, (C(*CH*$_3$)$_3$)).

^{13}C NMR (101 MHz, $CDCl_3$) δ 173.13 (Cquat), 140.05-137.71-135.63-135.35-132.05-131.33-130.63-130.08-129.87-116.31 (C-Arom), 77.70 (C-3), 77.19 (C-5), 73.80 (*C*H$_2$Ph), 72.82 (C-1), 72.40 (C-4), 64.12 (C-7), 63.75 (C-6), 57.47 (O*C*H$_3$), 46.76 (C-2), 29.03 (C(*CH*$_3$)$_3$), 25.20 ppm (*C*H$_3$CO).

MS (ESI+) m/z calculated $[M+Na]^+$=706.32; found=706.56 (100%).

*C-[2-acetamido-4-O-benzyl-6-O-(tert-butyl diphenysilyl)-2-deoxy-3-O-(4-methoxybenzyl)-α-D-mannopyranosyl]-methyl methanesulfonate (**52**)*

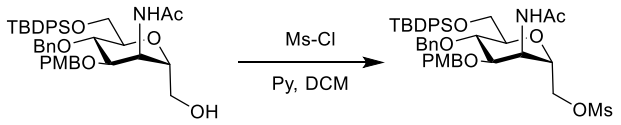

51 52

80%

51 (1.10 g, 1.60 mmol) was converted into **52** as described in *General procedure **I***.
The crude was purified by flash chromatography (Hex:EtOAc 6:4 to 4:6) to give **52** in 80% yield (975 mg, 1.28 mmol).

Characterization

^{1}H NMR (400 MHz, $CDCl_3$) δ 7.56-7.21 (m, 15H, H-Arom), 6.98 (d, *J*= 8.7 Hz, 2H, H-Arom), 6.74 (d, *J*= 8.7 Hz, 2H, H-Arom), 5.51 (d, *J*= 8.9 Hz, 1H, N*H*), 4.54 (d, *J*= 12.2 Hz, 1H, C*H*HPh), 4.48 (d, *J*= 12.2 Hz, 1H, C*H*HPh), 4.36 (d, *J*= 11.4 Hz, 1H, C*H*HPh), 4.21 (dd, *J*= 9.3, 3.5 Hz, 1H, H-2), 4.17 - 4.12 (m, 2H, H-7), 4.07 (d, *J*= 11.4 Hz, 1H, C*H*HPh), 3.94 (dt, *J*= 6.2, 3.0 Hz, 1H, H-5), 3.85 (dd, *J*= 6.5, 2.3 Hz, 2H, H-6), 3.76 (dd, *J*= 4.2, 2.6 Hz, 1H, H-4), 3.74-3.68 (m, 1H, H-1), 3.73 (s, 3H, OCH_3), 3.54 (t, *J*= 3.9 Hz, 1H, H-3), 1.75 (s, 3H, SO_2CH_3), 1.19 (s, 3H, CH_3CO), 0.98 ppm (s, 9H, $C(CH_3)_3$).

^{13}C NMR (101 MHz, $CDCl_3$) δ 171.83 (Cquat), 139.86-137.72-135.26-132.05-131.19-130.66-129.96, 116.29 (C-Arom), 77.54 (C-5), 77.39 (C-3), 74.27-73.90 (CH_2Ph), 72.88 (C-4), 72.15 (C-1), 72.02 (C-7), 63.75 (C-6), 57.45 (OCH_3), 47.07 (C-2), 39.62 (SO_2CH_3), 25.39 ($C(CH_3)_3$), 21.34 ppm (CH_3CO).

MS (ESI+) m/z calculated $[M+Na]^+$=784.30; found=784.46 (100%).

*Dimethyl C-[2-acetamido-4-O-benzyl-6-O-(tert-butyl diphenysilyl)-2-deoxy-3-O-(4-methoxybenzyl)-α-D-mannopyranosyl]methanephosphonate (**54**)*

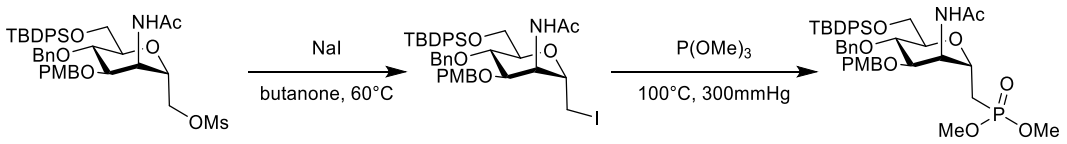

52 53 54

75%

52 (975 mg, 1.28 mmol) was converted into iodide **53** according to *General procedure **J***. The crude was treated with $P(OMe)_3$ according to *General procedure **K***.
Flash chromatography (EtOAc to EtOAc:MeOH 9:1) led to **54** (745 mg, 0,96 mmol) in 75% yield over two steps.

Characterization

^{1}H NMR (400 MHz, $CDCl_3$) δ 7.62 - 7.14 (m, 15H, H-Arom), 7.08 (d, *J*= 8.7 Hz, 2H, H-Arom), 6.75 (d, *J*= 8.7 Hz, 2H, H-Arom), 5.75 (d, *J*= 9.3 Hz, 1H, N*H*), 4.61 (d, *J*= 11.7 Hz, 1H, C*H*HPh), 4.52 (d, *J*= 11.7 Hz, 1H, C*H*HPh), 4.36 (d, *J*= 11.2 Hz, 1H, C*H*HPh), 4.28-4.25 (m, 1H, H-2), 4.26 (d, *J*= 11.0 Hz, 2H, C*H*HPh), 4.06-4.02 (m, 1H, H-1), 3.98 (dd, *J*= 10.5, 6.3 Hz, 1H, H-6a), 3.86-3.80 (m, 2H, H-4, H-6b), 3.76 - 3.72 (m, 1H, H-5), 3.71 (s, 3H, OCH_3), 3.67 - 3.63 (m, 1H, H-3), 3.56 (d, *J*= 10.9 Hz, 3H, POCH_3), 3.50 (d, *J*= 10.9 Hz, 3H, POCH_3), 2.06 - 1.86 (m, 2H, H-7), 1.80 (s, 3H, CH_3CO), 0.98 ppm (s, 9H, C(CH_3)$_3$).

^{13}C NMR (101 MHz, $CDCl_3$) δ 169.79 (*C*O), 138.02-135.61-135.53-133.24-133.16-130.00-129.79-129.47, 128.48-127.87, 127.77-114.03 (C-Arom), 75.74 (C-3), 74.97 (C-5), 73.08 (*C*H_2Ph), 71.58 (C-4), 71.50 (*C*H_2Ph), 68.46 (C-1), 62.03 (C-6), 55.30 (O*C*H_3), 52.78 (d, *J*= 5.9 Hz, PO*C*H_3), 52.14 (d, *J*= 5.9 Hz, PO*C*H_3), 48.89 (d, *J*= 13.2 Hz, C-2), 27.73 (d, *J*= 145.2Hz, C-7), 23.42 (C(*C*H_3)$_3$), 19.26 ppm (*C*H_3CO).

^{31}P NMR (162 MHz, $CDCl_3$) δ 31.37 ppm.

MS (ESI+) m/z calculated $[M+H]^+$=776.33; found=776.97 (100%).
m/z calculated $[M+Na]^+$=798.33; found=798.76 (40%).

*Methyl C-(2-acetamido-4-O-benzyl-6-O-(tert-butyl diphenysilyl)-2-deoxy-3-O-(4-methoxybenzyl)-α-D-mannopiranosyl)methanephopshonate triethylammonium salt (**55**)*

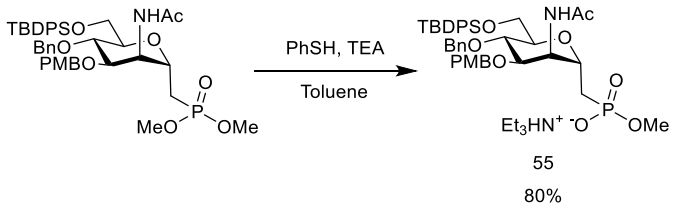

55

80%

54 (745 mg, 0,96 mmol) was converted into compound **55** as described in *General procedure **N***.

The crude was purified by flash chromatography (EtOAc to EtOAc:MeOH 8:2). The product, obtained as a mixture of acid and salts was passed through a column filled with Amberlite IR-120 resin, H^+ form. TEA was added in order to give compound **55** (663 mg, 0.77 mmol) as a single, triethylammonium salt in 80% yield.

Characterization

^{1}H NMR (400 MHz, $CDCl_3$) δ 7.69 (ddt, J = 17.0, 6.7, 1.5 Hz, 4H, H-Arom), 7.49 - 7.15 (m, 13H, H-Arom), 6.89 - 6.78 (m, 2H, H-Arom), 6.31 (d, J = 8.4 Hz, 1H, N*H*), 4.84 (d, *J*= 11.4 Hz, 1H C*H*HPh), 4.80-4.75 (m, 1H, H-2), 4.67 (d, *J*= 10.8 Hz, 1H, C*H*HPh), 4.55 (d, *J*= 11.2 Hz, 1H, C*H*HPh), 4.44 (d, *J*= 10.8 Hz, 1H, C*H*HPh), 4.26 (dt, *J*= 8.6, 5.0 Hz, 1H, H-1), 4.02 - 3.93 (m, 3H, H-3, H-6), 3.87 (t, *J*= 7.5 Hz, 1H, H-4), 3.80 (s, 3H, OC*H*$_3$), 3.70 (m, 1H, H-5), 3.58 (d, *J*= 10.6 Hz, 3H, POC*H*$_3$), 3.05 (q, *J*= 7.3 Hz, 6H, 3xC*H*$_2$CH$_3$), 2.19 - 1.90 (m, 2H, C-7), 1.97 (s, 3H, C*H*$_3$CO), 1.28 (t, *J*= 7.3 Hz, 9H, 3xCH$_2$C*H*$_3$), 1.07 ppm (s, 9H, C(C*H*$_3$)$_3$).

^{13}C NMR (101 MHz, $CDCl_3$) δ 135.84-135.68-130.29-129.87-128.49-127.89-113.97 (C-Arom), 77.16 (C-3), 74.32 (*C*H$_2$Ph), 74.22 (C-5), 73.37 (C-4), 71.98 (C-1), 71.35 (*C*H$_2$Ph), 62.83 (C-6), 55.40 (O*C*H$_3$), 51.90 (d, *J*= 5.4 Hz, PO*C*H$_3$), 49.46 (C-2), 45.45 (*C*H$_2$CH$_3$), 28.35 (d, *J*≈ 130 Hz, C-7), 23.71(C(*C*H$_3$)$_3$), 19.45(*C*H$_3$CO), 8.61 ppm (CH$_2$*C*H$_3$).

^{31}P NMR (162 MHz, $CDCl_3$) δ 22.20 ppm.

MS (ESI-) *m/z* calculated [M-TEA]$^-$=760.31; found=760.93 (100%)

4.3.3 Alternative phosphonate synthesis

*1-C allyl-4,6-O-benzylidene-1-deoxy-α-D-glucopiranoside (**66**)*

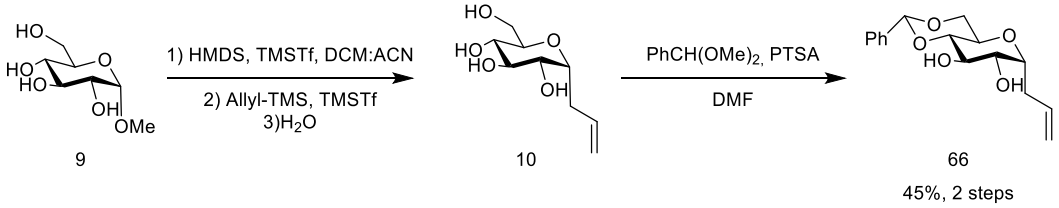

Methyl α-D glucopyranoside **9** (5.00 g, 25.75 mmol) was suspended in dry DCM:ACN 1:1 (75 mL, 0.3 M). HMDS (11.80 mL, 56.57 mmol) and TMSOTf (0.47 mL, 2.58 mmol) were added. The mixture was stirred for about 30' until the TLC (DCM:MeOH 8:2) showed the full conversion of **9** and then the generated NH_3 was removed in vacuo for 2 h.
Allyl-TMS (8.22 mL, 51.5 mmol) was added, followed by the slow addition of TMSOTf (4.66 mL, 51.5 mmol). After 20h, (TLC DCM:MeOH 8:2), cold H_2O (1.86 mL, 103 mmol) was added and the mixture was stirred for additional 30', after which the reaction was quenched with TEA, the solvent was removed under reduced pressure and several co-evaporations with toluene were performed in order to remove H_2O traces.
Intermediate **10** was converted into **66** according to *General procedure **C***.
The crude was purified by filtration on silica (Hex:EtOAc 2:8) to give **66** (3.39 g, 11.59 mmol) in 45% yield over 2 steps.

Characterization

^{1}H NMR (400 MHz, $CDCl_3$) δ 7.59 - 7.34 (m, 5H, H-Arom), 5.86 (dddd, *J*= 17.3, 10.1, 7.6, 6.2 Hz, 1H, H-8), 5.56 (s, 1H, C*H* benzylidene), 5.26 - 5.09 (m, 2H, H-7), 4.31 - 4.25 (m, 1H, H-6a), 4.20 (dt, *J*= 11.1, 4.9 Hz, 1H, H-1), 4.00 - 3.88 (m, 2H, H-2, H-3), 3.76 - 3.65 (m, 2H, H-6b, H-5), 3.50 (t, *J*= 8.8 Hz, 1H, H-4), 2.64 (d, *J*= 2.2 Hz, 1H, C3-O*H*), 2.61 - 2.50 (m, 1H, H-9), 2.48 ppm (d, *J* = 2.6 Hz, 1H, C2-O*H*).

^{13}C NMR (101 MHz, $CDCl_3$) δ 134.41 (C-8), 129.48-128.54-126.38 (C-Arom), 117.44 (C-9), 102.10 (*C*H benzylidene), 82.12 (C-4), 76.18 (C-1), 72.32 (C-2), 71.73 (C-3), 69.47 (C-6), 63.52 (C-5), 29.81 ppm (C-7).

MS (ESI+) *m/z* calculated $[M+Na]^+$=292.13; found=292.25 (100%).

*1-C allyl-3-O-acetyl-4,6-O-benzylidene-1-deoxy-α-D-glucopiranoside (**67**)*

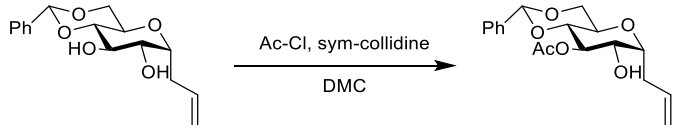

66 67

30%

Compound **66** (500 mg, 1.71 mmol) was dissolved in dry DCM (25 mL, 0.07 M). Sym-collidine (1.13 mL, 8.55 mmol) was added and the solution was cooled down to -20°C. Acetyl chloride (146 µL, 2.05 mmol) was added dropwise and the reaction progress was monitored by TLC (Hex:EtOAc 3:7).

After 15h, the reaction mixture was diluted with H_2O and washed 2x HCl 5% and 1x $NaHCO_3$ (saturated aqueous solution). The organic phase was dried over Na_2SO_4 and the solvent was removed under reduced pressure.

The crude was purified by flash chromatography (Hex:EtOAc 1:1 to 3:7) to give compound **67** (170 mg, 0.58 mmol) in 30% yield.

Characterization

^{1}H NMR (400 MHz, $CDCl_3$) δ 7.51 - 7.36 (m, 5H, H-Arom), 5.84 (ddt, *J*= 16.7, 10.4, 6.9 Hz, 1H, H-8), 5.53 (s, 1H, C*H* benzylidene), 5.25 - 5.13 (m, 3H, H-3, H-9), 4.29 (m, 1H, H-6a), 4.20 (dt, J = 10.6, 5.4 Hz, 1H, H-1), 4.01 (dt, *J*= 10.2, 5.4 Hz, 1H, H-2), 3.80 – 3.70 (m, 2H, H-5, H-6b), 3.64 (p, *J*= 9.4 Hz, 1H, H-4), 2.72 – 2.52 (m, 3H, H-7, O*H*), 2.18 ppm (s, 3H, C*H*$_3$CO).

^{13}C NMR (101 MHz, $CDCl_3$) δ 134.04 (C-8), 128.42-126.30 (C-Arom), 117.72 (C-9), 101.72 (*C*H benzylidene), 79.47 (C-4), 76.48 (C-1), 73.96 (C-3), 72.08 (C-2), 69.50 (C-6), 63.80 (C-5), 30.03 (C-7), 21.18 ppm (*C*H$_3$CO).

MS (ESI+) m/z calculated $[M+H]^+$=357.14; found=357.21 (100%).

*1-C allyl-3-O-acetyl-4-O-benzyl-6-O-(tert-butyldipenhylsilyl)-1-deoxy-α-D-glucopyranoside (**70**)*

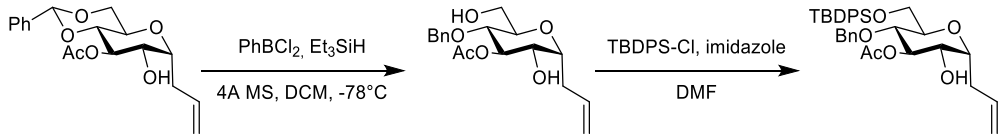

67 69 70

20%

Compound **67** (350 mg, 1.05 mmol) was converted into **69** according to *General procedure **D***.

The crude **69** was reacted with TBDPS-Cl as described in *General procedure **O***.

The crude was purified by flash chromatography (Hex:EtOAc 6:4 to 5:5) to give **70** (120 mg, 0.21 mmol) in 20% yield.

Characterization

^{1}H NMR (400 MHz, $CDCl_3$) δ 7.65 - 7.14 (m, 15H, H-Arom), 5.73 (ddt, *J*= 17.1, 10.1, 6.9 Hz, 1H, H-8), 5.13 - 4.93 (m, 3H, H-3, H-9), 4.63 - 4.52 (m, 2H, C*H*$_2$Ph), 3.87-3.74 (m, 5H, H-1, H-3, H-5, H-6), 3.66 (t, *J*= 5.0 Hz, 1H, H-4), 3.54 (ddd, *J*= 9.3, 6.1, 3.2 Hz, 1H, H-2), 2.93 (d, *J*= 9.2 Hz, 1H, O*H*), 2.41 - 2.30 (m, 2H, H-7), 1.86 (s, 3H, C*H*$_3$CO), 0.97 ppm (s, 9H, C(C*H*$_3$)$_3$).

MS (ESI+) m/z calculated $[M+H]^+$=597.27; found=597.57 (100%).

*1-C allyl-3-O-acetyl-2-azido-4-O-benzyl--6-O-(ter-butyldipenhylsilyl)-2-deoxy-α-D-mannopyranoside (**71**)*

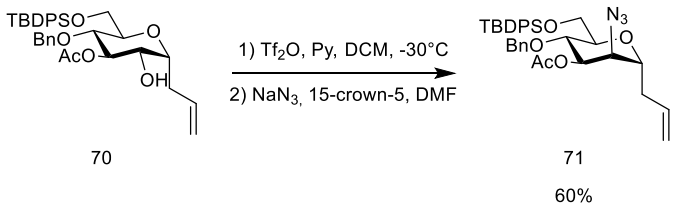

70 71

60%

Compound **70** (120mg, 0.21 mmol) was converted into **71** as described in *General procedure **E***.

The crude was purified by flash chromatography (Hex:EtOAc 6:4 to 5:5) to give **71** (75 mg, 0.126 mmol) in 60% yield.

Characterization

^{1}H NMR (400 MHz, $CDCl_3$) δ 7.69 - 7.09 (m, 15H, H-Arom), 5.82 - 5.65 (m, 1H, H-8), 5.28 - 5.17 (m, 1H, H-3), 5.14 - 5.00 (m, 2H, H-9), 4.60 (d, J = 11.5 Hz, 1H, C*H*HPh), 4.53 (d, *J*= 11.5 Hz, 1H, C*H*HPh), 3.93 - 3.85 (m, 2H, H-1, H-4), 3.85 - 3.73 (m, 3H, H-2, H-6), 3.65 (ddd, *J*= 8.6, 5.1, 3.4 Hz, 1H, H-5), 2.46 – 2.28 (m, 2H, H-7), 1.95 (s, 3H, C*H*$_3$CO), 0.99 ppm (s, 9H, C(C*H*$_3$)$_3$).

^{13}C NMR (101 MHz, $CDCl_3$) δ 135.94-135.76-134.93 (C-Arom), 133.20 (C-8), 129.81-128.60-127.86 (Arom), 118.37 (C-9), 74.73 (C-5), 74.32 (*C*H_2Ph), 73.27 (C-1), 73.17 (C-4), 72.78 (C-3), 62.78 (C-6), 60.73 (C-2), 34.92 (C-7), 26.71 (C(*C*H_3)$_3$), 20.94 ppm (*C*H_3CO).

*1-C allyl-4,6-O-benzylidene-1-deoxy-3-O-(4-methoxybenzyl)-α-D-glucopyranoside (**73**)*

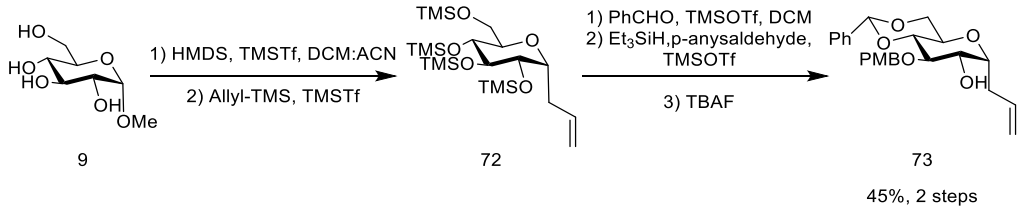

9 72 73

45%, 2 steps

Methyl α-*D*-glucopiranoside **9** (2.00g, 10mmol, 1 eq) was dissolved in 48 mL of DCM:ACN 1:1 (50mL, 0.2 M). HDMS (4.6 mL, 22 mmol, 2.2 eq) was added, followed by TMSOTf (0.18 mL, 1 mmol, 0.1 eq.). The mixture was stirred for 15 minutes and then the generated NH_3 was removed in vacuum for 2h. After the N_2 flush was restored, allyl-TMS (3.2 mL, 20 mmol, 2 eq) was added, followed by the slow addition of TMSOTf (1.81 mL, 10 mmol, 1 eq.). The reaction progress was monitored through TLC (DCM: MeOH 8:2).

After 48h, the reaction was quenched with TEA till neutrality. The solvent was removed under reduced pressure.

The crude was coevaporated with toluene and 4Å MS were added.

Crude **72** was dissolved in DCM (50 mL, 0.2 M) under Ar. Benzaldehyde was added (1.1 mL, 11 mmol, 1.1 eq.) and the solution was stirred for 30h. The mixture was then cooled to -78°C and stirred for additional 30'. TMSOTf (0.27 mL, 1.5 mmol, 0.15 eq.) was added dropwise and the reaction progress was monitored by TLC (9:1 Hex:AcOEt). After 2 h, the starting material was consumed.

Triethylsilane (1.8 mL, 11 mmol, 1.1 eq.) and p-anysaldehyde (1.5 mL, 12 mmol, 1.2 eq.) were added, followed by TMSOTf (0.14 mL, 0.75 mmol, 0.075 eq.). After 2h the starting material was consumed and TBAF (1M in THF, 20 mL, 20 mmol, 2 eq.) was added. The temperature was allowed to increase to RT and the solution was stirred overnight.

The reaction mixture was diluted with AcOEt, the MS were filtered over Celite and the organic phase was washed 2x$NaHCO_3$ (saturated aqueous solution) and once with brine. The solution was dried over Na_2SO_4 and the solvent removed under reduced pressure.

The crude was purified by flash chromatography (9:1 to 7:3 Hex:AcOEt) to give **73** (1.86 g, 4.5 mmol) in 45% yield.

Characterization

^{1}H NMR (400 MHz, $CDCl_3$) δ 7.39 - 7.17 (m, 5H, H-Arom), 7.13 (d, *J*= 8.7 Hz, 2H, H-Arom), 6.73 (d, *J*= 8.8 Hz, 2H, H-Arom), 5.76 – 5.56 (m, 1H, H-8), 5.44 (s, 1H, C*H* benzylidene), 5.04 - 4.92 (m, 2H, H-9), 4.82 (d, *J*= 11.0 Hz, 1H, C*H*HPh), 4.48 (d, *J*= 11.0 Hz, 1H, C*H*HPh), 4.10 (dd, *J*= 9.0, 3.0 Hz, 1H, H-6a), 4.04 – 3.93 (m, 1H, H-1), 3.74 (ddd, *J*= 8.3, 6.1, 1.5 Hz, 1H, H-2), 3.65 (s, 3H, OCH_3), 3.62 - 3.47 (m, 4H, H-3, H-4, H-5, H-6b), 2.40 - 2.27 ppm (m, 3H, H-7, O*H*).

^{13}C NMR (101 MHz, $CDCl_3$) δ 159.46-137.39 (H-Arom), 134.27 (C-8), 130.36-129.75-128.96-128.28-125.96 (H-Arom), 113.99 (C-9), 101.22 (*C*H benzylidene), 83.12-78.54 (C-3/C-4), 75.87 (C-1), 74.39 (CH_2Ph), 71.44 (C-2), 69.42 (C-6), 63.75 (OCH_3), 55.28 (C-5), 29.74 ppm (C-7).

MS (ESI+) m/z calculated $[M+H]^+$=435.19; found=435.27 (100%).

*1-C allyl-4-O-benzyl-6-O-(tert-butyldipenhylsilyl)-1-deoxy-3-O-(4-methoxybenzyl)-α-D-glucopyranoside (**75**)*

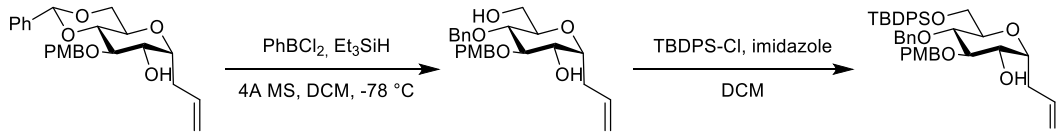

73 74 75

35%

Compound **73** (1.3 g, 3.15 mmol, 1 eq.) was converted into intermediate **74** according to *General procedure **D***.

The crude **74** was treated with TBPDS-Cl as described in *General procedure **O***.

The crude was purified by flash chromatography (Hex:EtOAc 7:3 to 5:5) to give compound **75** (718 mg, 1.10 mmol) in 35% yield over 2 steps.

Characterization

^{1}H NMR (400 MHz, $CDCl_3$) δ 7.76 – 7.66 (m, 4H, H-Arom), 7.54 – 7.27 (m, 11H, H-Arom), 7.20 – 7.13 (m, 2H, H-Arom), 6.91 – 6.81 (m, 2H, H-Arom), 5.81 (ddt, *J*= 17.1, 10.2, 6.9 Hz, 1H, H-8), 5.21 – 5.01 (m, 2H, H-7), 4.65-4.60 (m, 2H, 2xC*H*HPh), 4.57 (d, *J*= 11.5 Hz, 1H, C*H*HPh), 4.48 (d, *J*= 11.4 Hz, 1H, C*H*HPh), 4.10 – 4.02 (m, 1H, H-5), 4.01 – 3.95 (m, 2H, H-6), 3.89 – 3.85 (m, 1H, H-1), 3.83 (s, 3H, OC*H*$_3$), 3.81 – 3.77 (m, 1H, H-3), 3.74 (ddd, *J*= 4.4, 3.2, 1.0 Hz, 1H, H-4), 3.60 (dd, *J*= 4.7, 2.4 Hz, 1H, H-2), 3.05 (brs, 1H, O*H*), 2.47 – 2.32 (m, 2H, H-9), 1.07 ppm (s, 9H C(C*H*$_3$)$_3$).

^{13}C NMR (101 MHz, $CDCl_3$) δ 135.76-135.20-135.18-134.79 (C-Arom), 134.69 (C-8), 129.94-129.70-129.65-129.27-128.51-127.93-127.82 (C-Arom), 116.89 (C-9), 113.92 (C-Arom), 76.21 (C-3), 75.44 (C-5), 73.79 (C-4), 72.56 (*C*H$_2$Ph), 72.40 (*C*H$_2$Ph), 70.32 (C-1), 68.72 (C-2), 61.87 (C-6), 55.29 (O*C*H$_3$), 33.92 (C-7), 26.83 ppm (C(*C*H$_3$)$_3$).

MS (ESI+) m/z calculated $[M+Na]^+$=675.32; found=675.45 (100%).

*1-C allyl-2-azido-4-O-benzyl-6-O-(ter-butyldipenhylsilyl)-2-deoxy-3-O-(4-methoxybenzyl)-α-D-glucopiranoside (**48**)*

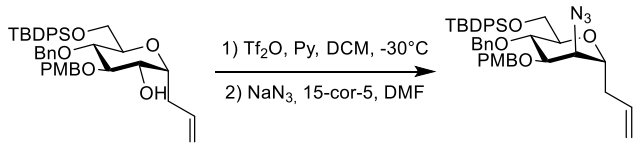

75 48

60%

Compound **75** (718 mg, 1.10 mmol, 1 eq.) was converted into **48** according to G*eneral procedure **E***.

The crude was purified by flash chromatography to give **48** (450 mg, 0.66 mmol) in 60% yield.

Characterization

^{1}H NMR (400 MHz, $CDCl_3$) δ 7.59 (ddd, *J*= 8.1, 5.1, 1.4 Hz, 4H, H-Arom), 7.40 - 7.09 (m, 13H, H-Arom), 6.79 - 6.68 (m, 2H, H-Arom), 5.82 - 5.57 (m, 1H, H-8), 5.06 - 4.92 (m, 2H, H-9), 4.62 (d, *J*= 11.4 Hz, 1H, C*H*HPh), 4.53 – 4.45 (m, 3H, C*H*HPh, CH_2Ph), 3.92 - 3.75 (m, 5H, H-1, H-3, H-6, H-4), 3.72 (s, 3H, OCH_3), 3.69 - 3.63 (m, 1H, H-5), 3.49 (dd, *J*= 5.1, 2.9 Hz, 1H, H-2), 2.36 – 2.17 (m, 2H, H-7), 0.97 ppm (s, 9H, C(CH_3)$_3$).

^{13}C NMR (101 MHz, $CDCl_3$) δ 138.05-135.74-135.58 (C-Arom), 134.79(C-8), 133.54-129.74-128.43-127.67-127.60 (C-Arom),117.69 (C-9), 113.89 (C-Arom), 77.60 (C-3), 74.95 (C-5), 73.80 (*C*H_2Ph), 73.58 (C-4), 72.25 (*C*H_2Ph), 72.08 (C-1), 62.69 (C-6), 60.39 (C-2), 55.28 (O*C*H_3), 35.25 (C-7), 26.82 ppm (C(*C*H_3)$_3$).

MS (ESI+) m/z calculated $[M+Na]^+$=700.32; found=700.37 (30%).

m/z calculated $[M+Na-N_2]^+$=682.32; found=682.46 (100%).

4.3.4 Oligosaccharides synthesis

*[N-(benzyloxycarbonyl)aminopropyl (2-acetamido-3-O-acetyl-4-O-benzyl-2-deoxy-β-D-mannopyranosidyl]methyl C-[2-acetamido-4,6-di-O-benzyl-2-deoxy-3-O-(4-methyoxybenzyl)-α-D-mannopyranosyl]methanephosphonate (**58**)*

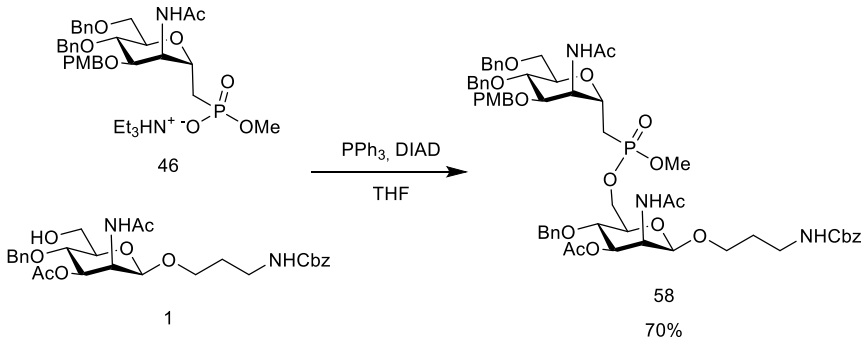

Mannoside **1** (109mg, 0.20 mmol) and phosphonate **46** (130mg, 0.182 mmol) were coupled together in Mitsunobu conditions, as described in *General procedure **R***.

The crude was purified by flash chromatography (EtOAc to EtOAc:MeOH 8:2) to give **58** (110 mg phosphorous diastereomer 1 + 30 mg phosphorous diastereomer 2, 0.123 mmol) in 70% yield.

Characterization

^{1}H NMR (400 MHz, $CDCl_3$) δ 8.64 – 8.54 (m, 1H, N*H*Ac), 7.43 – 7.24 (m, 20H, H-Arom), 7.13 (d, *J*= 8.5 Hz, 2H, H-Arom), 6.88 (d, *J*= 8.5 Hz, 2H, H-Arom), 5.86 – 5.76 (m, 1H, N*H*), 5.20 – 5.07 (m, 3H, N*H*, CH_2Ph), 5.02 (dd, *J*= 9.7, 3.7 Hz, 1H, H-3), 4.79 – 4.56 (m, 6H, H-1, H-2, 2xCH_2Ph), 4.56 – 4.10 (m, 8H, H-1', H-2', H-6a,b, 2xCH_2Ph), 4.09 – 3.94 (m, 2H, H-4, H-4'), 3.90 – 3.63 (m, 11H, H-3', H-5', H-7a, H-6'a,b, 2xOCH_3), 3.62 – 3.52 (m, 1H, H-7b), 3.45 (d, *J*= 9.3 Hz, 1H, H-5), 3.39 – 3.10 (m, 2H, H-9a,b), 2.25 – 2.08 (m, 5H, CH_2P, CH_3CO), 2.02 (s, 3H, CH_3CO), 1.88 (s, 3H, CH_3CO), 1.83 – 1.71 ppm (m, 2H, H-8a,b).

^{13}C NMR (101 MHz, $CDCl_3$) δ 171.64-170.23-169.86 (*C*O), 156.49 (*C*O Cbz), 137.94 - 129.95-129.29-128.49-128.03-127.80-127.67-114.13 (C-Arom), 99.39 (C-1), 75.56 (C-3'), 75.08 (*C*H_2Ph), 74.53 (C-3, C-5), 73.82 (C-4'), 73.41 (*C*H_2Ph), 72.83 (*C*H_2Ph), 72.13 (C-4/5'), 71.94 (C-4/5'), 71.55 (*C*H_2Ph), 68.46 (H-1'), 68.32 (C-6'), 67.61 (C-7), 66.55

(*C*H_2Ph), 66.23 (C-6), 55.33 (O*C*H_3), 53.89 (P(O)O*C*H_3), 50.26 (C-2), 48.77 (C-2'), 38.47 (C-9), 29.69 (C-8), 29.51 (d, J ~ 148 Hz, *C*H_2P), 23.40 (*C*H_3CO), 22.78 (*C*H_3CO), 20.97 ppm (*C*H_3CO).

^{31}P NMR (162 MHz, $CDCl_3$) δ 30.39 ppm.

MS (ESI+) m/z calculated $[M+H]^+$=1163.21; found=1163.24 (100%).

*[N-(benzyloxycarbonyl)aminopropyl (2-acetamido-3-O-acetyl-4-O-benzyl-2-deoxy-β-D-mannopyranosidyl]methyl C-[2-acetamido-3-O-acetyl-4,6-di-O-benzyl-2-deoxy)-α-D-mannopyranosyl]methanephosphonate sodium salt (**57**)*

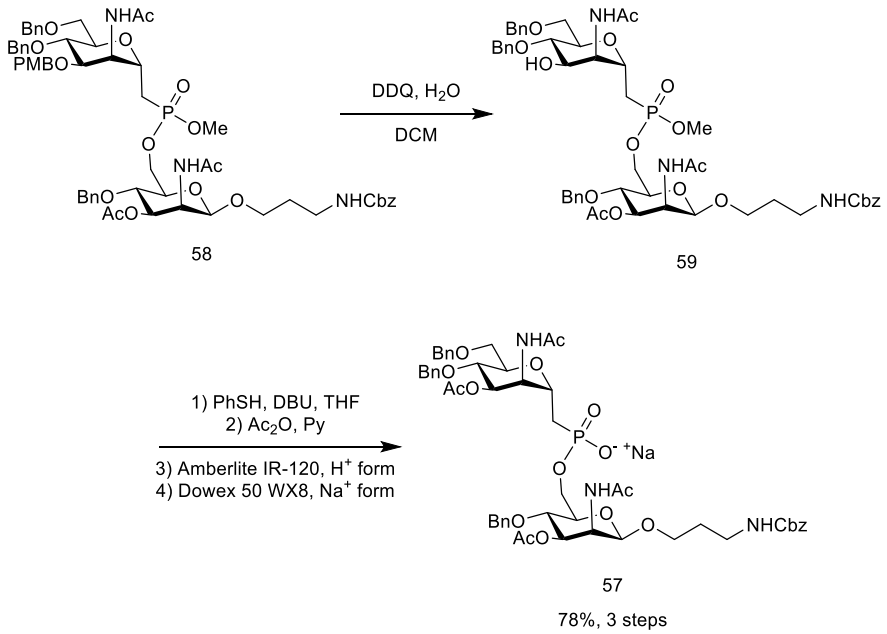

Dimer **58** (40 mg, 0.035 mmol, as a mixture of phosphorous diastereomers) was converted into **59** according to *General procedure **M***.

The crude was then converted into **57** through a sequence of *General procedures **N*** and ***A***.

The crude was purified by flash chromatography (EtOAc to EtOAc:MeOH 8:2).

The phosphonate was passed through a column filled with Amberlite IR-120 H^+ form and through one filled with Dowex 50 WX8 Na^+ form to give the sodium salt **57** in 78% yield.

Characterization

^{1}H NMR (400 MHz, MeOD) δ 7.40 – 7.19 (m, 20H, H-Arom), 5.19 (dd, J = 7.1, 4.1 Hz, 1H, H-3'), 5.07 (d, *J*= 3.3 Hz, 2H, CH_2Ph), 5.00 (dd, *J*= 9.3, 3.9 Hz, 1H, H-3), 4.73 – 4.46 (m, 10H, 3xCH_2Ph, H-1, H-2, H-4, H-2'), 4.38 – 4.30 (m, 1H, H-6a), 4.23 (td, *J*= 11.3, 10.8, 5.2 Hz, 2H, H-6b, H-1'), 3.95 - 3.69 (m, 5H, H-7a, H-4'. H-5', H-6'), 3.60-3.51 (m, 2H, H-5, H-7b), 3.19 (t, *J*= 6.6 Hz, 2H- H-9), 2.46 – 2.10 (m, 2H, H-7'), 2.00 (s, 3H, CH_3CO), 1.98 (s, 3H, CH_3CO), 1.96 (s, 3H, CH_3CO), 1.94 (s, 3H, CH_3CO), 1.78-1.70 ppm (m, 2H, H-8).

^{13}C NMR (101 MHz, MeOD) δ 128.24-128.17-128.05-128.01-127.78-127.62-127.58-127.45 (C-Arom), 98.51 (C-1), 76.67 (C-4), 74.57 (C-3), 74.42 (C-5), 74.33 (*C*H_2Ph), 73.66 (*C*H_2Ph), 73.26 (*C*H_2Ph), 72.75 (C-4',C-5'), 71.54 (C-3'), 71.19 (C-1'), 68.42 (C-6'), 66.82 (C-7), 65.98 (*C*H_2Ph), 64.58 (C-6), 50.68 (C-2), 50.14 (d, J=15 Hz, C-2'), 50.02 (C-9), 37.56 (C-8), 28.35 (d, J=156 Hz, C-7'), 21.22-19.62 ppm (*C*H_3CO).

^{31}P NMR (162 MHz, MeOD) δ 26.45 ppm.

MS (ESI+) m/z calculated $[M+2Na]^+$=1092.40; found=1092.49 (100%).

MS (ESI-) m/z calculated [M] =1046.40; found=1046.92 (100%).

*[N-(benzyloxycarbonyl)aminopropyl (2-acetamido-3-O-acetyl-4-O-benzyl-2-deoxy-β-D-mannopyranosidyl]methyl C-[2-acetamido-4-O-benzyl-6-O-(tert-butyldiphenylsilyl)-2-deoxy-3-O-(4-methyoxybenzyl)-α-D-mannopyranosyl]methanephosphonate (**60**)*

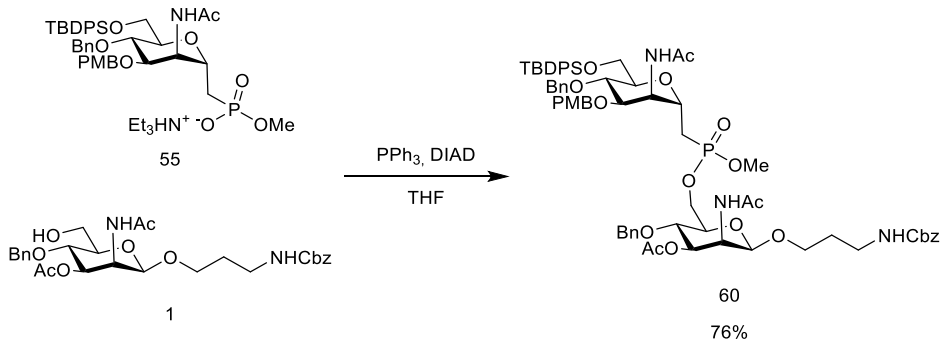

Mannoside **1** (50mg, 0.092 mmol) and phosphonate **55** (83mg, 0.096 mmol) were coupled together in Mitsunobu conditions, as described in *General procedure **R***.
The crude was purified by flash chromatography (EtOAc to EtOAc:MeOH 95:5) to give **60** (90 mg phosphorous diastereomer 1 + traces of phosphorous diastereomer 2, 0.070 mmol) in 76% yield.

Characterization

^{1}H NMR (400 MHz, $CDCl_3$) δ 7.93 (d, *J*= 9.7 Hz, 1H, N*H*), 7.62 (dq, *J*= 8.4, 1.6 Hz, 5H, H-Arom), 7.45 – 7.21 (m, 20H, H-Arom), 7.16 (d, *J*= 8.8 Hz, 2H, H-Arom), 6.86 (d, *J*= 8.7 Hz, 2H, Arom), 5.77 (d, *J*= 9.4 Hz, 1H, N*H*), 5.27 (t, *J*= 5.9 Hz, 1H, N*H*), 5.17 – 5.05 (m, 2H, CH_2Ph), 5.00 – 4.90 (m, 1H, H-3), 4.74 – 4.64 (m, 4H, H-2, C*H*HPh, CH_2Ph), 4.62 – 4.46 (m, 3H, H-1, 2xC*H*HPh), 4.38 – 4.18 (m, 5H, H-6a, H-2', H-6', C*H*HPh), 4.07-3.94 (m, 3H, H-4, H-1', H-4'), 3.91 – 3.76 (m, 3H, H7a, H-5', H-6'), 3.78 (s, 3H, OCH_3), 3.74-3.72 (m, 1H, H-3'), 3.55-3.51 (m, 1H, H-7b), 3.51 (d, *J* = 11.0 Hz, 3H, POCH_3), 3.41 – 3.35 (m, 1H, H-5), 3.31-3.27 (m, 1H, H-9a), 3.23 – 3.13 (m, 1H, H-9b), 2.13 – 2.01 (m, 2H, H7'), 2.05 (s, 3H, CH_3CO), 1.97 (s, 3H, CH_3CO), 1.88 (s, 3H, CH_3CO), 1.78-1.74 (m, 2H, H-8), 1.06 ppm (s, 9H, C(CH_3)$_3$).

^{13}C NMR (101 MHz, $CDCl_3$) δ 137.59-132.11-132.00-130.65-130.57-129.91-129.71-116.24 (C-Arom), 101.47 (C-1), 77.80 (C-3'), 77.36 (C-5'), 77.15 (*C*H_2Ph), 76.63 (C-3,C-5), 74.92 (*C*H_2Ph), 74.22 (C-4), 73.82 (*C*H_2Ph), 73.14 (C-1'), 70.47 (C-4'), 69.28 (C-7),

68.64 (C-6), 63.92 (*C*H_2Ph Cbz), 57.44 (C-6'), 55.76 (O*C*H_3), 52.15 (PO*C*H_3), 50.83 (C-2), 50.67 (d, *J*≈18, C-2'), 40.35 (C-9), 31.88 (d, *J*=145, C-7'), 31.60 (C-8), 28.99 (C(*C*H_3)$_3$), 24.53-23.04-21.30 ppm (*C*H_3CO).

^{31}P NMR (162 MHz, $CDCl_3$) δ 30.27 ppm.

MS (ESI+) m/z calculated $[M+Na+H]^+$=1311.49; found=1311.12 (100%).

*[N-(benzyloxycarbonyl)aminopropyl (2-acetamido-3-O-acetyl-4-O-benzyl-2-deoxy-β-D-mannopyranosidyl)methyl C-(2-acetamido-4-O-benzyl-2-deoxy-3-O-(4-methyoxybenzyl)-α-D-mannopyranosyl]methanephosphonate (**61**)*

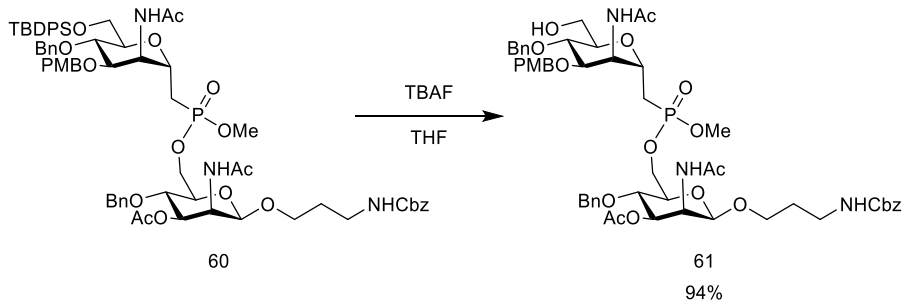

60 61

94%

Compound **60** (200 mg, 0.155 mmol) was reacted with TBAF as described in *General procedure **P.***

The crude was purified by flash chromatography (EtOAc to EtOAc:MeOH 95:5) to give **61** (150 mg, 0.143 mmol) in 94% yield.

Characterization

^{1}H NMR (400 MHz, $CDCl_3$) δ 7.51 – 7.44 (m, 1H), 7.37 – 7.22 (m, 10H), 7.05 (d, *J* = 8.2 Hz, 2H), 6.84 (d, *J* = 8.2 Hz, 2H), 5.55 (d, *J* = 9.5 Hz, 1H), 5.01 (s, 2H), 4.88 (dd, *J* = 10.0, 3.7 Hz, 1H), 4.68 – 4.35 (m, 6H), 4.34 – 4.25 (m, 1H), 4.16 (d, *J* = 10.3 Hz, 2H), 4.07 (dd, *J* = 11.6, 5.5 Hz, 1H), 3.97 (s, 1H), 3.85 (t, *J* = 9.6 Hz, 1H), 3.74 (d, *J* = 1.7 Hz, 3H), 3.70 (d, *J* = 11.1 Hz, 2H), 3.56 (d, *J* = 11.1 Hz, 1H), 3.47 (s, 1H), 3.32 (dd, *J* = 13.3, 6.2 Hz, 1H), 3.15 (tq, *J* = 12.7, 7.4, 6.9 Hz, 3H), 2.23 – 1.87 (m, 1H), 1.98 (s, 2H), 1.91 (d, *J* = 3.3 Hz, 3H), 1.75 (s, 3H), 1.68 ppm (s, 2H).

^{13}C NMR (101 MHz, $CDCl_3$) δ 130.05, 128.63, 128.48, 128.12, 127.92, 127.64, 114.31, 99.24, 75.45, 75.07, 74.71, 74.32, 72.38, 71.97, 71.48, 67.42, 66.53, 64.64, 58.25, 55.37, 54.11, 50.23, 48.80, 29.52, 23.35, 22.95, 20.98, 14.26 ppm.

^{31}P NMR (162 MHz, $CDCl_3$) δ 32.66 ppm.

MS (ESI+) m/z calculated $[M+Na]^+$=1072.43; found=1072.89 (100%).

[N-(Benzyloxycarbonyl)aminopropyl (2-acetamido-3-O-acetyl-4-O-benzyl-2-deoxy-β-D-mannopyranosidyl) methyl C-(2-acetamido-4-O-benzyl-2-deoxy-3-O-(4-methyoxybenzyl)-α-D-mannopyranosyl)methanephosphonyl]methyl C-(2-acetamido-4,6-O-dibenzyl-2-deoxy-3-O-(4-methyoxybenzyl))-α-D-mannopyranosyl)]methanephosphonate ***(62)***

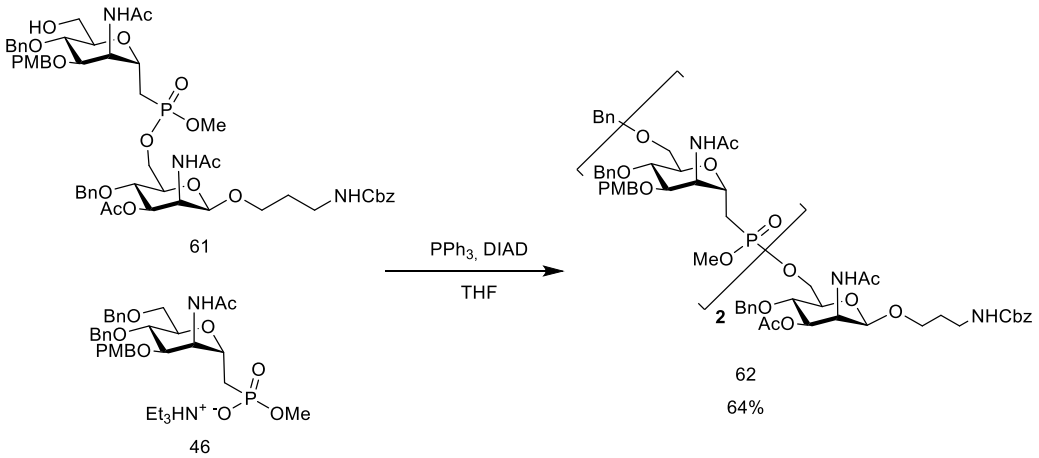

Dimer **61** (140 mg, 0.133 mmol) was coupled to phosphonate **46** (115 mg, 0.16 mmol) in Mitsunobu conditions, as described in *General procedure **P***.

The crude was purified by flash chromatography (EtOAc to EtOAc:MeOH 95:5) to give **62** (140mg, 0.085 mmol, mixture of 4 phosphorous diastereomers) in 64% yield.

Characterization

^{1}H NMR (400 MHz, $CHCl_3$) δ 7.89 (d, *J*= 9.6 Hz, 1H), 7.41 – 7.24 (m, 30H), 7.12 (d, *J*= 8.5 Hz, 2H), 6.86 (dt, *J*= 8.7, 3.6 Hz, 4H), 5.80 (d, *J*= 9.3 Hz, 1H), 5.33 (s, 1H), 5.16 – 5.06 (m, 3H), 4.99 (dd, *J*= 9.6, 3.8 Hz, 1H), 4.86 (d, *J*= 11.1 Hz, 1H), 4.78 – 4.71 (m, 2H), 4.61 (ddd, *J*= 12.6, 7.6, 2.9 Hz, 6H), 4.54 – 4.37 (m, 4H), 4.37 – 4.19 (m, 4H), 4.07 – 3.94 (m, 1H), 3.90 – 3.64 (m, 20H), 3.57 (h, *J*= 6.7, 5.9 Hz, 1H), 3.45 (d, *J*= 9.6 Hz, 1H), 3.21 (td, *J*= 12.9, 11.5, 5.2 Hz, 4H), 2.28 (ddd, *J*= 15.1, 10.4, 7.8 Hz, 1H), 2.06 (s, 4H), 2.02 (s, 5H), 2.01 (s, 3H), 1.85 ppm (s, 3H).

^{13}C NMR (101 MHz, $CDCl_3$) δ 171.69, 170.47, 169.90, 159.65, 159.41, 156.54, 138.13, 137.91, 130.01, 129.91, 129.31, 128.48, 128.02, 127.92, 127.75, 126.65, 114.10, 113.91, 104.14, 99.43, 76.40, 75.59, 74.94, 74.64, 74.41, 73.73, 73.39, 72.87, 72.77, 72.63, 71.88, 71.53, 70.91, 69.84, 68.42, 68.28, 67.65, 66.51, 65.69, 55.31, 54.10, 53.77, 50.13, 49.95,

48.78, 48.61, 48.48, 48.34, 38.41, 30.01, 29.51, 28.54, 27.08, 23.38, 23.08, 22.77, 21.97, 21.75, 20.99 ppm.

^{31}P NMR (162 MHz, $CDCl_3$) δ 29.76, 27.89 ppm.

MS (ESI+) m/z calculated $[M+Na]^+$=1667.66; found=1667.44 (10%).

MS (ESI-) m/z calculated $[M+Cl]^-$=1680.11; found=1679.72 (100%).

MALDI (HCCA) m/z calculated $[M+Na]^+$=1667.66; found=1667.9 (100%).

4.3 Synthesis of Lipid A derivatives

4.3.1 Acceptor synthesis

*Imidazole-1-sulfonyl azide hydrogen sulfate (**82**)*

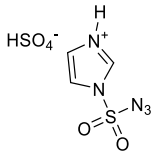

82

NaN_3 (5g, 77mmol, 1 eq.) was suspended in dry EtOAc (77ml, 1 M) and sulfuryl chloride (6.2ml, 77mmol, 1 eq.) was added over 10 minutes at 0°C. The temperature was left to increase to RT and the mixture was stirred overnight.

The suspension was cooled down to 0°C, imidazole (10g, 146mmol) was added in portions and the mixture was stirred at that temperature for 4 hours.

The solution was then basified with $NaHCO_3$ (150ml, saturated aqueous solution), the two phases were separated and the organic phase was washed with H_2O, dried over Na_2SO_4, filtered and cooled down to 0°C. H_2SO_4 (98%) (4.1ml, 77mmol, 1 eq.) was added slowly and the mixture was stirred for 30 minutes. The generated white precipitate was filtered on Buckner funnel and washed with a little amount of EtOAc.

The obtained solid was dried in vacuo pump to obtain **82** in 48% yield (10g, 37.2mmol).

Characterization

The spectroscopic data are in agreement with those reported in literature [120].

*1,3,4,6-tetra-O-acetyl-2-azido-2-deoxy-D-glucopyranose (**86**)*

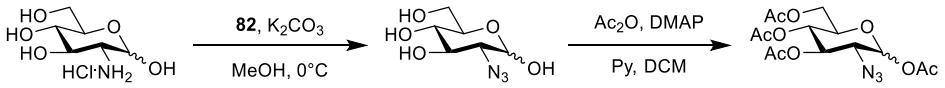

81 83 86

95%, 2 steps

Glucosamine hydrochloride (6.69g, 31mmols) was dissolved in MeOH. K_2CO_3 anhydrous (12.9g, 93mmol) was added slowly at 0°C. After 15 miuntes, imidazole-1-sulfonyl azide hydrogen sulfate (10g, 37.2mmol) was added in portions, followed by $CuSO_4 \cdot 5H_2O$ (78mg, 0.31mmol). The reaction progress was monitored through RPTLC (ACN:MeOH:H_2O 5:2:0.5). After 8 hours the starting material was consumed, and the solvent was removed under reduced pressure.

The crude **83** was converted into **86** as described in *General procedure **A***.

Purification by filtration on silica (Hex:EtOAc 6:4) led to **86** (11g, 29.47mmol) in 95% yield over 2 steps as a 2:1 mixture of the α and β anomers.

Characterization

The spectroscopic data are in agreement with those reported in literature [132].

*Thexyldimethylsilyl 3,4,6-tri-O-acetyl-2-azido-2-deoxy-β-D-glucopyranoside (**88**)*

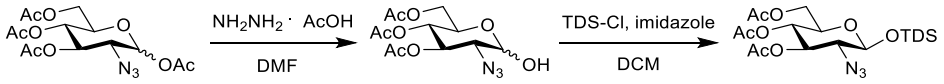

86 87 88

89%, 2 steps

Compound **86** (10g, 26.83mmol) was converted into **87** according to *General procedure **O***. The crude was reacted with TDS-Cl as described in *General procedure **Q*** to give **88**. The crude was purified by flash chromatography (Hex:EtOAc 7:3 to 6:4), leading to **88** (10g, 24mmol) with 89% yield over two steps.

Characterization

The spectroscopic data are in agreement with those reported in literature [132].

*Thexyldimethylsilyl 2-azido-4,6-O-benzylidene-2-deoxy-β-D-glucopyranoside (**85**)*

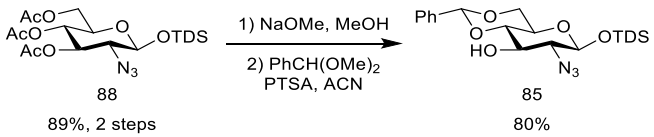

88 — 89%, 2 steps

85 — 80%

Compound **88** (10g, 24mmol) was deacetylated according to *General procedure **B***.
The crude was treated with benzaldehyde dimethyl acetal and PTSA as described in *General procedure **C*** to give **85**.
Flash chromatography (Hex:EtOAc 7:3) led to compound **85** (8.35 g, 19.2 mmol) in 80% yield over two steps.

Characterization

^{1}H NMR (400 MHz, $CDCl_3$) δ 7.34 - 7.10 (m, 5H, H-Arom), 5.33 (s, 1H, C*H* benzylidene), 4.43 (d, *J*= 7.7 Hz, 1H, H-1), 4.09 (dd, *J*= 10.5, 5.0 Hz, 1H, 6-a), 3.58 (t, *J*= 10.3 Hz, 1H, 6-b), 3.42 (dd, *J*= 9.3, 1.5 Hz, 1H, H-3), 3.36 (t, *J*= 9.1 Hz, 1H, H-4), 3.19 (ddd, *J*= 10.1, 9.1, 5.0 Hz, 1H, H-5), 3.15 - 3.04 (m, 1H, H-2), 2.52 (brs, 1H, O*H*), 1.49 (h, *J*= 7.1 Hz, 1H, C*H* TDS), 0.72 (s, 3H, CH_3 TDS), 0.70 (s, 9H, CH_3 TDS), 0.02 (s, 3H, CH_3Si TDS), 0.00 ppm (s, 3H, CH_3Si TDS).

^{13}C NMR (101 MHz, $CDCl_3$) δ 136.87-129.36-128.38-126.29 (C-Arom), 102.00 (*C*H benzylidene), 97.40 (C-1), 80.76 (C-4), 71.92 (C-3), 69.13 (C-2), 68.58 (C-6), 66.26 (C-5), 33.88 (*C*H TDS), 24.81 (Cquat TDS), 19.98 (*C*H_3Si TDS), 19.82 (*C*H_3Si TDS), 18.50 (*C*H_3Si TDS), 18.40 (*C*H_3Si TDS), -2.11 (*C*H_3Si TDS), -3.18 ppm (*C*H_3Si TDS).

MS (ESI+) *m/z* calculated $[M+Na]^+$=458.22; found=458.43 (100%).

*Thexyldimethylsilyl 3-O-acetyl-2-azido-4,6-O-benzylidene-2-deoxy-β-D-glucopyranoside (**96**)*

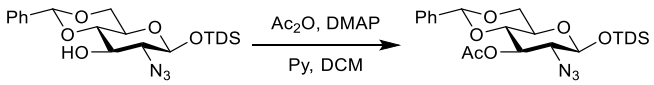

85 96

90%

Compound **85** (3.4g, 7.81mmol) was acetylated according to *General procedure **A***.
The crude was purified by filtration on silica (Hex:EtOAc 7:3) to give **96** (3.4g, 7.12mmol) in 91% yield.

Characterization

^{1}H NMR (400 MHz, $CDCl_3$) δ7.48-7.30 (m, 5H, H-Arom), 5.48 (s, 1H, C*H* benzylidene), 5.13 (t, *J*= 9.8 Hz, 1H, H-3), 4.69 (d, *J*= 7.5 Hz, 1H, H-1), 4.29 (dd, *J*= 10.3, 5.0 Hz, 1H, H-6a), 3.78 (t, *J*= 10.3 Hz, 1H, H-6b), 3.63 (t, *J*= 9.5 Hz, 1H, H-4), 3.48 (dd, *J*= 5.0, 10.3 Hz, 1H, H-5), 3.43-3.36 (dd, *J*= 7.5, 9.8 Hz, 1H, H-2), 2.13 (s, 3H, C*H*$_3$CO), 1.67 (hept, *J*= 6.8, 1H, CH TDS), 0.96-0.78 (m, 12 H, 4xC*H*$_3$ TDS), 0.22 (s, 3H, C*H*$_3$Si TDS), 0.21 ppm (s, C*H*$_3$Si TDS).

^{13}C NMR (101 MHz, $CDCl_3$) δ169.88 (Cquat), 136.98-129.25-128.38-126.28 (C-Arom), 101.66 (C-benzylidene), 97.61 (C-1), 78.85 (C-4), 71.29 (C-3), 68.68 (C-6), 67.45 (C-2), 66.66 (C-5), 34.01 (*C*H TDS), 21.02 (*C*H$_3$CO), 20.07-19.94-18.64-18.53 (*C*H$_3$ TDS), -2.03 (*C*H$_3$Si TDS), -3.09 ppm (*C*H$_3$Si TDS).

MS (ESI+) *m/z* calculated $[M+Na]^+$=500.23; found=500.31 (100%).

*Thexyldimethylsilyl 3-O-acetyl-2-azido-4-O-benzyl-2-deoxy-β-D-glucopyranoside (**79**)*

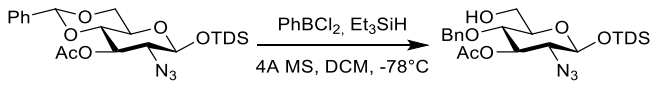

96 79

93%

96 (600 mg, 1.26 mmol) was converted into **79** as described in G*eneral procedure **D***.
The crude was purified by flash chromatography (Hex:EtOAc 8:2) to give pure **79** (560 mg, 1.17 mmol) in 93% yield.

Characterization

^{1}H NMR (400 MHz, $CDCl_3$) δ 7.42-7.25 (m, 5H), 5.06 (dd, *J*=10.4, 9.3 Hz, 1H, H-3), 4.46 (d, *J*= 7.7, 1H, H-1), 4.63 (d, *J*= 3.7 Hz, 2H, C*H*$_2$Ph), 3.88 (ddd, *J*= 12.2, 5.3, 2.7 Hz, 1H, H-6a), 3.74 (ddd, *J*= 11.9, 8.3, 3.9, 1H, H-6b), 6.65 (t, *J*= 9.5 Hz, 1H, H-4), 3.42 (ddd, *J*= 9.8, 4.1, 2.6 Hz, 1H, H-5), 3.30 (dd, *J*= 10.4, 7.7 Hz, 1H, H-2), 2.05 (s, 3H, C*H*$_3$CO), 1.80 (dd, *J*= 8.4, 5,4, 1H, O*H*), 1.67 (hept, *J*= 6.8, 1H, CH TDS), 0.92 (s, 3H, CH_3 TDS), 0.90 (s, 9H, CH_3 TDS), 0.22 (s, 3H, CH3Si TDS), 0.21 ppm (s, 3H, CH3Si TDS).

^{13}C NMR (101 MHz, $CDCl_3$) δ169.98 (Cquat), 137.65 (Cquat), 128.70, 128.16, 127.94 (C-Ar), 97.01 (C-1), 75.72 (C-4), 75.40 (C-5), 74.72 (*C*H_2Ph), 74.14 (C-3), 67.01 (C-2), 61.89 (C-6), 34.07 (CH TDS), 25.30 (Cquat), 21.07 (CH_3CO), 20.11-20.10-18.57-18.54 (CH_3 TDS), -1.96 (CH_3Si TDS), -3.00 ppm (CH_3Si TDS).

MS (ESI+) *m/z* calculated $[M+Na]^+$=502.25; found=502.42 (100%).

4.3.2 Donor synthesis

*Thexyldimethylsilyl 3,4,6-tri-O-acetyl-2-N-(9H-fluoren-9-yl)methyl-2-deoxy-β-D-glucopyranoside (**94**)*

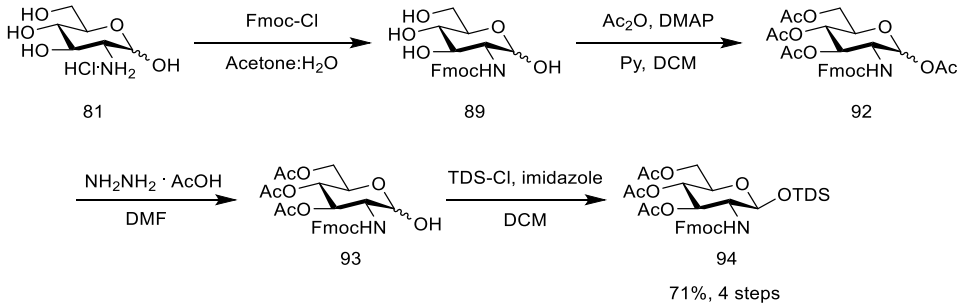

Glucosamine hydrochloride (10g, 46.5 mmol, 1 eq.) was dissolved in a mixture of H_2O and acetone 1:1 (240 mL, 0.2M). Fmoc-Cl (18.1 g, 70 mmol, 1.5 eq.) and $NaHCO_3$ (7g, 93 mmol, 2 eq.) were added.

The reaction progress was followed by TLC (EtOAc:MeOH:H_2O 7:2:1). After 2 h the reaction was completed, and the solvent was evaporated under reduced pressure and the residue dissolved in toluene and evaporated several times to remove traces of water.

Crude **89** was acetylated according to *General procedure **A*** to give acetylated compound **92**.

Deprotection of the anomeric position of **92** was carried out as described in *General procedure **Q*** to give compound **93**.

The crude was reacted with TDS-Cl according to *General procedure **O***.

Flash chromatography (Hex:EtOAc 8:2 to 6:4) led to the desired compound **94** (22.12 g, 33.02 mmol) in 71% yield over 4 steps.

Characterization

^{1}H NMR (400 MHz, Acetone-d_6) δ 7.96 – 7.19 (m, 8H, H-Arom), 6.65 (d, *J*= 9.4 Hz, 1H, N*H*), 5.30 (t, *J*= 10.0 Hz, 1H, H-3), 5.06 (d, *J*= 8.0 Hz, 1H, H-1), 4.96 (t, *J*= 9.7 Hz, 1H, H-4), 4.39 – 4.29 (m, 1H, C*H*H Fmoc), 4.22 (m, 3H, H-6a, H-6b, C*H* Fmoc), 4.11 (d, *J*= 11.9 Hz, 1H, C*H*H Fmoc) 3.90 – 3.77 (m, 1H, H-5), 3.64 (q, *J*= 9.5 Hz, 1H, H-2), 2.02 (s, 3H, CH_3CO), 2.00 (s, 3H, CH_3CO), 1.93 (s, 3H, CH_3CO), 1.62 (hept, *J*= 6.9 Hz, 1H, C*H* TDS), 0.98 (s, 3H, CH_3 TDS), 0.96 (s, 9H, CH_3 TDS), 0.30 (s, 3H, CH_3Si TDS), 0.29 (s, 3H, CH_3Si TDS).

^{13}C NMR (101 MHz, Acetone-d_6) δ 170.81,170.30, 157.00, 145.32, 142.29 (Cquat), 128.51, 127.91, 126,10, 126.02, 120.80 (C-Arom), 97.00 (C-1), 73.42 (C-3), 72.56 (C-5), 70.39 (C-4), 67.19 (C-6), 63.29 (*C*H_2 Fmoc), 47.97 (C-2), 34.89 (*C*H TDS), 25.07 (Cquat), 20.93, 20.89, 20.71(CH_3CO), 19.15 (CH_3 TDS), -1.49 (CH_3Si TDS), -2.90 ppm (CH_3Si TDS).

MS (ESI+) *m/z* calculated $[M+Na]^+$=692.30; found=692.42 (100%).

*Thexyldimethylsilyl 3-O-acetyl-4,6-O-benzylidene-2-N-(9H-fluoren-9-yl)methyl-2-deoxy-β-D-glucopyranoside (**95**)*

METHOD I

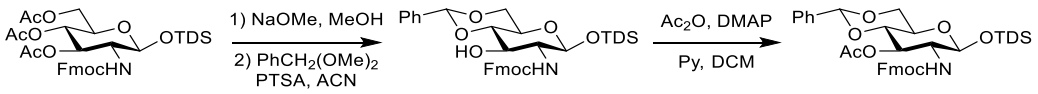

94 91 95

y= 66% over 3 steps

Compound **94** (1 g, 1.49 mmol, 1 eq.) was suspended in MeOH (10 mL, 0.15 M) and MeONa (8 mg, 0.15 mmol, 0.1 eq.) was added. The pH was checked (it should be between 7 and 8). The reaction was stirred at room temperature and followed by TLC (DCM: MeOH 9:1). After 20' the reaction was completed, Amberlite IR-120 resin, H^+ form was added to neutralize MeONa, the resin was filtered off and the solvent was evaporated.

The crude was converted into compound **91** following *General procedure **C***.

The crude **91** was acetylated according to *General procedure **A***.

Flash chromatography (Hex:EtOAc 9:1 to 7:3) led to compound **95** (663 mg, 0.98 mmol) in 66% over 3 steps.

METHOD II

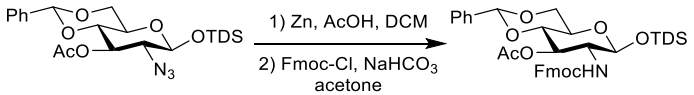

96 95

50%

Compound **96** (500 mg, 1.05 mmol) was dissolved in DCM (10.5 mL, 0.1 M). Zn (746 mg, 10.5 mmol) and AcOH (113 µL) were sequentially added. The reaction mixture was stirred at RT and monitored by TLC (Hex: AcOEt 7:3). After 18 h, additional 1.50 g of Zn and 230 µL of AcOH were added. The reaction mixture was stirred for further 48 h, after which, the insoluble material was filtered over Celite and the solvent was evaporated under reduced pressure.

The crude was dissolved in DCM (11.5 mL, 0.1 M), Fmoc-Cl (360 mg, 1.38 mmol, 1.2) and DIPEA (240 µL, 1.38 mmol) were added and the reaction progress was monitored by TLC (Hex:EtOAc 6:4). After 18h, the solvent was removed under reduced pressure.
The crude was purified by flash chromatography (Hex:EtOAc 8:2 to 7:3) to give **95** (365 mg, 0.55 mmol) in 50% yield.

Characterization

^{1}H NMR (400 MHz, Acetone-d_6) δ 7.95 – 7.20 (m, 13H, H-Arom), 6.64 (d, *J* = 9.7 Hz, 1H, N*H*), 5.65 (s, 1H, C*H* benzylidene), 5.32 (t, *J* = 9.9 Hz, 1H, H-3), 5.11 (d, *J* = 7.9 Hz, 1H, H-1), 4.44 – 4.17 (m, 4H, CH_2 Fmoc, H-6a, C*H* Fmoc), 3.85 (t, *J* = 9.8 Hz, 1H, H-6b), 3.85 (t, *J* = 9.8 Hz, 1H, H-4), 3.66 (m, 1H, H-2), 3.56 (td, *J* = 9.7, 5.0 Hz, 2H, H-5), 1.95 (s, 3H, CH_3CO), 1.62 (hept, *J* = 6.9 Hz, 1H, C*H* TDS), 0.87 (s, 3H, CH_3 TDS), 0.82 (s, 9H, CH_3 TDS), 0.19 (s, 3H, CH_3Si TDS), 0.17 ppm (s, 3H, CH_3Si TDS).

^{13}C NMR (101 MHz, Acetone) δ 170.71-157.08-145.34-139.06 (Cquat), 130.09-129.82-129.04-128.73-128.13-127.89-127.39-126.35-126.26-121.02 (C-Arom), 102.19 (*C*H benzylidene), 97.96 (C-1), 80.23 (C-4), 72.81 (C-3), 69.43 (C-6), 67.54 (C-5), 67.42 (*C*H_2 Fmoc), 59.81 (C-2), 48.20 (*C*H Fmoc), 35.05 (*C*H TDS), 25.69 (*C*H_3CO), 20.68 (*C*H_3Si TDS), 19.16 ppm (*C*H_3Si TDS).

MS (ESI+) *m/z* calculated $[M+Na]^+$=696.30; found=696.48(100%).

*3-O-acetyl-4,6-O-benzylidene-2-N-(9H-fluoren-9-yl)methyl-2-deoxy-D-glucopyranose (**97**)*

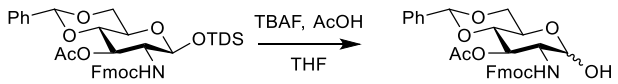

95 97

82%

Anomeric silyl ether of compound **95** (1.3 g, 2.01 mmol) was removed according to *General procedure **P***.

The crude was purified by flash chromatography (DCM: MeOH 30:1) to give **97** (847 mg, 1.6 mmol) in 82% yield as a (about 8:2) mixture of α and β anomers.

Characterization (α anomer)

^{1}H NMR (400 MHz, Acetone-d_6) δ 7.86 (d, *J*= 7.5 Hz, 2H, H-Arom), 7.57 (dd, *J*= 17.7, 7.5 Hz, 2H, H-Arom), 7.50 – 7.32 (m, 9H, H-Arom), 6.25 (d, *J* = 9.7 Hz, 1H, N*H*), 5.65 (s, 1H, C*H* benzylidene), 5.39 (t, *J* = 9.9 Hz, 1H, H-3), 5.28 (d, *J* = 4 Hz, 1H, H-1), 4.41-4.35 (m, 1H, C*H*H Fmoc), 4.29-4.17 (m, 3H, H-6a, C*H*H Fmoc, C*H* Fmoc), 4.13-4.09 (m, 1H, H-5), 4.08-4.07 (m, 1H, H-2), 3.99-3.79 (m, 2H, H-4, H-6b), 1.95 ppm (s, 3H, CH_3CO).

^{13}C NMR (101 MHz, Acetone-d_6) δ 129.60-128.83-128.56-128.00-127.92-127.20-126.16-120.82 (C-Arom), 102.19 (*C*H benzylidene), 93.42 (C-1), 80.55 (C-4),72.81 (C-3), 70.78 (C-6), 69.25 (*C*H_2 Fmoc), 63.59 (C-5), 55.90 (C-2), 47.94 (*C*H Fmoc), 25.69 ppm (*C*H_3CO).

MS (ESI+) *m/z* calculated $[M+Na]^+$=554.19; found=554.37(100%).

*O-(3-O-acetyl-4,6-O-benzylidene-2-deoxy-2-N-(9-fluorenylmethoxycarbonylamino)-α-D-glucopyranosyl trichloroacetimidate (**80**)*

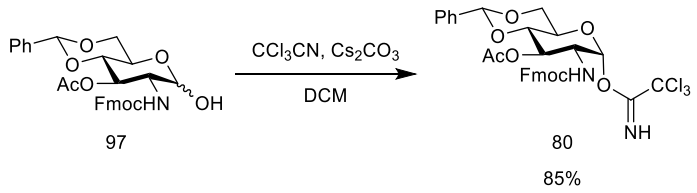

Compound **97** (212 mg, 0.40 mmol, 1 eq.) was dissolved in DCM (4 mL, 0.1 M). Thrichloroacetonitrile (780 µL, 0.80 mmol, 2 eq.) and Cs_2CO_3 (67 mg, 0.20 mmol, 0.5 eq.) were added. The reaction progress was monitored by TLC (Hex: AcOEt 1:1).

After 1h the reaction was completed. The crude was diluted with DCM, the organic layer was washed with $NaHCO_3$ and brine, dried on Na_2SO_4, filtered and the solvent was evaporated.

The reaction crude was purified by flash chromatography (Hex: AcOEt 8:2 to 7:3 with 1% of TEA) to give **80** (166 mg, 0.25 mmol) in 65% yield, as α anomer.

Characterization

^{1}H NMR (400 MHz, Acetone-d_6) δ 9.52 (s, 1H, C=N*H*), 7.86 (d, *J*= 7.5 Hz, 2H, H-Arom), 7.62-7.55 (m, 2H, H-Arom), 7.50 – 7.32 (m, 9H, H-Arom), 6.50 (d, *J* = 3.7 Hz, 1H, H-1), 6.45 (d, *J* = 8.7 Hz, 1H, N*H*), 5.73 (s, 1H, C*H* benzylidene), 5.49 (t, *J* = 10.0 Hz, 1H, H-3), 4.48 - 4.19 (m, 5H, H-6, CH_2 Fmoc, C*H* Fmoc), 4.15 – 4.00 (m, 2H, H-2, H-5), 3.89 (t, *J* = 10.0 Hz, 1H, H-4), 2.05 ppm (s, 3H, CH_3CO).

4.3.3 Disaccharide synthesis

Thexyldimethylsilyl 6-O-[3-O-acetyl-4,6-O-benzylidene-2-deoxy-2-(9-fluorenylmethoxycarbonylamino)-β-D-glucopyranosyl]-3-O-acetyl-2-azido-4-O-benzyl-2-deoxy-β-D-glucopyranoside (77)

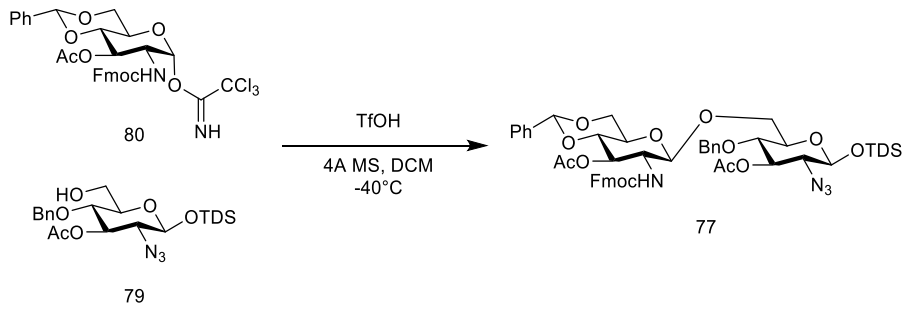

Acceptor **79** (165 mg, 0.344 mmol, 1 eq.) and donor **80** (298 mg, 0.44 mmol, 1.3 eq.) were coevaporated with toluene and dried in vacuo overnight.

Freshly activated 4 Å MS were added to the mixture of donor and acceptor, followed by the addition of DCM (5mL, 0.07 M), under Ar atmosphere. The solution was stirred for 30' at RT and for additional 15' at -45°C. TfOH (5µL, 0,051 mmol, 0.15 eq.) was slowly added to the reaction mixture. The reaction progress was monitored by HPTLC (Hex:EtOAc 7:3). After 1h, the temperature was allowed to increase to -25°C. After 4h at -25°C, HPTLC showed full disappearance of the donor and the reaction was quenched by the addition of TEA till neutral pH.

MS were filtered over Celite and the solvent was evaporated in vacuo.

The crude was purified by flash chromatography (Hex:AcOEt 8:2 to 7:3), to afford disaccharide **77** (240 mg, 0.24 mmol) in 67% yield as a pure β anomer.

Characterization

^{1}H NMR (400 MHz, Acetone-d_6) δ 7.86 (d, *J* = 7.6 Hz, 2H, H-Arom), 7.67 – 7.26 (m, 16H, H-Arom), 6.85 (d, *J* = 8.9 Hz, 1H, N*H*), 5.68 (s, 1H, C*H* benzylidene), 5.40 (t, *J* = 9.9 Hz, 1H, H-3'), 5.10 – 5.01 (m, 1H, H-3), 4.98 (d, *J* = 8.3 Hz, 1H, H-1'), 4.81 (d, *J* = 7.7 Hz, 1H, H-1), 4.70 (d, *J* = 11.1 Hz, 1H, C*H*HPh), 4.58 (d, *J* = 11.0 Hz, 1H, C*H*HPh), 4.40 - 4.30 (m, 2H, H-6a', C*H*H Fmoc), 4.21 – 4.05 (m, 3H, H-6a,C*H*H Fmoc, C*H* Fmoc), 3.96 - 3.89 (m, 1H, H-6b), 3.89 – 3.64 (m, 5H, H-4, H-5, H-2', H-4', H-6b'), 3.62-3.55 (m, 1H, H-5'), 3.38

– 3.30 (m, 1H, H-2), 1.96 (s, 6H, 2x C*H*$_3$CO), 1.73 (hept, 1H, C*H* TDS), 0.95 (s, 3H, C*H*$_3$ TDS), 0.94 (d, *J* = 2.1 Hz, 9H, 3xC*H*$_3$ TDS), 0.28 (s, 3H, C*H*$_3$Si), 0.27 ppm (s, 3H, C*H*$_3$Si).

^{13}C NMR (101 MHz, Acetone-d_6) δ 169.66-169.09-155.94-144.19-143.93-141.16-138.44-137.89 (Cquat), 128.75-128.15-127.99-127.95-127.64-127.56-127.05-126.99-126.29-125.15-125.10-119.92 (C-Arom), 101.82 (C*H* benzylidene), 101.08 (C-1'), 96.45 (C-1), 78.86/76.04/74.07 (C-4/C-5/C-4') 74.29 (*C*H$_2$Ph), 73.81 (C-3), 71.79 (C-3'), 68.28 (C-6'), 68.03 (C-6), 66.87 (C-2), 66.35 (*C*H$_2$ Fmoc), 66.30 (C-5'), 56.68 (C-2), 47.00 (*C*H Fmoc), 33.87 (*C*H TDS), 19.96-19.54 (CH_3CO), 17.97 (CH_3 TDS), -2.42 (CH_3Si TDS), -3.88 ppm (CH_3Si TDS).

MS (ESI+) *m/z* calculated $[M+Na]^+$=1015.41; found=1015.47(100%)

4.3.4 Fatty acid chains synthesis

*tert-Butyl (triphenylphosphoranylidene)acetate (**103**)*

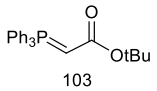

103

To a solution of Ph_3P (8.8 g, 33.8 mmol) in THF (20 mL) tert-butyl bromoacetate was added dropwise (5 mL, 33.8 mmol). The reaction was stirred RT overnight. The white precipitate was filtered, washed with Et_2O and dried in vacuo to afford tert-butyl acetate triphenylphosphonium bromide in 93% yield (14.4 g, 31.4 mmol).

To a suspension of tert-butyl acetate triphenylphosphonium bromide (13.8 g, 30.1 mmol) in H_2O (250 mL, 0.12 M) a solution of NaOH (1.5 g, 37.5 mmol) in H_2O (50 mL, 0.77M) was added dropwise at 0°C. After 20', the precipitate was filtered and washed with H_2O until neutral pH and dried to give **103** (11.3g, 30 mmol) in quantitative yield.[133]

*tert-Butyl (E)-2-hexadecenoate (**104**)*

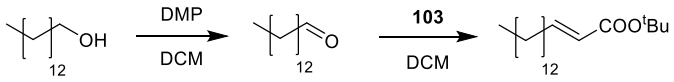

99 101 104

90%

Tetradecanol **99** (1.00g, 4.67 mmol) was dissolved in DCM (47 mL, 0.1 M). DMP (3.97g, 9.33 mmol) was added and the mixture was stirred overnight before being quenched by the addition of 40 mL $Na_2S_2O_3$ (saturated aqueous solution) and 40 mL $NaHCO_3$ (saturated aqueous solution). After 30', the organic and the aqueous phases were separated, and the organic phase was washed with H_2O and brine and dried over Na_2SO_4.

After salt filtration, the solvent was evaporated in vacuo to give aldehyde **101**.

The crude was dissolved in DCM (23 mL, 0.2 M). tert-Butyl (triphenylphosphoranylidene) acetate **103** (2.34 g, 6.2 mmol) was added and the solution was stirred for 3h at RT.

The solvent was concentrated in vacuo and 100 mL of Et_2O/hexane (1:1) were added. The insoluble material was removed by filtration over Celite.

The filtrate was concentrated, and the residue was purified by flash chromatography (Hex:Et_2O 92:8 to 85:15) to give **104** (1.31g, 4.20 mmol) in 90% yield.

Characterization

^{1}H NMR (400 MHz, $CDCl_3$) δ 6.86 (dt, *J*= 15.6, 6.9 Hz, 1H, H-3), 5.73 (dt, *J*= 15.6, 1.6 Hz, 1H, H-2), 2.16 (dq, *J*= 1.7, 6.9 Hz, 2H, H-4), 1.54-1.37 (m, 2H, H-15), 1.48 (s, 9H, C(C*H*$_3$)$_3$), 1.37-1.20 (m, 20H, H-5 - H-14), 0.88 ppm (t, *J*= 6.9 Hz, 3H, H-16).

^{13}C NMR (101 MHz, $CDCl_3$) δ 166.21 (Cquat), 148.36 (C-3), 122.86 (C-2), 79.94 (Cquat), 32.07 (C-4), 31.97-28.84 (C-5 - C-14), 28.17 (C(*C*H$_3$)$_3$), 22.69 (C-15), 14.12 (C-16) ppm.

*tert-Butyl (2S,3R)-2,3-Dihydroxyhexadecanoate (**106**)*

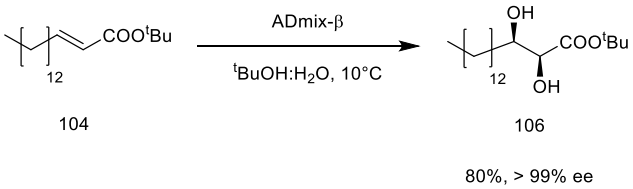

104 106

80%, > 99% ee

Potassium ferricyanide(III) (257 mg, 0.78 mmol), K_2CO_3 (108mg, 0.78 mmol), [$(DHQD)_2$PHAL] (2mg, 0.0026 mmol) and OsO_4 (50 µl of a 0.01M solution in H_2O, 0.5 µmol) were stirred in a 1:1 *t*-BuOH:H_2O mixture (1.3 mL, 0.2 M) at RT for 15'.

Methanesulfonamide (25 mg, 0.26 mmol) was added and the mixture was cooled to 10 °C. A solution of **104** (80 mg, 0.26mmol in 1 ml of a 1:1 *t*-butanol:H_2O mixture) was introduced and the mixture was stirred at 10 °C. The reaction progress was monitored by TLC (Hex:EtOAc 8:2).

After 12 h, the reaction was quenched by the addition of Na_2SO_3 (400 mg), followed by stirring at RT for further 2 h. The mixture was subsequently extracted with 3xEtOAc and the organic extracts were washed with 2M aqueous KOH, dried over Na_2SO_4, filtered, and concentrated in vacuo.

Purification by flash chromatography (Hex:EtOAc 9:1 to 8:2) led to **106** (72mg, 0.21 mmol) in 80% yield.

Characterization

^{1}H NMR (400 MHz, $CDCl_3$) δ 3.97 (dd, *J*= 5.0, 2.3 Hz, IH, H-2), 3.84 (m, IH, C-3), 3.07 (d, *J*= 5.0 Hz, 1H, C2-O*H*), 1.84 (d, *J*= 9.2 Hz, 1H, C3-O*H*), 1.65-1.43 (m, 2H, H-4), 1.55 (s, 9H, C(C*H*$_3$)$_3$), 1.43-1.25 (m, 22H, H-5 - H-15), 0.88 ppm (t, *J*= 6.6 Hz, 3H, H-16).

^{13}C NMR (101 MHz, $CDCl_3$) δ 173.07 (Cquat), 83.29 (Cquat), 73.26 (C-2), 72.86 (C-3), 34.14 (C-4), 31.92-22.84 (C-5 - C-15), 28.17 (C(*C*H$_3$)$_3$), 14.26 (C-16) ppm.

MS (ESI+) *m/z* calculated $[M+Na]^+$=367.29; found=367.20 (100%)

[α]D^{31}= +15.2 (c 1.0, $CHC1_3$).

*tert-Butyl (2R,3R)-3-Acetoxy-2-chlorohexadecanoate (**108**)*

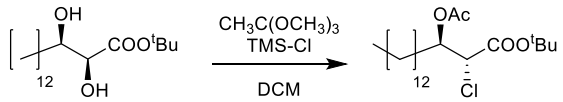

106 108

60%

A solution of **106** (2.7g, 7.84 mmol), trimethy orthoacetate (1.5 mL, 11.76 mmol) and chlorotrimethylsilane (1.5 mL, 11,76 mmol) in DCM (52 mL, 0.15M) was stirred at RT for 72h. The reaction progress was monitored by TCL (Hex:EtOAc 9:1).

The reaction mixture was concentrated in vacuo, and the residue was purified by flash chromatography (Hex to Hex:Et_2O 8:2) to give **108** (1.9 g, 4.7 mmol) in 60% yield.

Characterization

^{1}H NMR (400 MHz, $CDCl_3$) δ 5.29 (ddd, *J*= 7.4, 6.3, 4.4 Hz, 1H, H-3), 4.38 (d, *J*= 6.3 Hz, 1H, H-2), 2.09 (s, 3H, C*H*$_3$CO), 1.70 (m, 2H, H-4), 1.50 (s, 9H, C(C*H*$_3$)$_3$), 1.40-1.22 (m, 22H, H-5 - H-15), 0.91 ppm (m, 3H, H-16).

^{13}C NMR (101 MHz, $CDCl_3$) δ 169.88 (Cquat), 166.01 (Cquat), 84.8 (Cquat), 73.49 (C-3), 59.39 (C-2), 33.51 (C-4), 29.59-29.28 (C-5 - C-15), 27.77 (C(*C*H$_3$)$_3$), 20.89 (*C*H$_3$CO), 14.11 ppm (C-16).

MS (ESI+) *m/z* calculated $[M+Na]^+$=427.27; found=427.16 (100%).

*tert-Butyl (R)-3-Acetoxyhexadecanoate (**109**)*

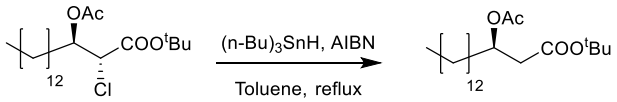

108 109

50%

108 (200mg, 0.454 mmol) was dissolved in toluene. Tri-n-butyltin hydride (159 µL, 0.59 mmol) and AIBN (4 mg, 0.023 mmol) were added. The solution was refluxed for 24h and the reaction progress was monitored by TLC (Hex:EtOAc 9:1).
The solvent was removed in vacuo and the residue was purified by flash chromatography (Hex to Hex:EtOAc 9:1) to give **109** (84 mg, 0.227 mmol) in 50% yield.

Characterization

^{1}H NMR (400 MHz, $CDCl_3$) δ 5.22 (m, 1H, H-3), 2.47 (dd, *J*= 15.2, 7.1 Hz, 1H, H-2a), 2.45 (dd, *J*= 15.2, 5.6 Hz, 1H, H-2b), 2.04 (s, 3H, C*H*$_3$CO), 1.65-1.20 (m, 24H, H-4 - H-15), 1.45 (s, 9H, C(C*H*$_3$)$_3$), 0.88 ppm (t, *J*= 6.6 Hz, 3H, H-16).

^{13}C NMR (101 MHz, $CDCl_3$) δ 170.46 (Cquat), 169.85 (Cquat), 80.93 (Cquat), 71.01 (C-3), 40.77 (C-4), 34.25 (C-2), 32.07-21.27 (C-5 - C-15), 28.16 (C(*C*H$_3$)$_3$), 20.89 (*C*H$_3$CO), 14.11 ppm (C-16).

MS (ESI+) *m/z* calculated $[M+Na]^+$=393.31; found=393.30 (100%).

*tert-Butyl (R)-3-Hydroxyhexadecanoate (**110**)*

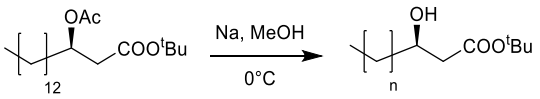

109 110: n=12

80%

To a solution of **109** (130mg, 0.35mmol) in MeOH (3.5 mL, 0.1 M) was added NaOMe (0.035 mmol) in MeOH (freshly prepared from Na). The mixture was stirred at 0°C and the reaction progress was monitored by TLC (Hex:EtOAc 8:2). After 2h, the reaction was quenched by the addition of AcOH and the solvent was evaporated in vacuo.
The crude was purified by flash chromatography (Hex:EtOAc 9:1 to 8:2) to give **110** (90 mg, 0.28 mmol) in 80% yield.

Characterization

^{1}H NMR (400 MHz, $CDCl_3$) δ 3.95 (m, 1H, H-3), 3.06 (d, *J*= 3.9 Hz, IH, O*H*), 2.42 (dd, *J*= 16.4, 3.1 Hz, IH, H-2a), 2.31 (dd, *J*= 16.4, 9.0 Hz, IH, H-2b), 1.53-1.20 (m, 24H, H-4 -H-15), 1.46 (s, 9H, C(CH_3)$_3$), 0.88 ppm (t, *J*= 6.6 Hz, 3H, H-16).

^{13}C NMR (101 MHz, $CDCl_3$) δ 68.33 (C-3), 42.48 (C-2), 36.35 (C-4), 32.09-22.85 (C-5 - C-15), 28.30 (C(CH_3)$_3$), 14.26 ppm (C-16).

MS (ESI+) *m/z* calculated $[M+Na]^+$=351.30; found=351.32 (100%)

*tert-Butyl (E)-2-heptadecenoate (**105**)*

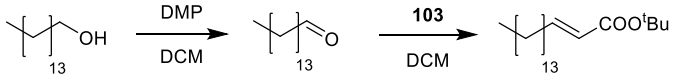

100 102 105

90%

Pentadecanol (10.0 g, 44 mmol) was dissolved in DCM (220 mL, 0.2 M). DMP (37.30 g, 88 mmol) was added and the mixture was stirred overnight before being quenched by the addition of 200 mL $Na_2S_2O_3$ (saturated aqueous solution) and 200 mL $NaHCO_3$ (saturated aqueous solution). After 30', the organic and the aqueous phases were separated, and the organic phase was washed with H_2O and brine and dried over Na_2SO_4. The solvent was evaporated in vacuo to give aldehyde **102**.

The crude was dissolved in DCM (220 mL, 0.2 M). tert-Butyl (triphenylphosphoranylidene) acetate **103** (23.4 g, 62 mmol) was added and the solution was stirred for 3h at RT.

The solvent was removed in vacuo and 300 mL of Et_2O/hexane (1:1) were added. The insoluble material was removed by filtration over Celite.

The filtrate was concentrated in vacuo, and the residue was purified by flash chromatography (Hex:Et_2O 92:8 to 85:15) to give **105** (13.0g, 42.0 mmol) in 90% yield.

Characterization

^{1}H NMR (400 MHz, $CDCl_3$) δ 6.86 (dt, *J*= 15.5, 7.0 Hz, 1H, H-3), 5.73 (dt, *J*= 15.5, 1.6 Hz, 1H, H-2), 2.16 (qd, *J*= 7.0, 1.6 Hz, 2H, H-4), 1.48 (s, 9H, C(C*H*$_3$)$_3$), 1.45-1.38 (m, 2H, H-16), 1.37-1.20 (m, 22H, H-5 - H-15), 0.84 ppm (t, *J*= 6.9 Hz, 3H, H-17).

^{13}C NMR (101 MHz, $CDCl_3$) δ 166.21 (Cquat), 148.36 (C-3), 122.86 (C-2), 79.94 (Cquat), 32.07 (C-4), 31.97-28.84 (C-5 - C-15), 28.16 (C(*C*H$_3$)$_3$), 22.70 (C-16), 14.12 ppm (C-17).

*tert-Butyl (2S,3R)-2,3-Dihydroxyheptadecanoate (**107**)*

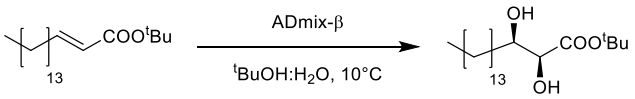

105 107

80%, > 99% ee

Potassium ferricyanide(III) (15.78 g, 47.93 mmol), K_2CO_3 (6.59 g, 47.93 mmol), [$(DHQD)_2PHAL$] (125 mg, 0.16 mmol) and OsO_4 (0.5 mL of a 0.001 M solution in H_2O, 0.5 μmol) were stirred in a 1:1 *t*-BuOH:H_2O mixture (50 mL, 0.2 M) at RT for 15'.

Methanesulfonamide (1.52 g, 15.98 mmol) was added and the mixture was cooled to 10 °C. A solution of **105** (5.2 g, 15.98 mmol in 10 ml of a 1:1 *t*-BuOH:H_2O mixture) was introduced and the mixture was stirred at 10 °C. The reaction progress was monitored by TLC (Hex:EtOAc 8:2).

After 12 h, the reaction was quenched by the addition of Na_2SO_3 (15 g), followed by stirring at RT for further 2 h. The mixture was subsequently extracted with 3xEtOAc and the organic extracts were washed with 2M aqueous KOH, dried over Na_2SO_4, filtered, and concentrated in vacuo.

Purification by flash chromatography (Hex:EtOAc 9:1 to 8:2) led to compound **107** (13.76 g, 38.34 mmol) in 80% yield.

Characterization

^{1}H NMR (400 MHz, $CDCl_3$) δ 3.96 (d *J*= 2.3 Hz, 1H, H-2), 3.84 (d, *J*= 6.1 Hz, 1H, C-3), 3.06 (brs, 1H, C2-O*H*), 1.82 (brs, 1H, C3-O*H*), 1.65-1.43 (m, 2H, H-4), 1.55 (s, 9H, C(C*H*$_3$)$_3$), 1.43-1.25 (m, 24H, H-5 - H-16), 0.88 ppm (t, *J*= 6.6 Hz, 3H, H-17).

^{13}C NMR (101 MHz, $CDCl_3$) δ 172.92 (Cquat), 83.15 (Cquat), 73.11 (C-2), 72.71 (C-3), 33.99 (C-4), 31.92-22.69 (C-5 - C-16), 28.03 (C(*C*H$_3$)$_3$), 14.12 ppm (C-17).

[α]D^{31}= +16.4 (c 1.0, $CHC1_3$).

References

(1) Xavier, N. M. Special Issue " Carbohydrates 2018 ." **2020**, 2018–2019.

(2) Rouzic, E. M. Meningitis Epidemics in Africa : A Brief Overview. **2007**, 7–11.

(3) Hollingshead, S.; Tang, C. M. An Overview of Neisseria Meningitidis. In *Neisseria meningitidis: Methods and Protocols*; Seib, K. L., Peak, I. R., Eds.; Springer New York: New York, NY, 2019; pp 1–16.

(4) Torres-Sánchez, M. I.; Draghetti, V.; Panza, L.; Lay, L.; Russo, G. Synthesis of the Phosphono Analogue of the Dimeric Subunit of Neisseria Meningitidis Type A Capsular Polysaccharide. *Synlett* **2005**, No. 7, 1147–1151.

(5) Torres-Sanchez, M. I.; Zaccaria, C.; Buzzi, B.; Miglio, G.; Lombardi, G.; Polito, L.; Russo, G.; Lay, L. Synthesis and Biological Evaluation of Phosphono Analogues of Capsular Polysaccharide Fragments from Neisseria Meningitidis A. *Chem. – A Eur. J.* **2007**, *13*, 6623–6635.

(6) Enotarpi, J.; Tontini, M.; Balocchi, C.; van der Es, D.; Auberger, L.; Balducci, E.; Carboni, F.; Proietti, D.; Casini, D.; Filippov, D. V.; et al. A Stabilized Glycomimetic Conjugate Vaccine Inducing Protective Antibodies against Neisseria Meningitidis Serogroup A. *Nat. Commun.* **2020**, *11* (1), 1–9.

(7) Gao, Q.; Zaccaria, C.; Tontini, M.; Poletti, L.; Costantino, P.; Lay, L. Synthesis and Preliminary Biological Evaluation of Carba Analogues from Neisseria Meningitidis A Capsular Polysaccharide. *Org. Biomol. Chem.* **2012**, *10* (33), 6673.

(8) Vangala, M.; Hotha, S. Synthesis of 1,2,3-Triazolyl Analog of Neisseria Meningitidis A Capsular Polysaccharide. *J. Carbohydr. Chem.* **2018**, *37* (7–8), 393–413.

(9) Berry, D.; Lynn, F.; Lee, C.-H.; Frasch, C.; Bash, M. Effect of O Acetylation of Neisseria Meningitidis Serogroup A Capsular Polysaccharide on Development of Functional Immune Responses. *Infect. Immun.* **2002**, *70*, 3707–3713.

(10) Galanos, C.; Luderitz, O.; Rietshel, E. T.; Westphal, O.; Brade, H.; Brade, L.; Freudenberg, M.; Schade, U.; Imoto, M.; Yoshimura, H.; et al. Synthetic and Natural Escherichia Coli Free Lipid A Express Identical Endotoxic Activities. *Eur. J. Biochem.* **1985**, *148* (1), 1–5.

(11) Noel Masihi, K.; Lange, W.; Brehmer, W.; Ribi, E. Immunobiological Activities of Nontoxic Lipid A: Enhancement of Nonspecific Resistance in Combination with Trehalose Dimycolate against Viral Infection and Adjuvant Effects. *Int. J. Immunopharmacol.* **1986**, *8* (3), 339–345.

(12) Coler, R. N.; Bertholet, S.; Moutaftsi, M.; Guderian, J. A.; Windish, H. P.; Baldwin, S. L.; Laughlin, E. M.; Duthie, M. S.; Fox, C. B.; Carter, D.; et al. Development and Characterization of Synthetic Glucopyranosyl Lipid Adjuvant System as a Vaccine Adjuvant. *PLoS One* **2011**, *6* (1), e16333.

(13) Erturk-Hasdemir, D.; Oh, S. F.; Okan, N. A.; Stefanetti, G.; Gazzaniga, F. S.; Seeberger, P. H.; Plevy, S. E.; Kasper, D. L. Symbionts Exploit Complex Signaling to Educate the Immune System. *Proc. Natl. Acad. Sci. U. S. A.* **2019**, *116* (52), 26157–26166.

(14) Coico, R. Gram Staining. *Curr. Protoc. Microbiol.* **2006**, *00* (1), A.3C.1-A.3C.2.

(15) Beveridge, T. J. Use of the Gram Stain in Microbiology. *Biotech. Histochem.* **2001**, *76* (3), 111–118.

(16) Silhavy, T. J.; Kahne, D.; Walker, S. The Bacterial Cell Envelope. **2010**, 1–17.

(17) Silipo, A.; Molinaro, A. *Endotoxins: Structure, Function and Recognition - The Diversity of the Core Oligosaccharide in Lipopolysaccharides*; Wang, X., Quinn, P. J., Eds.; Springer New York, 2010.

(18) Raetz, C. R. H.; Whitfield, C. Lipopolysaccharide Endotoxins. *Annu. Rev. Biochem.* **2002**, *71* (1), 635–700.

(19) Mazgaeen, L.; Gurung, P. Recent Advances in Lipopolysaccharide Recognition Systems. *Int. J. Mol. Sci.* **2020**, *21* (2).

(20) Lindberg, A. A. Polyosides (Encapsulated Bacteria). *Comptes Rendus l'Académie des Sci. - Ser. III - Sci. la Vie* **1999**, *322* (11), 925–932.

(21) Weintraub, A. Immunology of Bacterial Polysaccharide Antigens. *Carbohydrate Research*. Elsevier BV November 14, 2003, pp 2539–2547.

(22) Yatim, K. M.; Lakkis, F. G. A Brief Journey through the Immune System. *Clin. J. Am. Soc. Nephrol.* **2015**, *10* (7), 1274–1281.

(23) Alberts, B.; Johnson, A.; Lewis, J.; Raff, M.; Roberts, K.; Walter, P. Innate Immunity. In *Molecular Biology of the Cell. 4th edition*; Garland Science, 2002.

(24) Kawai, T.; Akira, S. The Roles of TLRs, RLRs and NLRs in Pathogen Recognition. *Int. Immunol.* **2009**, *21* (4), 317–337.

(25) Delves, P. J.; Roitt, I. M. The Immune System. *N. Engl. J. Med.* **2000**, *343* (1), 37–49.

(26) Vidya, M. K.; Kumar, V. G.; Sejian, V.; Bagath, M.; Krishnan, G.; Bhatta, R. Toll-like Receptors: Significance, Ligands, Signaling Pathways, and Functions in Mammals. *Int. Rev. Immunol.* **2018**, *37* (1), 20–36.

(27) Schroeder, H. W. J.; Cavacini, L. Structure and Function of Immunoglobulins (Author Manuscript). *J. Allergy Clin. Immunol.* **2010**, *125*, S41–S52.

(28) Ionescu, L.; Urschel, S. Memory B Cells and Long-Lived Plasma Cells. *Transplantation* **2019**, *103* (5), 890–898.

(29) Janeway's Immunobiology. Ninth Edition by Kenneth Murphy, Casey Weaver, Allan Mowat, Leslie Berg, David Chaplin, Charles A. Janeway, Paul Travers, and Mark Walport. *Q. Rev. Biol.* **2018**, *93* (1), 59.

(30) WHO. Vaccines and Immunization. *https://www.who.int/health-topics/vaccines-and-immunization#tab=tab_1*.

(31) Jenner, E. Origin of My Inquiry. *Med. Phys. J.* **1801**, *5* (28), 505–508.

(32) Gross, C. P.; Sepkowitz, K. A. The Myth of the Medical Breakthrough: Smallpox, Vaccination, and Jenner Reconsidered. *Int. J. Infect. Dis.* **1998**, *3* (1), 54–60.

(33) Riedel, S. Edward Jenner and the History of Smallpox and Vaccination. *Baylor Univ. Med. Cent. Proc.* **2005**, *18* (1), 21–25.

(34) Pearce, J. Louis Pasteur and Rabies: A Brief Note. *J. Neurol. Neurosurg. Psychiatry* **2002**, *73* (1), 82–82.

(35) Barrett, P. N.; Mundt, W.; Howard, M. K. Vero Cell Platform in Vaccine Production : Moving towards Cell Culture-Based Viral Vaccines. **2009**, 607–618.

(36) Enders, J. F.; Weller, T. H.; Robbins, F. C. Cultivation of the Lansing Strain of Poliomyelitis Virus in Cultures of Various Human Embryonic Tissues. *Science (80-.).* **1949**, *109* (2822), 85–87.

(37) Delany, I.; Rappuoli, R.; De Gregorio, E. Vaccines for the 21st Century. *EMBO Mol. Med.* **2014**, *6* (6), 708–720.

(38) Gotschlich, E. C.; Liu, T. Y.; Artenstein, M. S. Human Immunity to the Meningococcus. *J. Exp. Med.* **1969**, *129* (6), 1349–1365.

(39) Plotkin, S. History of Vaccination. *Proc. Natl. Acad. Sci.* **2014**, *111* (34), 12283–12287.

(40) Schneerson, R.; Barrera, O.; Sutton, A.; Robbins, J. B. Preparation, Characterization, and Immunogenicity of Haemophilus Influenzae Type b Polysaccharide-Protein Conjugates. *J. Exp. Med.* **1980**, *152* (2), 361–376.

(41) Rappuoli, R.; De Gregorio, E.; Costantino, P. On the Mechanisms of Conjugate Vaccines. *Proc. Natl. Acad. Sci.* **2019**, *116* (1), 14–16.

(42) Point, W. Development and Chimpanzee Testing of a Vaccine against Human Hepatitis B. **1976**, *700*, 694–700.

(43) Charlton Hume, H. K.; Vidigal, J.; Carrondo, M. J. T.; Middelberg, A. P. J.; Roldão, A.; Lua, L. H. L. Synthetic Biology for Bioengineering Virus-like Particle Vaccines. *Biotechnol. Bioeng.* **2019**, *116* (4), 919–935.

(44) Pizza, M. Identification of Vaccine Candidates Against Serogroup B Meningococcus by Whole-Genome Sequencing. *Science (80-.).* **2000**, *287* (5459), 1816–1820.

(45) Male, D.; Brostoff, J.; Roth, D. B.; Roitt, I. Immunology. 7th. *England, OX5 1GB, Kidlington, Elsevier Ltd Publ.* **2006**, *568*, 10.

(46) Baxter, D. Active and Passive Immunity, Vaccine Types, Excipients and Licensing. *Occup. Med. (Chic. Ill).* **2007**, *57* (8), 552–556.

(47) Mak, T. W.; Saunders, M. E. Vaccines and Clinical Immunization. In *The Immune Response*; Mak, T. W., Saunders, M. E. B. T.-T. I. R., Eds.; Elsevier: Burlington, 2006; pp 695–749.

(48) Minor, P. D. Live Attenuated Vaccines : Historical Successes and Current Challenges. *Virology* **2015**, *479–480*, 379–392.

(49) Sanders, B.; Koldijk, M.; Schuitemaker, H. *Inactivated Viral Vaccines*; 2015.

(50) Nascimento, I. P.; Leite, L. C. C. Recombinant Vaccines and the Development of New Vaccine Strategies. *Brazilian J. Med. Biol. Res. = Rev. Bras. Pesqui. medicas e Biol.* **2012**, *45* (12), 1102–1111.

(51) Plotkin, S. .; Mortimer, A. *Short History of Vaccination*, 2nd ed.; 1994.

(52) Ramon G. Sur l'augmentation Anormale de l'antitoxine Chez Les Chevaux Producteurs de Serum Ntidiphterique. *Bull Soc Cetr Med Vet* **1925**, 227–234.

(53) McKee, A. S.; Marrack, P. Old and New Adjuvants. *Curr. Opin. Immunol.* **2017**, *47*, 44–51.

(54) Coffman, R. L.; Sher, A.; Seder, R. A. Review Vaccine Adjuvants : Putting Innate Immunity to Work. *Immunity* **2010**, *33* (4), 492–503.

(55) Goto, N.; Akama, K. Histopathological Studies of Reactions in Mice Injected with Aluminum-Adsorbed Tetanus Toxoid. *Microbiol. Immunol.* **1982**, *26* (12), 1121–1132.

(56) Paul, W. E.; Zhu, J. How Are T(H)2-Type Immune Responses Initiated and Amplified? *Nat. Rev. Immunol.* **2010**, *10* (4), 225–235.

(57) Lindblad, E. B. Aluminium Compounds for Use in Vaccines. *Immunol. Cell Biol.* **2004**, *82* (5), 497–505.

(58) Olive, C. Pattern Recognition Receptors: Sentinels in Innate Immunity and Targets of New Vaccine Adjuvants. *Expert Rev. Vaccines* **2012**, *11*, 237–256.

(59) Duthie, M. S.; Windish, H. P.; Fox, C. B.; Reed, S. G. Use of Defined TLR Ligands as Adjuvants within Human Vaccines. *Immunol. Rev.* **2011**, *239* (1), 178–196.

(60) Volkin, D. B.; Burke, C. J.; Sanyal, G.; Middaugh, C. R. Analysis of Vaccine Stability. *Dev. Biol. Stand.* **1996**, *87*, 135–142.

(61) Cancogni, D.; Fusari, M.; Poggi, N.; Lay, L. Major Advances in the Development of Synthetic Oligosaccharide-Based Vaccines. In *Polysaccharides: Bioactivity and Biotechnology*; Ramawat, K. G., Mérillon, J.-M., Eds.; Springer International Publishing: Cham, 2015; pp 2065–2116.

(62) Mond, J. J.; Lees, A.; Snapper, C. M. T Cell-Independent Antigens Type 2. *Annu. Rev. Immunol.* **1995**, *13* (1), 655–692.

(63) Lepow, M. L.; Goldschneider, I.; Gold, R.; Randolph, M.; Gotschlich, E. C. Persistence of Antibody Following Immunization of Children with Groups A and C

Meningococcal Polysaccharide Vaccines. *Pediatrics* **1977**, *60* (5), 673–680.

(64) Lesinski, G. B.; Westerink, M. A. Novel Vaccine Strategies to T-Independent Antigens. *J. Microbiol. Methods* **2001**, *47* (2), 135—149.

(65) Avery, B. Y. O. T.; Goebel, W. F. Chemo - Immunological Studies on Conjugated Carbohydrate-Proteins. **1931**.

(66) Colombo, C.; Pitirollo, O.; Lay, L. Recent Advances in the Synthesis of Glycoconjugates for Vaccine Development. *Molecules* **2018**, *23* (7).

(67) Mitchison, N. A. The Carrier Effect in the Secondary Response to Hapten-Protein Conjugates. II. Cellular Cooperation. *Eur. J. Immunol.* **1971**, *1* (1), 18–27.

(68) Avci, F. Y.; Li, X.; Tsuji, M.; Kasper, D. L. A Mechanism for Glycoconjugate Vaccine Activation of the Adaptive Immune System and Its Implications for Vaccine Design. *Nat. Med.* **2011**, *17* (12).

(69) Berti, F.; Adamo, R. Recent Mechanistic Insights on Glycoconjugate Vaccines and Future Perspectives. *ACS Chem. Biol.* **2013**, *8* (8), 1653–1663.

(70) Sun, X.; Stefanetti, G.; Berti, F.; Kasper, D. L. Polysaccharide Structure Dictates Mechanism of Adaptive Immune Response to Glycoconjugate Vaccines. *Proc. Natl. Acad. Sci.* **2019**, *116* (1), 193 LP – 198.

(71) Costantino, P.; Rappuoli, R.; Berti, F. The Design of Semi-Synthetic and Synthetic Glycoconjugate Vaccines. *Expert Opin. Drug Discov.* **2011**, *6* (10), 1045–1066.

(72) Ferna, V.; Rodriguez, A.; Baly, A.; Herrera, L.; Izquierdo, M.; Villar, A.; Valde, Y.; Cosme, K.; Deler, M. L.; Montane, M.; et al. Polysaccharide Vaccine Against Haemophilus Influenzae Type B. **2004**, *305* (July), 522–526.

(73) Roy, R. New Trends in Carbohydrate-Based Vaccines. *Drug Discov. Today Technol.* **2004**, *1* (3), 327–336.

(74) Stein-Zamir, C.; Shoob, H.; Abramson, N.; Block, C.; Keller, N.; Jaffe, J.; Valinsky, L. Invasive Meningococcal Disease Epidemiology and Characterization of Neisseria Meningitidis Serogroups, Sequence Types, and Clones; Implication for Use of Meningococcal Vaccines. *Hum. Vaccin. Immunother.* **2019**, *15* (1), 242–248.

(75) Attarpour-Yazdi, M. M.; Ghamarian, A.; Mousaviehzadeh, M.; Davoudi, N. Identification of the Serotypes of Bacterial Meningitis Agents; Implication for Vaccine Usage. *Iran. J. Microbiol.* **2014**, *6* (4), 211–218.

(76) Jennings, H. J.; Bhauacharjee, A. K.; Bundle, D. R.; Kenny, C. P.; Martin, A.; Smith, I. C. P. Structures of the Capsular Polysaccharides of Neisseria Meningitidis as Determined by 13C-Nuclear Magnetic Resonance Spectroscopy. *J. Infect. Dis.* **1977**, *136* (578–583).

(77) Yazdankhah, S. P.; Caugant, D. A. Neisseria Meningitidis: An Overview of the Carriage State. *J. Med. Microbiol.* **2004**, *53* (Pt 9), 821–832.

(78) Rosenstein, N. E.; Perkins, B. A.; Stephens, D. S.; Popovic, T.; Hughes, J. M. Meningococcal Disease. *N. Engl. J. Med.* **2001**, *344* (18), 1378–1388.

(79) Nadel, S. Treatment of Meningococcal Disease. *J. Adolesc. Heal.* **2016**, *59* (2), S21–S28.

(80) Wu, H. M.; Harcourt, B. H.; Hatcher, C. P.; Wei, S. C.; Novak, R. T.; Wang, X.; Juni, B. A.; Glennen, A.; Boxrud, D. J.; Rainbow, J.; et al. Emergence of Ciprofloxacin-Resistant Neisseria Meningitidis in North America. *N. Engl. J. Med.* **2009**, *360* (9), 886–892.

(81) Batty, E. M.; Cusack, T.; Thaipadungpanit, J.; Watthanaworawit, W.; Carrara, V.; Sihalath, S.; Hopkins, J.; Soeng, S.; Ling, C.; Turner, P.; et al. International Journal of Infectious Diseases The Spread of Chloramphenicol-Resistant Neisseria Meningitidis in Southeast Asia. *Int. J. Infect. Dis.* **2020**, *95*, 198–203.

(82) States, M.; Strate-, W. H. O.; Group, A.; Membres, E. Meningococcal Vaccines: WHO Position Paper, November 2011. *Wkly. Epidemiol. Rec.* **2011**, *86* (47), 521–539.

(83) Burman, C.; Serra, L.; Nuttens, C.; Presa, J.; Balmer, P.; York, L. Meningococcal Disease in Adolescents and Young Adults: A Review of the Rationale for Prevention through Vaccination. *Hum. Vaccin. Immunother.* **2019**, *15* (2), 459–469.

(84) Gasparini, R.; Panatto, D.; Bragazzi, N. L.; Lai, P. L.; Bechini, A.; Levi, M.; Durando, P.; Amicizia, D. How the Knowledge of Interactions between Meningococcus and the Human Immune System Has Been Used to Prepare Effective *Neisseria Meningitidis* Vaccines. *J. Immunol. Res.* **2015**, *2015*, 189153.

(85) Laforce, F. M.; Borrow, R.; Preziosi, M. Documenting the Results of a Successful Partnership : A New Meningococcal Vaccine for Africa. **2015**, *61* (Suppl 5), 389–390.

(86) Djingarey, M. H.; Barry, R.; Bonkoungou, M.; Tiendrebeogo, S.; Sebgo, R.; Kandolo, D.; Lingani, C.; Preziosi, M.-P.; Zuber, P. L. F.; Perea, W.; et al. Effectively Introducing a New Meningococcal A Conjugate Vaccine in Africa: The Burkina Faso Experience. *Vaccine* **2012**, *30 Suppl 2*, B40-5.

(87) Toma, L.; Legnani, L.; Rencurosi, A.; Poletti, L.; Russo, G. Modeling of Synthetic Phosphono and Carba Analogues of N -Acetyl- a - D -Mannosamine 1-Phosphate , the Repeating Unit of the Capsular Polysaccharide from Neisseria Meningitidis Serovar A †. **2009**, 3734–3740.

(88) Calloni, I.; Unione, L.; Jiménez-Osés, G.; Corzana, F.; Del Bino, L.; Corrado, A.; Pitirollo, O.; Colombo, C.; Lay, L.; Adamo, R.; et al. The Conformation of the Mannopyranosyl Phosphate Repeating Unit of the Capsular Polysaccharide of Neisseria Meningitidis Serogroup A and Its Carba-Mimetic. *European J. Org. Chem.* **2018**, *2018* (33), 4548–4555.

(89) Lay, L. Manuscript in Preparation.

(90) Berry, D. S.; Lynn, F.; Lee, C.-H.; Frasch, C. E.; Bash, M. C. Effect of O Acetylation of Neisseria Meningitidis Serogroup A Capsular Polysaccharide on Development of Functional Immune Responses. *Infect. Immun.* **2002**, *70* (7), 3707 LP – 3713.

(91) Torres-Sanchez, M. I.; Zaccaria, C.; Buzzi, B.; Miglio, G.; Lombardi, G.; Polito, L.; Russo, G.; Lay, L. Synthesis and Biological Evaluation of Phosphono Analogues of Capsular Polysaccharide Fragments from Neisseria Meningitidis A. *Chem. - A Eur. J.* **2007**, *13* (23), 6623–6635.

(92) Teodorovi, P.; Oscarson, S. Synthesis of Stable C-Phosphonate Analogues of Neisseria Meningitidis Group A Capsular Polysaccharide Structures Using Modified Mitsunobu Reaction Conditions. **2006**, No. Scheme 1, 4485–4490.

(93) Casero, F.; Cipolla, L.; Lay, L.; Nicotra, F.; Panza, L. Stereoselective Synthesis of the Isosteric Phosphono Analogues of N -Acetyl- r - D -Glucosamine 1-Phosphate and N -Acetyl- r - D -Mannosamine 1-Phosphate. **1996**, *3263* (6), 3428–3432.

(94) Manea, F.; Bindoli, C.; Fallarini, S.; Lombardi, G.; Polito, L.; Lay, L.; Bonomi, R.; Mancin, F.; Scrimin, P. Multivalent, Saccharide-Functionalized Gold Nanoparticles as Fully Synthetic Analogs of Type a Neisseria Meningitidis Antigens. *Adv. Mater.* **2008**, *20* (22), 4348–4352.

(95) Fallarini, S.; Buzzi, B.; Giovarruscio, S.; Polito, L.; Brogioni, G.; Tontini, M.; Berti, F.; Adamo, R.; Lay, L.; Lombardi, G. A Synthetic Disaccharide Analogue from Neisseria Meningitidis A Capsular Polysaccharide Stimulates Immune Cell Responses and Induces Immunoglobulin G (IgG) Production in Mice When Protein- Conjugated. **2015**.

(96) Henriques, P.; Dello Iacono, L.; Gimeno, A.; Biolchi, A.; Romano, M. R.; Arda, A.; Bernardes, G. J. L.; Jimenez-Barbero, J.; Berti, F.; Rappuoli, R.; et al. Structure of a Protective Epitope Reveals the Importance of Acetylation of Neisseria Meningitidis Serogroup A Capsular Polysaccharide. *Proc. Natl. Acad. Sci.* **2020**, 202011385.

(97) Wang, Y.; Yan, Q.; Wu, J.; Zhang, L. H.; Ye, X. S. A New One-Pot Synthesis of α-Gal Epitope Derivatives Involved in the Hyperacute Rejection Response in Xenotransplantation. *Tetrahedron* **2005**, *61* (17), 4313–4321.

(98) Ishihara, K.; Kurihara, H.; Yamamoto, H. An Extremely Simple, Convenient, and Selective Method for Acetylating Primary Alcohols in the Presence of Secondary Alcohols. *J. Org. Chem.* **1993**, *58* (15), 3791–3793.

(99) Joseph, A. A.; Verma, V. P.; Liu, X. Y.; Wu, C. H.; Dhurandhare, V. M.; Wang, C. C. TMSOTf-Catalyzed Silylation: Streamlined Regioselective One-Pot Protection and Acetylation of Carbohydrates. *European J. Org. Chem.* **2012**, No. 4, 744–753.

(100) Bennek, J. A.; Gray, G. R. An Efficient Synthesis of Anhydroalditols and Allyl C-Glycosides. *J. Org. Chem.* **1987**, *52* (5), 892–897.

(101) Baudry, D.; Ephritikhine, M.; Felkin, H. Isomerisation of Allyl Ethers Catalysed by the Cationic Iridium Complex [Ir(Cyclo-Octa-1{,}5-Diene)(PMePh2)2]PF6. A

Highly Stereoselective Route to Trans-Propenyl Ethers. *J. Chem. Soc.{,} Chem. Commun.* **1978**, No. 16, 694–695.

(102) Gaul, C.; Njardarson, J. T.; Danishefsky, S. J. The Total Synthesis of (+)-Migrastatin. *J. Am. Chem. Soc.* **2003**, *125* (20), 6042–6043.

(103) Yang, D.; Zhang, C. Ruthenium-Catalyzed Oxidative Cleavage of Olefins to Aldehydes. *J. Org. Chem.* **2001**, *66* (14), 4814–4818.

(104) Lee, D. G.; Chen, T.; Wang, Z. Heterogeneous Permanganate Oxidations. 5. The Preparation of Aldehydes by Oxidative Cleavage of Carbon-Carbon Double Bonds. *J. Org. Chem.* **1993**, *58* (10), 2918–2919.

(105) Cohen, R. J.; Fox, D. L.; Eubank, J. F.; Salvatore, R. N. Mild and Efficient Cs2CO3-Promoted Synthesis of Phosphonates. *Tetrahedron Lett.* **2003**, *44* (47), 8617–8621.

(106) Ma, X.; Xu, Q.; Li, H.; Su, C.; Yu, L.; Zhang, X.; Cao, H.; Han, L.-B. Alcohol-Based Michaelis–Arbuzov Reaction: An Efficient and Environmentally-Benign Method for C–P(O) Bond Formation. *Green Chem.* **2018**, *20* (15), 3408–3413.

(107) Alex, C.; Visansirikul, S.; Zhang, Y.; Yasomanee, J. P.; Codee, J.; Demchenko, A. V. Synthesis of 2-Azido-2-Deoxy- and 2-Acetamido-2-Deoxy-D-Manno Derivatives as Versatile Building Blocks. *Carbohydr. Res.* **2020**, *488*, 107900.

(108) Akira, S.; Uematsu, S.; Takeuchi, O. Pathogen Recognition and Innate Immunity. *Cell* **2006**, *124* (4), 783–801.

(109) Komaniecka, I.; Choma, A.; Lindner, B.; Holst, O. The Structure of a Novel Neutral Lipid A from the Lipopolysaccharide of Bradyrhizobium Elkanii Containing Three Mannose Units in the Backbone. *Chem. – A Eur. J.* **2010**, *16* (9), 2922–2929.

(110) Coats, S. R.; Pham, T.-T. T.; Bainbridge, B. W.; Reife, R. A.; Darveau, R. P. MD-2 Mediates the Ability of Tetra-Acylated and Penta-Acylated Lipopolysaccharides to Antagonize Escherichia Coli Lipopolysaccharide at the TLR4 Signaling Complex. *J. Immunol.* **2005**, *175* (7), 4490–4498.

(111) Ziaco, M.; Go, S.; Traboni, S.; Razim, A.; Casillo, A.; Iadonisi, A.; Gamian, A.; Corsaro, M. M.; Bedini, E. Development of Clickable Monophosphoryl Lipid A Derivatives toward Semisynthetic Conjugates with Tumor-Associated Carbohydrate Antigens. **2017**, *595*.

(112) Edelman, R. The Development and Use of Vaccine Adjuvants. *Mol. Biotechnol.* **2002**, *21* (2), 129–148.

(113) Chen, C.; Zhang, C.; Li, R.; Wang, Z.; Yuan, Y.; Li, H.; Fu, Z.; Zhou, M.; Zhao, L. Monophosphoryl-Lipid A (MPLA) Is an Efficacious Adjuvant for Inactivated Rabies Vaccines. *Viruses* **2019**, *11* (12), 1118.

(114) Chung, H.; Pamp, S. J.; Hill, J. A.; Surana, N. K.; Edelman, S. M.; Troy, E. B.; Reading, N. C.; Villablanca, E. J.; Wang, S.; Mora, J. R.; et al. Gut Immune

Maturation Depends on Colonization with a Host-Specific Microbiota. *Cell* **2012**, *149* (7), 1578–1593.

(115) Rinninella, E.; Raoul, P.; Cintoni, M.; Franceschi, F.; Miggiano, G. A. D.; Gasbarrini, A.; Mele, M. C. What Is the Healthy Gut Microbiota Composition? A Changing Ecosystem across Age, Environment, Diet, and Diseases. *Microorganisms* **2019**, *7* (1).

(116) Dasgupta, S.; Erturk-Hasdemir, D.; Ochoa-Reparaz, J.; Reinecker, H.-C.; Kasper, D. L. Plasmacytoid Dendritic Cells Mediate Anti-Inflammatory Responses to a Gut Commensal Molecule via Both Innate and Adaptive Mechanisms. *Cell Host Microbe* **2014**, *15* (4), 413–423.

(117) Mazmanian, S. K.; Round, J. L.; Kasper, D. L. A Microbial Symbiosis Factor Prevents Intestinal Inflammatory Disease. *Nature* **2008**, *453* (7195), 620–625.

(118) Ochoa-Repáraz, J.; Mielcarz, D. W.; Wang, Y.; Begum-Haque, S.; Dasgupta, S.; Kasper, D. L.; Kasper, L. H. A Polysaccharide from the Human Commensal Bacteroides Fragilis Protects against CNS Demyelinating Disease. *Mucosal Immunol.* **2010**, *3* (5), 487–495.

(119) Alhawi, M.; Stewart, J.; Erridge, C.; Patrick, S.; Poxton, I. R. Bacteroides Fragilis Signals through Toll-like Receptor (TLR) 2 and Not through TLR4. *J. Med. Microbiol.* **2009**, *58* (Pt 8), 1015—1022.

(120) Potter, G. T.; Jayson, G. C.; Miller, G. J.; Gardiner, J. M. An Updated Synthesis of the Diazo-Transfer Reagent Imidazole-1-Sulfonyl Azide Hydrogen Sulfate. *J. Org. Chem.* **2016**, *81* (8), 3443–3446.

(121) O'Ferrall, R. A. M.; Slae, S. β-Elimination of 9-Fluorenylmethanol in Aqueous Solution: An E1cB Mechanism. *J. Chem. Soc. B* **1970**, No. 0, 260–268.

(122) Ravindranathan Kartha, K. P.; Mukhopadhyay, B.; Field, R. A. Practical De-O-Acylation Reactions Promoted by Molecular Sieves. *Carbohydr. Res.* **2004**, *339* (3), 729–732.

(123) Oikawa, M.; Kusumoto, S. On a Practical Synthesis of β-Hydroxy Fatty Acid Derivatives. *Tetrahedron: Asymmetry* **1995**, *6* (4), 961–966.

(124) Frigerio, M.; Santagostino, M.; Sputore, S. A User-Friendly Entry to 2-Iodoxybenzoic Acid (IBX). *J. Org. Chem.* **1999**, *64* (12), 4537–4538.

(125) Sharpless, K. B.; Amberg, W.; Bennani, Y. L.; Crispino, G. A.; Hartung, J.; Jeong, K. S.; Kwong, H. L.; Morikawa, K.; Wang, Z. M. The Osmium-Catalyzed Asymmetric Dihydroxylation: A New Ligand Class and a Process Improvement. *J. Org. Chem.* **1992**, *57* (10), 2768–2771.

(126) Dale, J. A.; Dull, D. L.; Mosher, H. S. α-Methoxy-α-Trifluoromethylphenylacetic Acid, a Versatile Reagent for the Determination of Enantiomeric Composition of Alcohols and Amines. *J. Org. Chem.* **1969**, *34* (9), 2543–2549.

(127) Hoye, T. R.; Jeffrey, C. S.; Shao, F. Mosher Ester Analysis for the Determination of

Absolute Configuration of Stereogenic (Chiral) Carbinol Carbons. *Nat. Protoc.* **2007**, *2* (10), 2451–2458.

(128) Seco, J. M.; Quiñoá, E.; Riguera, R. Assignment of the Absolute Configuration of Polyfunctional Compounds by NMR Using Chiral Derivatizing Agents. *Chem. Rev.* **2012**, *112* (8), 4603–4641.

(129) Oikawa, M.; Kusumoto, S. On a Practical Synthesis of B-Hydroxy Fatty Acid Derivatives. **1995**, *6* (4), 961–966.

(130) Still, W. C.; Kahn, M.; Mitra, A. Rapid Chromatographic Technique for Preparative Separations with Moderate Resolution. *J. Org. Chem.* **1978**, *43* (14), 2923–2925.

(131) Gottlieb, H. E.; Kotlyar, V.; Nudelman, A. NMR Chemical Shifts of Common Laboratory Solvents as Trace Impurities. *J. Org. Chem.* **1997**, *62* (21), 7512–7515.

(132) Morelli, L.; Lay, L. Synthesis of Neisseria Meningitidis X Capsular Polysaccharide Fragments. *Arkivoc* **2012**, *2013* (2), 166–184.

(133) Zhang, L.-D.; Zhou, T.-T.; Qi, S.-X.; Xi, J.; Yang, X.-L.; Yao, Z.-J. Total Syntheses of Lycoposerramine-V and 5-Epi-Lycoposerramine-V. *Chem. – An Asian J.* **2014**, *9* (10), 2740–2744.